THE UNIVERSITY *of* EDINBURGH

Systematic analysis of protein-protein interactions of oncogenic human papillomavirus

Ramya M. Gundurao

A thesis presented for the degree of
Doctor of Philosophy,
The University of Edinburgh

February 2013

Division of Pathway Medicine
College of Medicine and Veterinary Medicine
The University of Edinburgh

DECLARATION

I hereby declare that this thesis and the work presented in it are my own.

I confirm that:

- This work was done wholly or mainly while in candidature for a research degree at this University.
- Where any part of this thesis has previously been submitted for a degree or any other qualification at this University or any other institution, this has been clearly stated.
- Where I have consulted the published work of others, this is always clearly attributed.
- Where I have quoted from the work of others, the source is always given. With the exception of such quotations, this thesis is entirely my own work.
- I have acknowledged all main sources of help.
- Where the thesis is based on work done by myself jointly with others, I have made clear exactly what was done by others and what I have contributed myself.

Ramya M. Gundurao

University of Edinburgh

ABSTRACT

Human papilloma virus (HPV) is a ubiquitous virus implicated in a growing list of cancers, particularly cervical cancer- the second most common cancer among women worldwide. Although persistent infection with high-risk oncogenic HPVs such as types -16 or -18 is necessary, additional factors like co-infection with other viruses can play a role in cancer progression. Protein-protein interactions play a central role in the infection, survival and proliferation of the virus in the host. Although some interactions of HPV proteins are well characterised, it is essential to discover other key viral interactions to further improve our understanding of the virus and to use this knowledge for the development of newer biomarkers and therapeutics.

The aim of this study was to systematically analyse the interactions of HPV-16 proteins using yeast two-hybrid (Y2H). To achieve this, a clone collection of the viral proteome was generated by recombinatorial cloning and three independent Y2H screens were performed: (i) Intra-viral screen to identify interactions among the HPV-16 proteins; (ii) Inter-viral screen to identify interactions with proteins of Herpes Simplex Virus (HSV) which is suggested to be a co-factor; and (iii) Virus-host screen to identify novel cellular binding partners. The intra-viral Y2H screen confirmed some of the previously known interactions and also identified binding of the E1 and E7 proteins. Deletion mutagenesis was performed to map the interaction domains to the amino-terminal 92 amino acids of E1 and carboxy-terminal CxxC domain of E7. Replication assays suggest a possible repression of E1-mediated episomal replication by direct binding of E7. The inter-viral Y2H screen identified interactions of HPV proteins with seventeen HSV-1 proteins including transcriptional regulator ICP4 and neurovirulance factor ICP34.5. The biological relevance of these interactions in the context of co-infection is discussed. The virus-host screen performed against a human cDNA library identified 54 interactions, a subset of which was validated by biochemical pull-down assays. The

functional relevance of an interaction between E7 and a proto-oncogene spermatogenic leucine zipper protein (SPZ1) was further investigated suggesting a role of SPZ1 in E7-mediated cell proliferation.

The work presented in this thesis identifies several novel interactions of HPV proteins. Future work will involve the in-depth elucidation of biological relevance of these interactions. In particular, the interactions of E7 with E1 and SPZ1 are of great interest to improve our understanding of the life cycle and pathogenesis of the virus which can be applied for improved strategies of prevention and treatment of malignancies caused by HPV.

ACKNOWLEDGEMENTS

Obtaining a PhD has been a goal ever since I was in high school. I am blessed to be surrounded by inspiring people who have played a huge role in achieving this. *Mom and Dad*, you have always encouraged me to do my best in everything, been there through all my small successes and failures, stood behind me in all the decisions I have taken and given me the confidence to achieve this, thank you. The credit for all my achievements goes to you both; I hope I have made you proud. My sister, *Rashmi*, thank you for always believing in me, for never letting me become overconfident, for correcting every mistake and inspiring me to become like you. Thanks to my brother-in-law, *Harish* for all the encouragement and my lovely niece, *Stuti* who always brings a smile on my face.

I would like to thank my two teachers who made me fall in love with Biology. *Suja Ma'am*, my Biology teacher in secondary school without who I would not be doing Biology, thank you very much. *Prathibha Ma'am*, my Biotechnology lecturer who has injected into me a bit of her passion for the subject and desire to keep learning and never stop aspiring and I am ever so thankful for that.

I would like to thank my supervisor *Prof Jürgen Haas* for the opportunity to do my PhD and encouraging me to expand my horizons and be independent in thinking and planning my project. Thank you for all your critical support, advice and encouragement. *Prof Heather Cubie*, my second supervisor during my PhD, you are a tremendous inspiration and through every phase of my PhD, talking to you has always encouraged me. Your knowledge and support has been a valuable asset to me. Thank you for your constant support.

I would like to thank the current and old members of Haas group, *Dr Samantha Griffiths* for answering my never ending questions, for all your reagents that I have used and for taking the time to proof-read my thesis. Thanks to *Rui Chen* and *Dr Alessandro Ceroni* for the much required pep talks, encouragement and thesis comments. Thanks to *Dr Suzanne Esper*, *Lakshmi Narayan Kaza* and *Dr Ola Hassanin* for all your help during my PhD. I would also like to thank the students who have provided valuable results towards my thesis, *Jenna Schafers*, *Annette Murr*, *Joe Sherwan* and *Tracy Mak*. Thanks to *Clark Russell* and *Peter Thomas* for being my English proof readers. I would like to say a special thanks to all my fellow PhD students who have sailed in the same boat as me, *Senthil Gandi, Shahida Syed, Fairus Noor Hassim, Wayne Hsieh, Rui Chen and Miriam Kaatz*. Thank you for welcoming me into the group, for all the lunch and coffee break craziness which kept me sane through the stressful PhD. I would have never enjoyed these years as much without you guys. Many thanks also to all the members of Division of Pathway Medicine for all the timely help throughout the course of my PhD. I would also like to thank the members of Scottish HPV reference lab, *Kate Cushieri*, *Catherine Moore*, *Maurice Canham* and *Johanna Pedraza* for all their advice and support.

I would like to thank the members of Max von Pettenkofer institute, Munich, who trained me in yeast two-hybrid, *Markus Heinzemann, Hannah Streibinger, Verena Hofer, Georg Malterer, Rose Dietlind* and especially *Suzanne Bailer* for all their help with the technique and making my stay in Munich wonderful. Thanks to *Prof Iain Morgan* and *Dr Mary Donaldson*, University of Glasgow for giving me an opportunity to do HPV replication assays in their lab and *Dr Andrew Macdonald* for all his valuable correspondence, suggestions and reagents.

Lastly I would like to thank *Abhishek*, my fiancé, for encouraging me to pursue my dream, for listening to me jump with joy when things went well and more often than not, complain when things didn't and mostly for being my biggest competition. Thank you for being my strength!

Dedicated to my grandmother,
Mrs Radha Bai

CONTENTS

LIST OF FIGURES

LIST OF TABLES

ABBREVIATIONS

AD	GAL4 DNA activation domain
A_E	Early polyadenylation site
A_L	Late pA
ATP	Adenosine triphosphate
att site	Recombination attachment site
bp	Base pair
BPV	Bovine papilloma virus
CIN	Cervical intraepithelial neoplasia
CMV	Cytomegalovirus
Co-IP	Co-immunoprecipitation
CRPV	Cottontail rabbit papilloma virus
C-terminus	Carboxy terminus
DBD	DNA-binding domain
ddH_2O	Double distilled water
DNA	Deoxyribonucleic acid
dATP	Deoxyadenosine triphosphate
dCTP	Deoxycytosine triphosphate
dTTP	Deoxytyrosine triphosphate
dGTP	Deoxyguanosine triphosphate
dNTP	Deoxynucleotide triphosphate
DMSO	Dimethyl sulphoxide
ds	Double stranded
E1BS	E1 binding site
E2BS	E2 binding site
EBV	Epstein-Barr virus
ECM	Extra-cellular matrix
ER	Endoplasmic reticulum
EV	Epidermodysplasia verruciformis
Fwd	Forward
GOI	Gene of interest
HPV	Human papillomavirus
HSIL	High-grade squamous intraepithelial lesion
HSV	Herpes simplex virus

Kb	Kilobase
kDa	KiloDalton
LCR	Long control region
LSIL	Low-grade squamous intraepithelial lesion
LUMIER	LUminiscence based Mammalian IntERactome assay
MGC	Mammalian gene collection
N-terminus	Amino terminus
ORF	Open reading frame
Ori	Origin of replication
pA	Polyadenylation site
PCNA	Proliferative cell nuclear antigen
PCR	Polymerase chain reaction
PPI	Protein-protein interactions
PsV	Pseudovirion
PV	Papilloma virus
QsV	Quasi virions
Rev	Reverse
RNA	Ribonucleic acid
ROPV	Rabbit oral papillomavirus
RPM	Rotations per minute
SDS	Sodium dodecyl sulphate
UAS	Upstream activation sequence
VLP	Virus like particles
Y2H	Yeast two-hybrid

Chapter 1:

Introduction

1.1 Papilloma Virus

Papilloma viruses (PVs) are small, epitheliotrophic, non-enveloped double-stranded (ds) deoxyribonucleic acid (DNA) viruses belonging to the *papillomaviridae* family. Cottontail rabbit papilloma virus (CRPV), which causes warts of cottontail rabbits, was the first PV to be identified (1). It specifically infected cutaneous epithelium and caused warts and tumours (it was the first DNA tumour virus identified) but was unable to infect any mucosal sites (1). Soon after its discovery, an oral papilloma virus was discovered in rabbits called rabbit oral papillomavirus (ROPV) which caused warts in the oral mucosa but was unable to infect non-mucosal epithelial sites (2). This led to the understanding that PVs are site-specific and two types of PVs exist- mucosal and cutaneous. Neither of these two viruses, CRPV or ROPV could infect any other mammals which further led to the conclusion that apart from being site-specific, PVs are also highly species-specific (3). Additionally, it was discovered that multiple PV types could infect the same species and exposure to one type of PV does not confer protective immunity against another (3). As PVs infect most known mammals and birds, there are 189 PV types known to date including 120 human papilloma viruses (HPV) (4).

1.1.1 Phylogeny

Historically, PVs were classified in the same family as polyomaviruses. The first PV to be completely sequenced was bovine papillomavirus 1 (BPV-1) (5), followed by several others which showed distinct differences between PVs and polyomaviruses in terms of gene organisation and sequence homology. The recognition of these differences between the two families led to the classification of PVs as a new family called *papillomaviridae* (6). The members of this family are now classified based on sequence homology of the L1 open reading frame (ORF) which is highly conserved (7). The

family is divided into genus (PVs with less than 60 % homology), species (60-70 % homology), types (71-89 % homology), subtypes (90-98 %) and variants (more than 98 % homology) (Figure 1.1). Based on this classification, there are twenty nine genera named by Greek letters. Since the number of genera is more than the Greek letters, further genera are named by adding the prefix 'dyo'. The species and types are denoted by numbers (4).

HPVs belong in the alpha, beta, gamma, mu and nu genera. Most alpha-PVs infect the genital mucosa and the medically important HPVs associated with malignant infections (classified as high-risk types), such as types -16 and -18 fall under this genus. However, within the alpha genus, there are also some HPV types which infect cutaneous epithelium causing benign skin warts such as types -2 and -57. The beta, gamma, mu, and nu viruses infect non-genital skin with beta HPVs involved in causing epidermodysplasia verruciformis (EV) specific lesions. All other genera contain animal PVs, with BPV and CRPV classified under the delta and kappa PVs respectively (4).

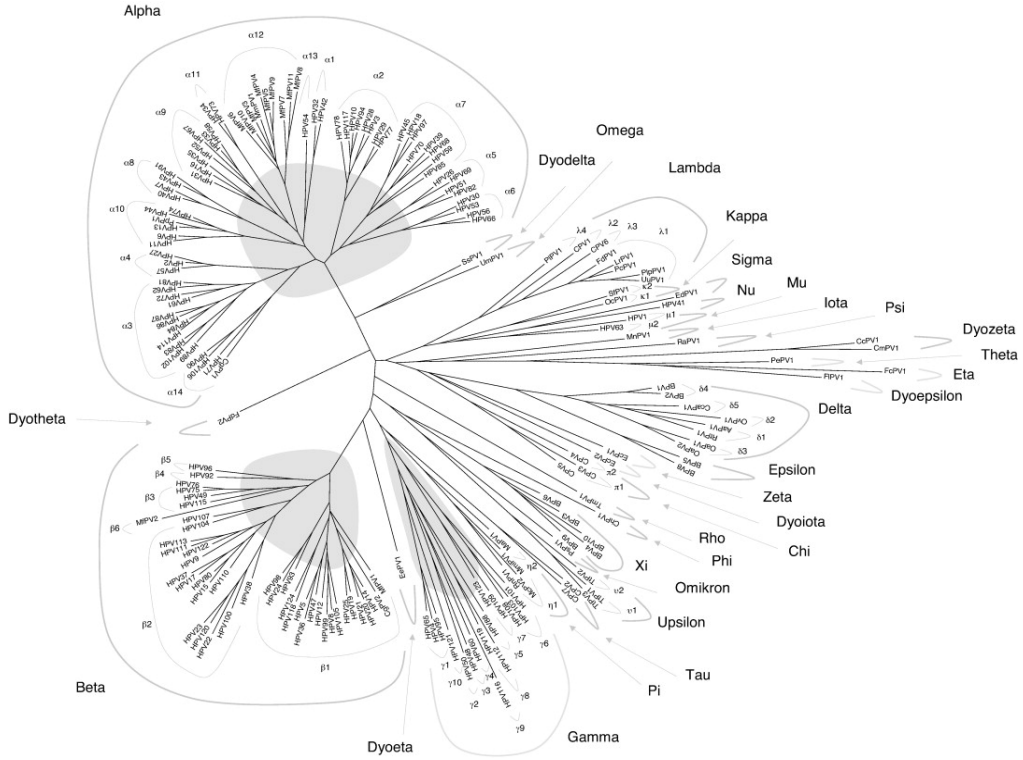

Figure 1.1: Classification of PVs. Phylogenetic tree of PVs based on sequence similarity of the L1 ORF. The outermost semicircular symbols refer to genera, the numbers at the end of each branch identify the species and other abbreviations refer to animal papillomavirus types. C-numbers refer to candidate HPV types. Figure reproduced with permission from reference (4).

1.1.2 Human Papilloma virus

HPV infects the skin and the genital mucosa of humans. Out of the 120 known HPVs, around 40 infect genital areas and these are further classified based on their disease association as high-risk types (HPV -16, -18, -31, -45) which cause malignant genital lesions and low-risk types (HPV -2, -6, -11, -57) that cause warts and benign lesions (8).

1.2 HPV Biology

1.2.1 HPV life cycle

The life cycle of HPV depends on differentiating epithelium (Figure 1.2). The stratified epithelium consists of a basal layer of keratinocytes. As the basal cells divide, a

population of cells remain in the basal layer and propagate whereas some cells migrate towards the upper layers of epithelium and exit the cell cycle. These cells differentiate to form the supra-basal epithelium made up of spinous and granular epithelial cells. The uppermost layer of epithelium is made of keratinised or non-keratinised mucosal epithelium (9).

HPV infects the basal cells by entry through micro-wounds in the epithelium. Upon infection, a series of viral gene expression occurs, which includes expression of early viral genes E1, E2, E5, E6 and E7 resulting in the replication of viral DNA into 20-100 episomes per cell (9). E1 and E2 are the first viral proteins expressed and they control the transcription of other viral genes and aid in replication. The E6 and E7 oncoproteins increase cell proliferation, leading to benign lesions and warts. In most cases of infection, the virus is maintained in an episomal state in the dividing basal cells. As the basal cells differentiate and move to the upper layers of epithelium, the expression of late proteins E4, L1 and L2 occurs. The expression of these proteins facilitates virion assembly followed by shedding of viral particles from the topmost layer (9).

While most HPV infections regress within two years (10), in some cases, integration of the viral DNA into the cellular genome occurs. Integration is randomly distributed with no preferential integration site on the human genome (11). However, it has been observed that the disruption of the E2 gene of HPV is often a consequence of integration (11). E2 controls the transcription of viral oncogenes E6 and E7 and its disruption leads to increased expression of E6 and E7 which induce a series of cellular processes causing the immortalisation of cells leading to cervical intraepithelial neoplasia (CIN) and cervical cancer (12).

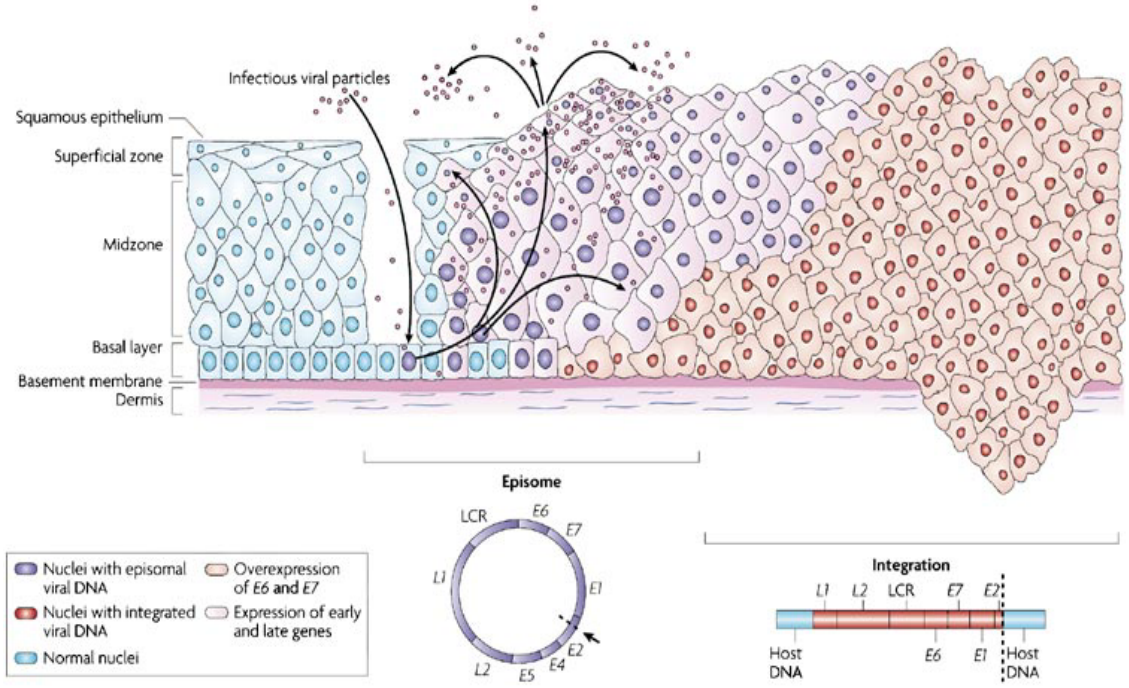

Figure 1.2: HPV life cycle in differentiating epithelium. The figure shows normal differentiation of stratified squamous epithelium in the leftmost corner (light blue). In the middle panel, HPV infected basal keratinocytes (shown in dark blue) with episomal viral genome divide and move on to supra-basal layers which remain in the cell cycle and continue to proliferate. Virions are produced and shed from the uppermost layer of epithelium. Cells with integrated genomes (red) are shown on the right panel. Integration causes immortalisation of cells and continuous proliferation leading to malignancy. Figure reproduced with permission from reference (13).

1.2.2 Genome organisation

HPV genome is made of eight kilobase (Kb) circular dsDNA. It is divided into three regions: (i) a long control region (LCR), containing the origin of replication (Ori) and promoter sites for transcription of genes; (ii) an early region coding region for the genes - E1, E2, E4, E5, E6, E7; (iii) a late region coding for genes L1 and L2. The three regions are separated by two polyadenylation (pA) sites for the early and late genes: early pA (A_E) and late pA (A_L) sites (Figure 1.3) (14)

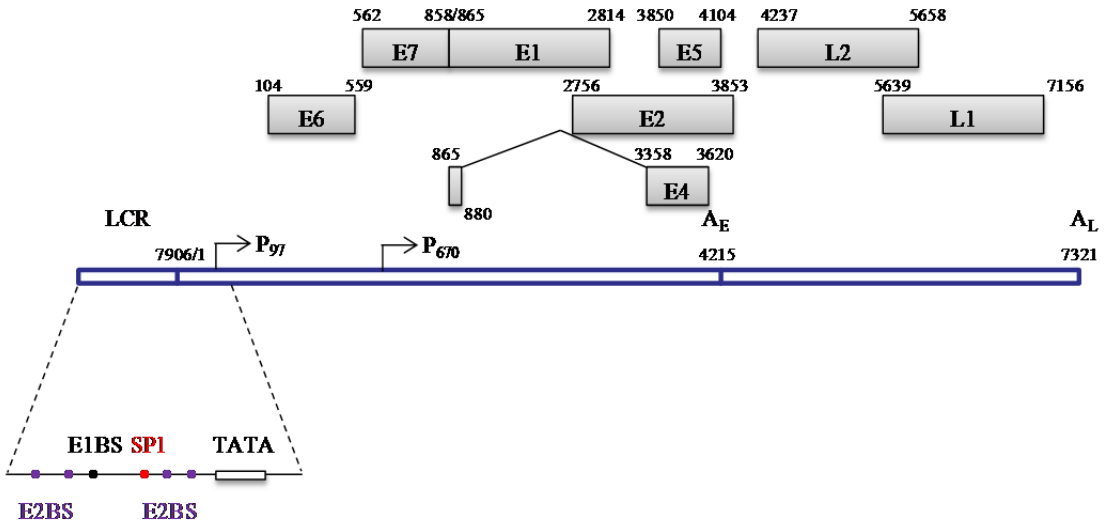

Figure 1.3: Schematic representation of HPV-16 genome. The figure shows the linear form of HPV-16 genome including the long control region (LCR), the early and the late regions. The main promoters p97 and p670 and the polyadenylation sites A_E and A_L are also shown. The ORF and the start and end sites are shown above. The LCR region is expanded below to show the four E2 binding sites (E2BS), one E1 binding site (E1BS), SP1 and TATA box. Figure recreated from reference (14).

1.2.3 Capsid structure

Studies of viral structure, infection and entry have been difficult due to the close link between differentiation epithelium and HPV lifecycle. However, in the recent years these problems were overcome by the discovery and use of virus like particles (VLPs), pseudovirions (PsV) and quasivirions (QV) (reviewed in reference (15)). VLPs are generated by transfecting plasmids expressing L1 alone or L1 and L2 proteins into *E.coli*, yeast or mammalian cells. The expression of these two proteins results in the formation of DNA free capsid particles which can be isolated by lysing the cells. PsVs are similar to VLPs but contain a reporter plasmid encased within the virion. QVs are a form of PsV with full-length recircularised viral genomes. QVs are therefore quite similar to native virions in structure and antigenicity. With the discovery of raft culture systems, which allow complete differentiation of epithelial layers, studies with native HPV virions are now possible (16,17).

HPV is a non-enveloped virus of about 52-55 nm diameter. It has a circular DNA encased in an icosahedral capsid. Two viral proteins, the major capsid protein L1 and the minor capsid protein L2 make up the capsid structure.

1.2.3.1 Capsid proteins L1 and L2

The two capsid proteins L1 and L2 interact with each other to form the capsid structure of the virus (18,19). L2 is organised into 72 pentamers called capsomeres in a T=7 lattice structure. There are 12 pentavalent and 60 hexavalent capsomeres (20). Within each capsomeres, one L2 is present stabilising the capsid structure (20). Being highly immunogenic, the L1 and L2 proteins are only expressed in the terminally differentiated cells which have limited immune surveillance (21). The capsid proteins are the first point of contact with the host cell and are involved in internalisation and nuclear transport of the virus (see Section 1.2.4).

1.2.4 Viral entry and internalisation

HPV infection occurs by binding of the virus particle to the basement membrane and the basal keratinocytes. Similar to most viruses, heparin sulphate proteoglycans (HSPGs) were the first receptors discovered as being necessary for HPV binding (21). There are three types of HSPGs: (i) syndecans, which are abundant in epithelial cells; (ii) glypicans, which are predominant in the central nervous system and (iii) secreted perlecans, abundant in extracellular matrix (ECM). Syndecan-1 which is predominantly expressed in epithelial cells and overexpressed in wound healing, is believed to be the predominant HPV receptor (22). However, as the ECM is also a primary attachment site, the secreted perlecans might also be involved. HSPG-independent infection of HPV-16 has also been shown which leads to the hypothesis that other secondary receptors might be involved. Some of these putative receptors are laminin-5 and α6-integrin (reviewed in reference (23)).

Cell surface interactions of the virus predominantly depend on the L1 capsid protein, while L2 interacts with secondary receptors (23). The first step of viral contact to the cell happens with a low-specificity binding of L1 to HSPGs which causes a conformational change in the capsid resulting in the unmasking of a specific region in the amino (N) terminus of L2, which is then cleaved by the proteinase furin. The proteolytic cleavage of L2 leads to further conformational change resulting in the binding of L2 to secondary receptors. The internalisation of HPV is a slow process compared to most viruses. Studies have shown an unusually long period of cell attachment before entry (reviewed in reference (24)). Internalisation of HPV particle occurs by endocytosis with two possible mechanisms, clathrin-mediated and caveolin-mediated (25). However, a recent study also suggests a clathrin and caveolin independent mechanism for internalisation of HPV-16 (26).

Once the virus has entered the cell, uncoating of virus occurs within the endosomes where the L1 protein is shed from the viral genome. The L2 protein is not necessary for viral uncoating however, it plays a role in removing the genome from the endosome (27). The trafficking of viral genome in the cytosol occurs along the microtubules. The L2 protein interacts with microtubules via a molecular motor protein complex called dynein to transport the viral genome towards the nucleus (28,29). L2 harbours nuclear localisation signal (NLS) which shuttles the genome into the nucleus (reviewed in reference (27)).

1.2.5 Viral replication

Most of the relevant literature available about PV replication comes from research on BPV-1 as it readily infects mouse fibroblasts. Since the mechanism of replication is highly conserved in the different members of the papillomavirus family, the results from BPV-1 can be extrapolated to HPVs.

Upon viral infection, expression of early proteins E1 and E2 initiate episomal replication. The minimum sequence required for replication is the Ori, which is located in the LCR of the genome (Figure 1.3). The Ori includes an E1 binding site (E1BS) and multiple E2 binding sites (E2BS) (30). Initiation of replication occurs by sequential assembly of replication machinery on the Ori (Figure 1.4). Initially, E2 forms a dimer and binds to the E2BS. By direct protein-protein interaction between E2 and E1, two molecules of E1 are brought together forming a hetero-tetramer of E1 and E2 (31). E1 is the viral replication factor that acts as an adenosine triphosphate (ATP) dependent helicase. Binding of E1 is not sequence-specific, but E2 maintains specificity of binding of E1. This is followed by ATP-dependent removal of E2 and addition of E1 dimer to the complex resulting in E1 homo-tetramer. In the next step, more E1 molecules are recruited to form two E1 trimers and subsequently two E1 hexamers. Each hexamer binds to one strand of DNA and separates the two strands thereby generating partial single-stranded DNA replication fork. E1 hexamers are then formed on the DNA and serve as DNA helicase. In the next step, host cell replication proteins are recruited for replication of the episome (32).

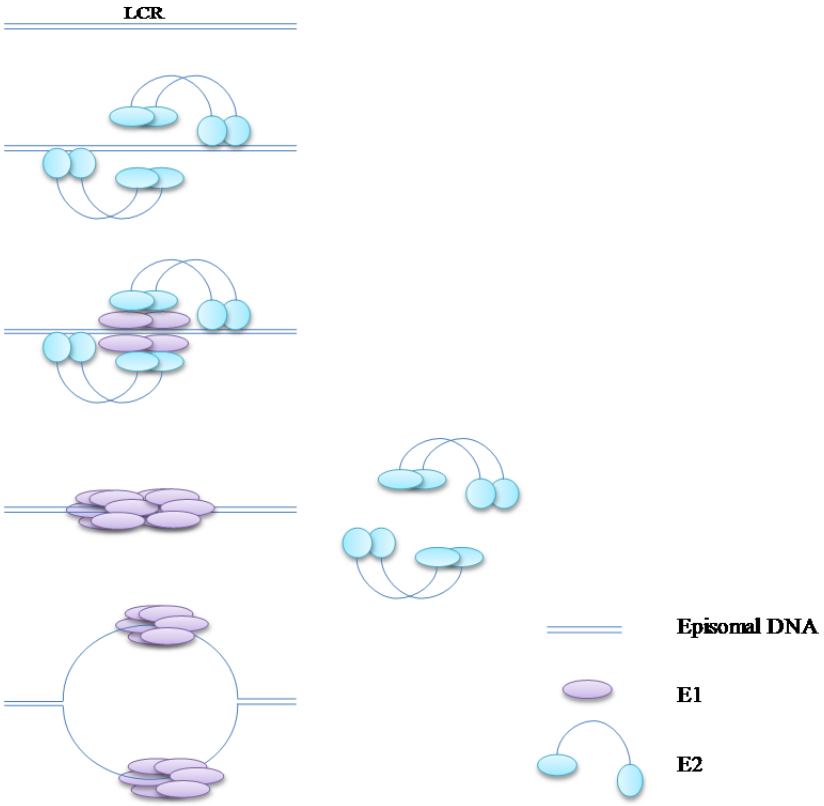

Figure 1.4: HPV episomal replication. Schematic representation of HPV episomal replication. The LCR of episome is shown with E2 (blue) and E1 (purple) proteins. E2 dimers bind to the LCR and recruit E1 followed by release of E2 and formation of E1 di-hexamer. Each hexamer binds to one strand of DNA and separates them to form a replication fork. Cellular replication machinery is then recruited for replication of the episome (not shown for simplicity). Figure recreated from reference (32).

1.2.5.1 Replication protein E1

The E1 protein is a 68 kDa nuclear phosphoprotein similar in form and function to SV40 large T antigen (33). It has ATPase and helicase activities (34) by which it is able to unwind DNA for replication. The carboxy (C) terminal region of E1 is responsible for DNA-binding, oligomerization, E2 binding, ATPase and helicase activities. E1 also binds to a number of cellular proteins and recruits them to the replication complex. Some of these interactors of E1 are listed in Figure 1.5 (35).

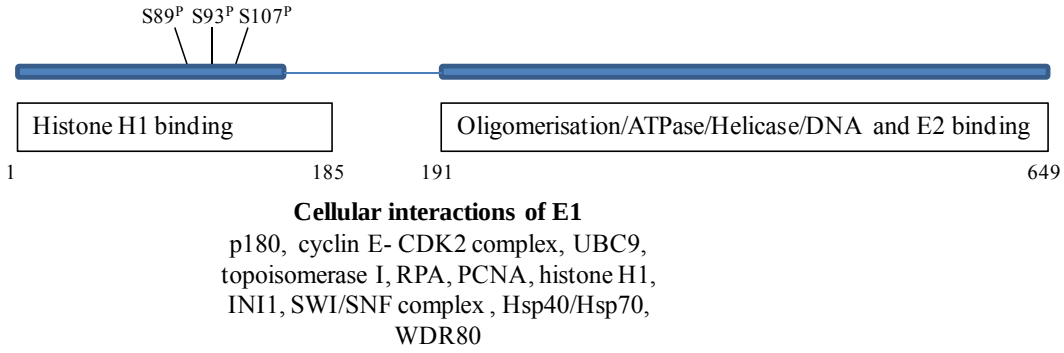

Figure 1.5: HPV E1 protein. Schematic representation of E1 protein with the N-terminus and C-terminus regions highlighted. The functions of the domains are shown below and the Serine (S) residues phosphorylated are highlighted. The cellular interacting partners of E1 are listed below. Figure recreated from reference (35).

In addition to its well characterised role in replication, E1 is involved in viral transcription and transformation. In BPV-1, E1 modulates the ability of E2 to transactivate viral promoters (36). Apart from the full-length E1, BPV1 also has a 23 kDa E1-M protein which is thought to be a transcriptional repressor (37). A similar E1-M protein has been found in HPV-11 (38). E1 also modulates the host cell cycle by its interactions with histone H1 and cyclin D1 (39,40). Mutations in E1 protein also increase the transformation and immortalisation of keratinocytes by HPV-16 (41).

1.2.6 Viral transcription

Viral transcription is tightly regulated by the differentiation stage of the host cells. Two major promoters control transcription in HPV-16. The early promoter p97 lies upstream of the E6 ORF and is responsible for early gene expression in basal cells of the epithelium. The p670 promoter lies within the E7 ORF region and is responsible for late gene expression of L1, L2 and E4 in terminally differentiated epithelial cells (42). Other minor promoters in the early regions of the genome have been described (43,44), however their activities in the context of the episomal HPV genome remains unknown.

Transcription is also regulated by regulatory cis elements present in the LCR (Figure 1.3), such as the consensus E2BS, ACC(N6)GGT by which E2, the transcriptional

activator/repressor regulates the transcription of E6 and E7. Additionally, cis elements present in the E7 ORF control the p670 promoter (43). Several transcription factor binding sites such as AP1 and SP1 are also present in the LCR (44).

The transcripts of HPV-16 do not contain any introns and viral transcripts are polycistronic undergoing extensive alternative splicing. Several mRNA transcripts coding for putatively spliced proteins have been characterised. The E1^E4 protein is a product of a spliced transcript resulting in the first five amino acids of E1 combined to E4 (45). The E2C fragment spliced to several other ORFs, E1^E2C (43), E8^E2C (46). Apart from these, some new splice positions of E6, E7 and E4 have also been identified, generating ORFs denoted as E4*, E6* and E7* (43). However, the role of many of these new transcripts and proteins are still unknown.

1.2.6.1 Transcriptional regulator protein E2

The E2 protein is the major transactivator of viral gene expression. It has an N-terminal transactivation domain of about 200 amino acids and a C-terminal DNA-binding and dimerisation domain of about 90 amino acids. The two domains are highly conserved between species and are joined by a variable linker (47). In BPV-1, three forms of E2 have been identified, the 48 kDa full-length E2 protein, which is a potent transcriptional activator and two other C-terminal forms, E2-TR and E8^E2 which act as transcriptional repressors. In some HPV types such as HPV -1, -11, -16, -31 and -33, a E8^E2C form of the protein is found which contains the C-terminal domain of E2 fused to the E8 ORF. This protein is a strong repressor of viral transcription via the p97 promoter and a regulator of viral replication which can be attributed to its interactions with cellular corepressor molecules such as TRIM28 (48) and NCoR1 (49).

.

The E2 protein activates transcription by binding to the E2BS in the LCR region and its interactions with cellular transcription factors such as AMF-1 (also called G-protein pathway suppressor 2 or GPS2) (50) and HNAP1 (51). However, it is also capable of

repressing transcription of the viral oncogenes E6 and E7 (52) and late genes (53). Another known function of E2 is its role in plasmid segregation by tethering the episome to mitotic chromosomes by its interaction with BRD4 (54), ChIR1 (55) and TopBP1 (56,57). E2 is intrinsically pro-apoptotic through its interactions with p53 (58) and caspase 8 (59) and overexpression of E2 in HPV transformed or untransformed cell lines causes abrogation of the cell cycle.

1.2.7 Encapsidation and release of virus

While replication and transcription of the virus is tightly regulated in the basal layer of epithelium, in the upper layers vegetative replication occurs. In the uppermost layer, formation of capsid and encapsidation of viral genome occurs followed by release of viral particles (9).

1.2.7.1 The E4 protein

The E4 protein is the most abundantly expressed viral protein (60). It is a late protein which accumulates in the cytoplasm in low-grade cervical neoplasia where vegetative viral replication occurs. Two new spliced forms in HPV-18, E2^E4C and E2^E4L (61) and one in HPV-16 E1^E4* have been identified (43) .

Being expressed in terminally differentiated cells of epithelium, E1^E4 plays a role in making the cell unstable and conducive for viral release (62). With its C-terminus, it can oligomerise to form filamentous networks (63). The N-terminus of E1^E4 can bind to the cytokeratin network by its interaction with keratin-18 (64–66). The multimers of E1^E4 are then cleaved by the protein calpain causing the collapse of cytokeratin network (67). Once the cytokeratin is disrupted, E1^E4 associates with the mitochondria causing a reduction in membrane potential leading the cell into apoptosis which supports the release of virus particles (62).

Apart from its function in terminally differentiated cells, overexpression of E1^E4 causes G2 arrest in cervical cancer cell lines HeLa and SiHa. This function has been localised to a proline-rich region between amino acids 17 and 45 which contains a NLS, a cyclin-binding motif, and a CDK phosphorylation site (68). Additionally, interaction of HPV-1 E1^E4 with other cellular factors such as Wee1 also aid in this function (69).

1.2.8 Cellular transformation

While most HPV infections are cleared within two years (10), in some cases it leads to cellular transformation and neoplasia (Figure 1.2). The oncoproteins E5, E6 and E7 are responsible for the necessary changes within a cell.

1.2.8.1 Transforming protein E7

The E7 oncoprotein of HPV plays a central role in the transformation and immortalisation of cells with co-operation from E6. It is a small protein made of 98 amino acids and shares structural and functional similarities with two viral oncoproteins, SV40 large T antigen and adenovirus E1A (70). Based on these similarities, the sequence of E7 is divided into three conserved regions CRI, CRII and CRIII (42) (Figure 1.6).

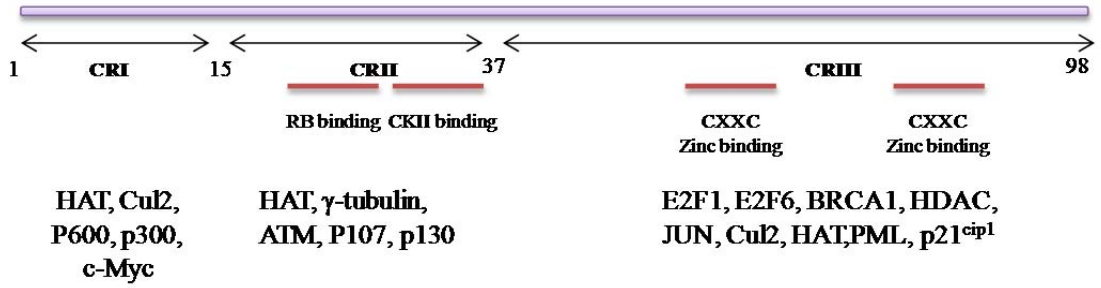

Figure 1.6: Schematic representation of E7 oncoprotein structure and functions. The length of E7 protein and the three conserved domains are shown above and the domains responsible for major functions of E7 such as binding to RB, CKII and the zinc-binding motifs are shown below. Protein interactions of the different domains of E7 are listed below. Figure recreated from reference (71).

One of the main functions of E7 is its binding and inactivation of pocket proteins RB, p107 and p130. RB is a cell cycle regulator implicated in most major cancers (reviewed in (72,73)). In G0 and early G1 phases of cell cycle, RB binds to and inactivates the E2F family of transcription factors that are necessary for the transcription of genes responsible for S-phase progression. During late G1, RB is phosphorylated by cyclin-dependent kinases (CDKs) and hyperphosphorylated RB releases E2F. The continuous expression of E2F responsive genes leads to uncontrolled cell division. Protein phosphatase PP1c acts by competing with CDKs to dephosphorylate RB in order to maintain control over cell cycle (74). In many cancers, RB is degraded by ubiquitination or maintained in hyperphoshorylated state for continued cell cycle progression (73). Regulation of RB by HPV E7 protein is a key factor in HPV infection. E7 binds to RB and releases E2F for constitutive expression of S-phase genes. E7 also mediates proteosomal degradation of RB (9) resulting in constitutive expression of E2F responsive genes and therefore continued proliferation. The LxCxE domain in the CRII domain and additional amino acids in the CRIII domain are necessary for E7 interaction with RB (75–77). Apart from its action via RB, E7 also directly interacts with E2F proteins and activates transcription of its downstream genes (78). Therefore, by its action through RB and E2F it maintains the cell in a continuous proliferative phase which is advantageous for the viral episomal replication and propogation. However another result of this excessive amount of cell proliferation is the progession towards immortalisation and neoplasia.

E7 targets a range of other proteins apart from RB, to induce a state of proliferation and transformation of the cell. Some of these interactions are highlighted in Figure 1.7. Of particular interest is its interaction with CDK inhibitors such as p21. p21 binds to the CDK–cyclin complex and to proliferation cell nuclear antigen (PCNA) and acts a cell cycle check point at G1. E7 interacts with p21 and prevents its functions thereby leading to continued progression through cell cycle which is also suggested to be a mechanism necessary for HPV episomal replication (79). The CRIII region of E7 has

two zinc-binding motifs CxxC which are necessary for metal-binding and for interaction of HPV with several cellular target proteins including MYC, a transcription factor that regulates cell proliferation (reviewed in (80)).

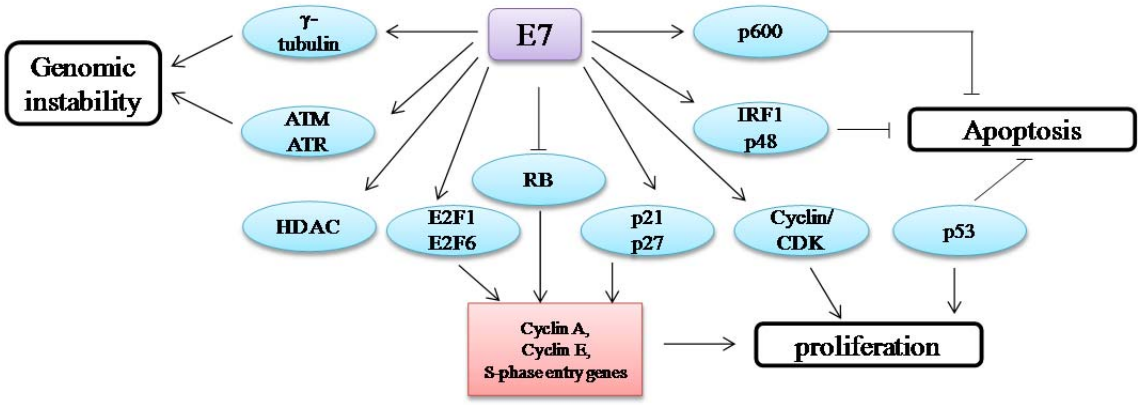

Figure 1.7: Schematic representation of the protein interactions and the pathways affected by E7. Proteins that E7 interacts with (blue) and transcriptionally activates (red) and the pathways that are implicated (black rectangles) by E7 are indicated. Figure recreated from reference (9).

1.2.8.2 Transforming protein E6

The E6 protein is one of the major oncogenes of the virus which causes inhibition of DNA damage-induced apoptosis. The degradation of RB by E7 and increased cell proliferation induces a p53 dependent DNA damage response in cells which is controlled by E6 (81). P53 is a tumour suppressor protein which is activated in response to DNA damage. Upon activation, it transcriptionally activates genes required for apoptosis and cell cycle arrest (82). In HPV infected cells, the activity of p53 is controlled by E6. E6 causes ubiquitin-mediated proteolysis of p53 through its interaction with the ubiquitin ligase E6-associated protein (E6AP) (83). This activity is specific to high-risk HPVs, whereas in low-risk HPVs, even though the E6 protein can bind to E6AP, this does not result in p53 degradation suggesting that additional mechanisms might be involved (9). E6 also induces self-ubiquitination of E6AP. This activity is retained by an E6 mutant that is unable to degrade p53 but capable of

immortalising epithelial cells, which indicates this is a necessary mechanism for immortalisation (84).

Additionally, E6 interferes with p53 activity by binding directly to it and interfering with its DNA-binding and transcriptional activity. The affinity of this interaction and inhibition of DNA-binding is higher in high-risk compared to low-risk HPV types (85). E6 also blocks the activity of histone acetyl transferases which stabilise p53 such as p300, CREB binding protein (CBP) and ADA3 (9).

Apart from its major role in p53 degradation, several additional mechanisms of immortalisation of cells by E6 have been reported. E6 binds to cellular PDZ domain containing proteins through a unique motif present in high-risk HPVs and acts as a bridge between them and E6AP, leading to their degradation. Several PDZ domain containing proteins are implicated as tumour suppressors and their degradation aids in blocking apoptosis by E6. Among the PDZ domain containing proteins degraded by E6 are human homologue of Drosphila scribble (hScrib), human homologue of Drosphila disc large (hDIg) and MAGI-1,2,3 (86,87).

E6 upregulates human telomerase (hTERT) and maintains telomere length which is a characteristic of most cancers (88). E6 does this by three possible mechanism: (i) by binding to activators of hTERT transcription factors such as MYC, MAX, SP1 and histone acetyltransferases and increasing transcriptional activation; (ii) degrading transcriptional repressors of hTERT, NFX1 via E6-AP; (iii) by interacting with NFX123 to increase hTERT levels through transcriptional and post-transcriptional mechanisms (89). Some of the protein interactions and functions of E6 oncoprotein are indicated in Figure 1.8.

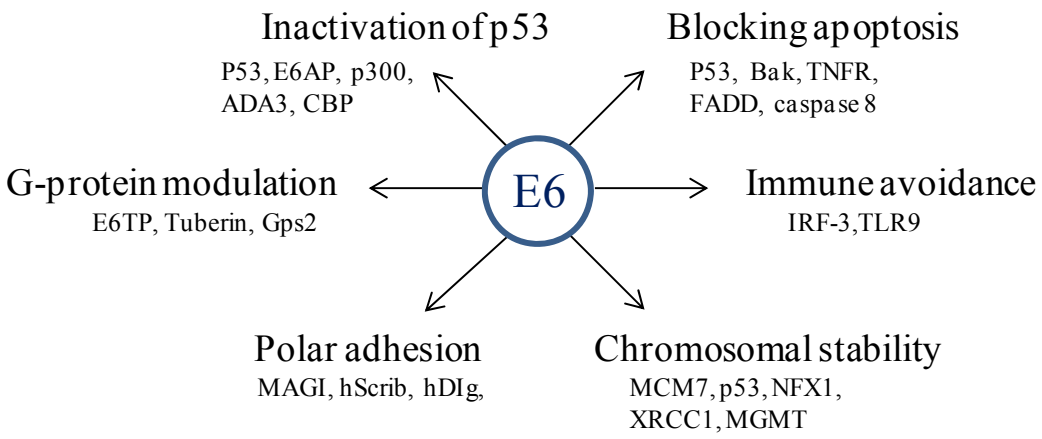

Figure 1.8: E6 cellular interactions. The multiple functions of E6 are represented in the figure. The proteins that E6 interacts with in order to mediate the given cellular responses are listed below. Figure recreated from reference (89).

1.2.8.3 Transforming protein E5

The E5 protein of HPVs is the third oncoprotein of the virus. It is a small hydrophobic membrane bound protein predominantly located in the endoplasmic reticulum (ER), golgi apparatus, endosomes and the nuclear membrane (90).

HPV-16 E5 causes transformation and increased growth in the presence of epithelial growth factor (EGF) and platelet derived growth factor (PDGF) receptors (91). E5 mediates signalling through EGFR and also enhances mitogen-activated protein kinase (MAPK) signalling pathway in cells independent of EGFR through ERK1/2 (92). E5 is also reported to activate ET-1/ETA receptor signalling (93). E5 suppresses the transcription of tumour suppressor p21 and increases expression of JUN and FOS (94,95). It also causes disruption of MHCII molecules (96,97). Several new host interactions of E5 have been discovered recently, such as BAP31 (98), karyopherin beta-3 , EVER and ZNT-1 (99) whose role in transformation are not yet clear.

1.2.9 Immune evasion

HPV is a very successful pathogen and it has evolved several mechanisms of immune evasion. The virus infects epithelial cells which have a differentiating lifecycle. By tightly synchronising its life cycle with that of differentiating epithelium and by generating virions in the topmost layer of the epithelium , the virus is able to evade an immune response to a great extent (100). HPV infection results in very low load of viral proteins, viremia and no inflammation or cell death (101). Therefore there is very little release of proinflammatory cytokines (100). A recent genome wide expression analysis study has shown that HPV actively downregulated a range of proinflammatory and chemotactic cytokines and antigen presenting cells (102). The antigen presenting cells in keratinocytes, Langerhans cells are shown to be reduced in cells infected with HPV from the alpha, gamma and mu but not beta genera (103). Another study has shown that HPV-8 causes a reduction in Langerhans cells possibly mediated by the loss of CCL20 (104,105). The viral oncoproteins E6 and E7 are able to disrupt the interferon signalling pathway particularly the Type 1 interferons which have antiviral and antiproliferative properties (106). The E6 protein inhibits IRF-3 activity (107) and E7 abrogates IFN-α induced signalling (108). Additionally, E5 causes disruption of MHC class II molecules (96,97). While most HPV infections are cleared with time, there is limited knowledge about its mechanism. There is evidence to suggest that in the naturally regressing anogenital warts, there is an infiltration of CD4+ and CD8+ T cells. Macrophages and expression of Th1 cytokines (109). However, about 10-20 % of the infected individuals lead on to have persistent infection with a high risk on progression in to cervical intraepithelial neoplasia (110).

1.3 HPV and human disease

1.3.1 Benign warts and lesions

HPVs are epitheliotropic viruses which cause several types of warts in different parts of the body (Table 1.1). Among the cutaneous HPVs, low-risk types -1 and -2 cause common warts in the skin such as flat warts and papillomas while high-risk cutaneous types such as types -5 and -8 are associated with epidermodysplasia verruciformis (EV) specific lesions. EV is a rare autosomal recessive disorder which increases susceptibility to certain HPV types. Infection with HPVs in these patients cause macules on the skin of the patients and can lead to squamous cell carcinoma (111). Mucosal HPVs infect the mucosal membranes of respiratory and genital regions. Genital HPVs are the most clinically relevant types. Low–risk mucosal HPVs cause warts in the genital skin and mucosa including the vulva, penis, scrotum, vaginal tract, cervix, and anal canal (42). High-risk mucosal HPVs are associated with causing cancer and CIN (8).

Classification	HPV types	Associated conditions
High-risk mucosal types	16,18,31,33,35,39, 45,51,52,56,58,59, 68, 73,82	Anogenital cancers, Oropharyngeal cancer (HPV-16 primarily)
Low risk mucosal types	6,11	Genital warts, recurrent respiratory papilloma, conjuctival papilloma
High-risk cutaneous types	5, 8	EV specific lesions , squamous cell carcinoma of the skin
Low-risk cutaneous types	1,2	Skin warts and papillomas

Table 1.1: Clinical manifestations of HPV types. The classification of HPV types and clinical associations of some or all of the HPV types are listed. Table is modified from reference (42).

1.3.2 HPVs and cancer

HPVs are associated with tumorigenesis and cancers. Cervical cancer is the most clinically significant cancer caused by HPV where persistent infection with high-risk HPVs is the necessary etiological factor (112). Other cancers associated with HPVs are skin cancers (reviewed in (113) and (114)), vulvar cancer (reviewed in (115)), anal cancer (116). There is also increasing evidence that HPV is associated with head and neck cancers particularly in the oropharynx and tonsillar regions (reviewed in (117)).

Cervical cancer is the most common cancer of women in developing countries and the second most common cancer in women worldwide. About 510,000 cases are reported each year (6). Over 99 % of cervical lesions contain DNA from one or many of the 15 types of high-risk HPVs with 70 % cases attributed to HPV-16 and HPV-18 (112)(118).

Most cancers occur by HPV infection in the transformation zone of the cervix, which is the region adjacent to the endo and exocervix. About 85 % of the cancers are of squamous cell origin, while the remaining are mainly adenocarcinomas, with a small number of cases being cell neuroendocrine tumors (119). Persistent infection of HPV causes dysplasia. The degree of dysplasia is determined by the amount of squamous epithelium replaced by continuously proliferating basal cells (Table 1.2). Papanicolaou (Pap) smear test is a standard test to identify the dysplastic cells (120).

Condition	Cytology	Histology
Normal	Normal	Normal
Mild dysplasia	LSIL	CIN 1
Moderate dysplasia	HSIL	CIN 2
Severe dysplasia	HSIL	CIN 3
In situ carcinoma	HSIL	CIN 3
Invasive carcinoma	HSIL	CIN 3

Table 1.2: Stages of cervical cancer. The dysplastic changes in the cell due to HPV infection and the cytological and histological staging of cervical cancer. LSIL- Low-grade squamous intraepithelial lesion, HSIL- High-grade squamous intraepithelial lesion, CIN- cervical intraepithelial neoplasia.

1.4 Risk factors for cervical cancer

Although persistent infection with high-risk HPV types is a necessary etiological factor for development of cervical cancer, several other factors are known to play a role in progression. Low age at first intercourse, high number of sexual partners, low age at the time of bearing children, high number of children (121), smoking (122) and long term use of hormonal contraceptives (123) increase the risk of cervical cancer.

In addition, there is evidence to show that co-infection with Chlamydia (124) or certain herpesviruses such as herpes simplex virus (HSV), cytomegalovirus (CMV) and Epstein-Barr virus (EBV) (125) are additional contributing factors, however their role is not well established. HSV-2 was believed to be the causative organism of cervical cancer as early as the 1970s (reviewed in reference (126)). Primary evidence came from sero-epidemiologic studies detecting HSV-2 DNA and HSV-2 specific antibodies (127) in cervical lesions. *In-vitro* studies have shown the transforming ability of inactivated HSV-2 in rat embryo cells (129) and of the *Bgl*II fragment of HSV-2 in NIH3T3 cells (130). More recently, there is evidence suggesting that HSV-1 might act as co-factor in

cervical cancer (131). It was now believed that HSV might be necessary to initiate carcinoma and HPV to maintain the transformed state (132).

1.5 Prevention and therapy

Two preventative vaccines Cervarix (Merck and Co) and Gardasil (Glaxosmithkline) have been approved for use against HPV infection and cervical cancer. These vaccines contain VLPs formed with L1 from different types of HPV and offer protection against these genotypes. Cervarix is a bivalent vaccine with protection against HPV-16 and -18 and Gardasil is quadrivalent with protection against types -6, -11, -16 and -18. Since more than 15 different high-risk HPV types are shown to be responsible for cervical cancer, vaccination against types -16 and -18 can potentially only prevent 71 % of cervical cancers worldwide, with higher percentage in Asia and Europe/North America (133). However, a vaccine containing at least seven most common HPV types would be necessary to prevent about 87 % of cervical cancers worldwide (133). The future of preventative vaccines is in creating cost effective vaccines conferring resistance against as many HPV types as possible.

Therapeutic targets for HPV and cervical cancer are concentrated towards E6 and E7 which are the most important oncogenes. Strategies under current research involve live vector, DNA, RNA, peptide and protein based targets (reviewed in (134)).

1.6 Summary of thesis

1.6.1 Hypothesis

Human papillomavirus- 16 is a medically important oncovirus. The use of preventative vaccines and early detection systems using pap smears have considerably reduced the burden of this virus-induced cervical cancer. But our basic understanding about the viral life cycle remains far from complete. One of the ways to improve our knowledge

about viral protein functions is to investigate its protein interactions. The hypothesis behind this PhD project is that a genome wide interactome study of the virus will provide valuable insights into the understanding of the virus. In order to address this issue, three main research questions were developed.

1. Are there any undiscovered interactions between the proteins of HPV-16?
2. Are there any direct protein interactions between HPV-16 and HSV-1?
3. Can a genome-wide interactome study of HPV-16 with human library provide us with novel interacting partners that can be targeted as biomarkers, therapeutics and for better disease management?

In order to address these research questions, a systematic analysis of protein interactions of the virus was performed using two high-throughput protein-protein interaction assays described below: (i) Yeast two-hybrid (Y2H) and LUminiscence-based Mammalian IntERactome assay (LUMIER) assays.

1.6.2 Research Techniques

1.6.2.1 The yeast two-hybrid system

The yeast two-hybrid (Y2H) system is a well-established technique for the detection of protein-protein interactions. Since it was first described using the GAL4 transcription factor for yeast *S.cerevisiea* (135), it has proved to be effective in identifying many interactions in biological systems. The system exploits the fact that the transcription factor GAL4 is composed of two domains, a DNA-binding domain (DBD) and an activation domain (AD) which are capable of initiating transcription provided they are in close proximity (135). In order to identify interactions between two proteins 'X' and 'Y' in the Y2H system, two hybrid proteins are generated; (i) the DBD fused to a protein 'X' (known as the bait protein); and (ii) the AD fused to a protein 'Y' (known as the prey protein). When the two fusion proteins are expressed in yeast, if X and Y

interact, the DBD and AD are brought in close proximity leading to the transcription of reporter genes under the regulation of an up-stream activation sequence (UAS) (Figure 1.9). The histidine (HIS) reporter gene used in this system allows the growth of yeast in medium lacking histidine. Another reporter MEL1, which encodes α-galactosidase causes breakdown of X-α-gal and can be used for semi-quantitative analysis of interactions.

Y2H can be used either to detect direct binary protein interactions between X and Y proteins or to screen a bait protein with a library of prey proteins. Direct interactions provide a quick and easy method to detect and verify interactions between two proteins. One of the applications of direct interactions is the ability to map the interaction binding sites of the proteins using deletion mutants and domains of proteins. This has previously been successfully used to identify binding domains of several interactions including HPV E1-E2 (31) and the dimerization of E7 (136). Also of importance is that semi-quantitative measurements can be made to calculate binding affinities of interactions (137). Library screens are able to identify new interaction partners of a protein. They can be performed as high-throughput experiments and provide extensive interactome data. The prey library can consist of full-length cDNAs or domains of proteins. It has been seen that individual domains interact better in Y2H which can be explained by the fact that protein domains fold independently of each other (138).

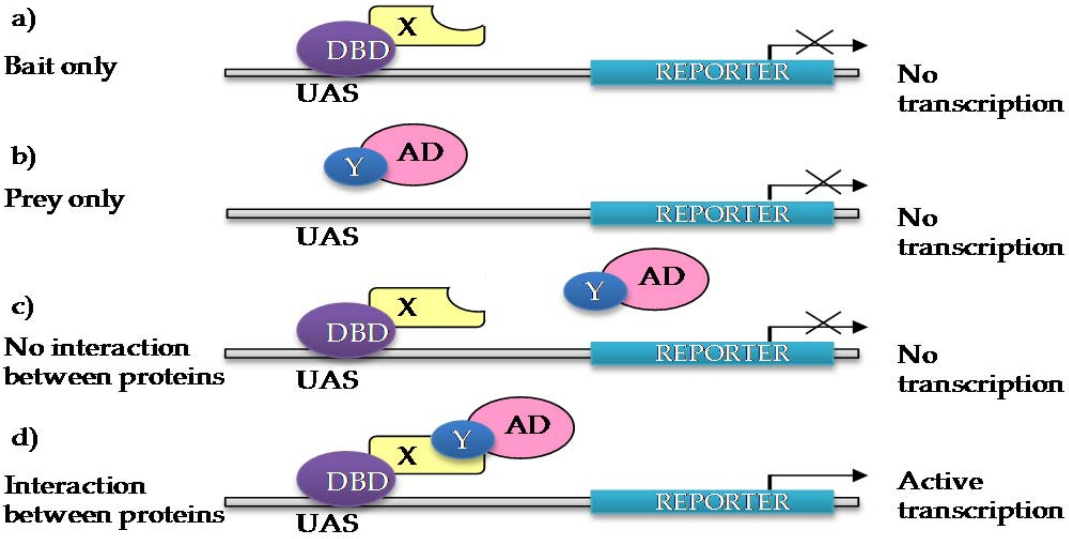

Figure 1.9: Schematic representation of Y2H system. The figure schematically illustrates the Y2H system. To test for an interaction between proteins X and Y, two fusion proteins are expressed in yeast, one with DNA-binding domain (DBD) of GAL4 (bait) and one with activation domain (AD) of GAL4 (prey). The DBD interacts with the upstream activation sequence (UAS). Transcription of the reporter gene depends on the two domains being in close proximity. In case of presence of bait or prey alone or if there is no interaction between the two (a, b, c), no reporter activation is seen. If the proteins X and Y interact, the DBD and AD are brought together and the reporter is expressed (d). Figure adapted and redrawn from ref (135).

Like most assays, Y2H has its own advantages and shortcomings. The popularity of the technique and the large amount of data that has been generated in the last two decades shows that the advantages irrefutably outweigh the limitations. Approximately 6000 human interactions have been identified to date using Y2H (137). Some of the key factors used in Y2H, their advantages, disadvantages and how these disadvantages are overcome are listed in Table 1.3. One of the concerns about the Y2H system is its high rate of false positives, which necessitates the validation of interactions, identified using other biochemical assays.

	Advantages	Disadvantages	Methods to overcome disadvantages
Performed in Yeast	*In-vivo* technique provides better biologically relevant data than *in-vitro* binding assays.	No post-translational modifications such as glycosylation, phosphorylation and formation of disulphide bridges as in higher eukaryotes	Co-transfection of genes expressing enzymes or addition of enzymes necessary for the post-translational modifications.
Use of GAL4 transcription system	Easy, inexpensive and quick. Identifies weak and transient interactions	Auto-activation of GAL4 transcription leading to false positives A third intermediate protein can be responsible for activation	Use of competitive inhibitor such as 3-AT Testing activity with empty plasmids as control
cDNA expression of fusion proteins	Use of fusion tags makes it an inexpensive, reliable and quick assay. Allows for use of two forms of fusion proteins (as baits with BD fusion and as preys with AD fusion)	Possible change in conformation of protein. High rate of false negatives Interactions may only occur in one direction (protein X as bait and Y as prey and vice versa)	Verify the confirmation by testing for known interactions Use of domains instead of full-length proteins Test interactions in both directions
Overexpression and nuclear localization of proteins	Identifies weak and transcient interactions	Changing subcellular localization of proteins within cell by artificial expression High rate of false positives	Validation of interaction by other biochemical assays
Semi-quantitative method	Useful in comparing affinities and mapping of interaction domains of interactions by mutagenesis		

Table 1.3: Y2H advantages and disadvantages. The key factors used in Y2H and their advantages and disadvantages are listed. Methods generally used to overcome any disadvantages are also listed (137)(138).

1.6.2.2 The LUMIER pull-down assay

LUminiscence-based Mammalian IntERactome assay was first described as a high-throughput PPI detection technique (139). The LUMIER assay is a variation of co-immunoprecipitation (co-IP) technique using luciferase readout. In order to detect interaction between two proteins X and Y, fusion proteins are generated, with protein X fused to a Protein A tag which can be immunoprecipitated (IP) by immunoglobin G (IgG) coated magnetic beads and protein Y is fused to a luciferase tag. Plasmids expressing both proteins are transfected into mammalian cells and whole cell lysate is used to immunoprecipate protein X. If the two proteins interact, the Y protein is co-immunoprecipitated and the luciferase signal is detected, if they do not interact, no luciferase signal is detected (Figure 1.10).

The LUMIER assay has several advantages over co-immunoprecipitation assays. It is highly sensitive and can be performed with small amounts of DNA and in high-throughput 96- or 384-well formats. It has been shown to have higher assay sensitivity of 36 % as compared to the Y2H assay with 25 % and other high-throughput assays such as mammalian protein-protein interactions trap (MAPPIT), protein complementation assay (PCA) and nucleic acid programmable protein array (NAPPA) in a comparative study (140).

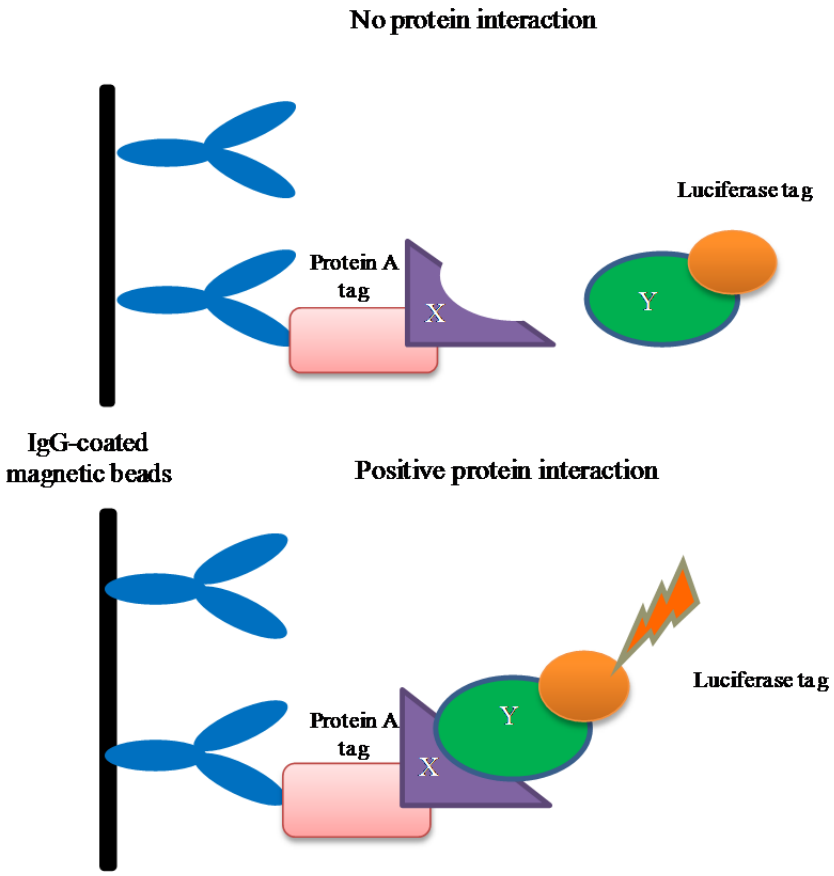

Figure 1.10: Schematic representation of LUMIER assay. To detect interaction between two proteins X and Y, fusion proteins with X fused to Protein A tag which is immunoprecipitated (IP) by IgG coated magnetic beads and protein Y is fused to a luciferase tag. After extensive washing, luciferase readout is measured. If X and Y do not interact, no luciferase signal is measured but if they interact, the Y protein is co-immunoprecipitated and luciferase signal is

Chapter 2:

Materials and methods

2.1 Materials

2.1.1 Reagents and Chemicals

Plasmids:

	Vector name	Feature	Source
1	pDONR207	Gateway® Donor vector	Invitrogen
2	pDONR223	Gateway® Donor vector	Invitrogen
3	pGADT7	Y2H prey	Clontech
4	pGBKT7	Y2H bait	Clontech
5	pCR3	Mammalian expression vector	Invitrogen
6	pCR3-N-MYC	N-terminal MYC tag	Invitrogen
7	pCR3-N-HA-dest	N-terminal HA tag	Invitrogen
8	pTREX-DEST30-PrA	N-terminal protein A fusion protein for LUMIER assay	DKFZ, Heidelberg
9	pcDNA3-RL-GW	N-terminal Renilla luciferase fusion protein for LUMIER assay	DKFZ, Heidelberg
10	p16OriM	Plasmid containing HPV-16 origin of replication	Iain Morgan, University of Glasgow (144)
11	pCMV-E1	pCMV plasmid with full-length HPV-16 E1	Iain Morgan, University of Glasgow (145)
12	pCMV-E2	pCMV plasmid with full-length HPV-16 E2	Iain Morgan, University of Glasgow (145)
13	pBR322-HPV-16	pBR322 with full-length HPV-16 genome cloned into *Bam*HI site	NIBSC, UK
14	pBR322-HPV-18	pBR322 with full-length HPV-18 genome cloned into *Bam*HI site	NIBSC, UK
15	pBabepuro E7 C24G	N-terminal Flag tag HPV-16 E7 mutant C24G	Andrew MacDonald, University of Leeds (146)
16	pGL3PCNA	Promoter region of PCNA (-560 to +60) cloned into pGL3 plasmid via *Nhe*I and *Xho*I restriction sites	Dr Georg Malterer, Max von Pettenkofer Institut

Table 2.1: List of plasmids used in this study. All the plasmids used in this study and their features and source are listed above.

Bacterial and yeast strains:

Electrocompetent *Escherichia coli* DH10β (Invitrogen)

Electrocompetent *Escherichia coli* 2T1R (Invitrogen)

Chemically competent *Escherichia coli* DH10β (Invitrogen)

AH109– *Saccharomyces cerevisea* mating type a

Y187- *Saccharomyces cerevisea* mating type α

Molecular weight markers:

GeneRuler™ DNA 1 kb ladder (MBI Fermentas)

GeneRuler™ DNA 100 bp ladder (MBI Fermentas)

Pageruler™ prestained protein Ladder (Thermoscientific)

DNA dyes:

6x DNA loading dye (MBI Fermentas)

SYBR® Safe DNA gel stain (Invitrogen)

Enzymes:

Gateway® LR clonase II enzyme mixture (Invitrogen)

Gateway® BP clonase II enzyme mixture (Invitrogen)

Restriction enzymes (NEB): *Bam*HI, *Ban*II, *Eco*RI, *Eco*RV, *Xho*I, *Xba*I, *Nhe*I, *Dpn*I, *Exo*III

Ribonuclease A (Sigma Aldrich®)

DNA oligos:

Primers and oligos were ordered from Metabion, Germany

DNA polymerase:

Expand Long Template PCR System (Roche diagnostics)

KOD DNA polymerase (Novagen)

BioMix™ red Taq polymerase (Bioline)

NEB Taq polymerase

Deoxynucleoside triphosphate:

10 mM each of dATP, dCTP, dGTP, and dTTP (Roche diagnostics)

DNA Probes:

Probes were obtained from mouse universal probe library (UPL) (Roche Diagnostics)

Antibodies:

Antibody	Supplier
Anti-HA high affinity, rat monoclonal, clone 3F10	Roche Diagnostics Cat# 11867423001
Anti-c-MYC, mouse monoclonal antibody, clone 9E11	Santa Cruz Biotechnology Cat# SC-47694
Anti-β-actin, rabbit monoclonal antibody, clone 13E5	Cell Signalling Cat# 5125
Anti-SPZ1 rabbit polyclonal antibody	Proteintech Cat# 18931-1-AP
Goat anti-mouse peroxidase coupled	Jackson Immunoresearch Cat# 115035062
Goat anti-rat peroxidase coupled	Jackson Immunoresearch Cat# 112005175
Goat anti-rabbit peroxidase coupled	Cell signalling Cat#7074
Alexa fluor®488 goat anti-mouse IgG	Invitrogen Cat# A-11001
Alexa fluor®594 goat anti-rat IgG	Invitrogen Cat# A-11007
Alexa Fluor® 680 goat anti-rabbit IgG	Invitrogen Cat# A-21109
Rabbit mAb IgG isotype control	Cell signalling Cat# 3900S
Rat IgG2a isotype control	Invitrogen Cat# R2A00

Table 2.2: List of antibodies used in this study.

Amino Acid supplement for yeast

Tryptophan (Sigma Aldrich®)- 20 mg/L

Leucine (Sigma Aldrich®)- 0.1 g/L

Antibiotics (Sigma-Aldrich®)

Ampicillin- 100 μg/ml,

Kanamycin- 50 μg/ml,

Gentamycin- 15 μg/ml

Yeast prey libraries

Mate and plate human testis library (Clontech)

Mate and plate mammalian gene collection library (Clontech)

Mate and plate lymph library (Clontech)

HSV-1 prey library (library of full-length and fragments of HSV-1 genes (141) (Appendix 2)

Transfection reagents

Lipofectamine 2000 (Invitrogen)

Lipofectamine LTX (Invitrogen)

Effectene (Qiagen)

Prolong Gold Anti-fade reagent with DAPI (Invitrogen)

Protein G Sepharose 4 Fast Flow (GE Healthcare)

2.1.2 Media, buffers and solutions

Media

2YT	1.6 % Bacto-tryptone (Difco®), 1 % yeast extract (Difco®), 0.5 % Sodium chloride (NaCl)
LB broth	1 % Bacto-tryptone (Difco®), 0.5 % yeast extract (Difco®), 1 % Sodium chloride (NaCl)
LB agar	LB broth, 1.5 % agar (Fluka®)
SD-LW	2.67 % minimal SD base (Clontech®) , 0.064 % –Leucine –Tryptophan drop-out supplement (Clontech®)
SD-LWH	2.67 % minimal SD base (Clontech®), 0.064 % –Leucine–Tryptophan–Histidine drop-out supplement (Clontech®)
YPD	2 % (w/v) Bacto-peptone (Difco®), 1 % (w/v) yeast extract (Difco®), 2 % glucose (Sigma Aldrich®)
YPDA	YPD medium, 0.002 % (w/v) adenine hemisulphate (Sigma Aldrich®)
YPD agar	YPD medium, 1.5 % (w/v) agar

Table 2.3: Recipes for bacterial and yeast media.

Cell line	Media
HEK293	DMEM (Lonza)/ 10 % FCS (Gibco)/ 1 % Penicillin/streptomycin (Lonza)
HEK293T	DMEM (Lonza)/ 10 % FCS (Gibco)/ 1 % Penicillin/streptomycin (Lonza)
HeLa	DMEM (Lonza)/ 10 % FCS (Gibco)/1 % Penicillin/streptomycin (Lonza)
SiHa	EMEM (Lonza)/ 2 mM L-glutamine (Lonza)/ 10 % FCS (Gibco)/ 1 % Penicillin/streptomycin (Lonza)
CaSki	RPMI-1640 (Lonza)/ 2 mM L-glutamine/ 10 % FCS (Gibco)/ 1 % Penicillin/streptomycin (Lonza)
BHK-21	EMEM (Lonza)/ 10 % FCS (Gibco)/ 1 % Penicillin/streptomycin (Lonza)
Cos7	DMEM (Lonza)/ 10 % FCS (Gibco)/1 % Penicillin/streptomycin (Lonza)

Table 2.4: Mammalian cell lines and media. The cell lines used in this study and their media and supplements are listed above.

Buffers

1x TAE: 0.04 M tris–acetate, 0.001 M EDTA, 5.7 % glacial acetic acid.

2x HBS: 50 mM HEPES, 10 mM KCl, 12 mM dextrose, 280 mM NaCl,1.5 mM Na_2PO_4, pH 7.05.

Alkaline lysis extraction Solution I: 50 mM glucose, 25 mM tris-Cl (pH 8.0) and 10 mM EDTA (pH 8.0), 100 μg/ml RNAse just before use.

Alkaline lysis extraction Solution II: 0.2 N sodium hydroxide and 1 % SDS.

Alkaline lysis extraction Solution III: 3 M potassium acetate and 11.5 % glacial acetic acid.

Yeast cracking buffer 1x stock: 8 M Urea, 5 % SDS, 40 mM tris-HCl (pH6.8),0.1 mM EDTA, 0.4 mg/ml Bromophenol blue

Yeast complete cracking buffer (for 1.13 ml): 1 ml Yeast cracking buffer 1x stock, 10 μlβ-mercaptoethanol, cOmplete inhibitor tablets (Roche, UK) (40 μl of stock – 1 tablet in 2 ml water) and phosStop (Roche, UK) (100 μl of stock – 1 tablet in 1 ml water)

Renilla assay buffer: 1.1 M NaCl, 2.2 mM Na_2EDTA, 220 mM K_xPO_4 pH 5.1, 0.44 mg/ml BSA, 2.5 μM coelenterazine

Solutions

Acrylamide/bisacrylamide solution (Sigma-Aldrich®): 30 %.

3-Amino-1, 2, 4-triazole (3-AT) (Sigma Aldrich®): 1 M stock.

Paraformaldehyde (PFA) (Thermo Scientific Cat# 28906): 4 % diluted in PBS.

4-methylumbelliferyl-β-xylobioside (Sigma Aldrich®): 1000x stock in dimethylformamide.

APS (Sigma Aldrich®): 10 % in water.

Coelenterazine (PJK Cat #260350): Diluted 1 mg coelenterazine in 2.36 ml of deoxygenated methanol/ HCl {8.7 ml of 35% HCl in 1 L methanol (Deoxygenated by pumping nitrogen gas through it on ice for 30 minutes)}.

HIRT buffer: 10 mM EDTA, 0.6 % SDS.

Immunofluoresence antibody dilution buffer: 1% BSA in PBS.

Immunofluoresence blocking buffer: 5 % normal goat serum (Sigma Aldrich®) in PBS.

Laemmli running buffer 2x: 4 % SDS, 20 % glycerol, 10 % β-mercaptoethanol, 0.004 % bromphenol blue and 0.125 M tris-Cl, pH 6.8.

LUMIER lysis buffer stock 1x: 22mM Tris pH 7.5, 275 mM NaCl, 1 % TritonX-100, 11 mM EDTA.

LUMIER lysis buffer per sample: 900 µl LUMIER lysis buffer stock 1x, 10 mM DTT, cOmplete inhibitor tablets (Roche, UK) (40 µl of stock – 1 tablet in 2 ml water) and phosStop (Roche, UK) (100 µl of stock – 1 tablet in 1 ml water) , 0.5 µl Benzonase (Novagen 70746, puritiy >90%).

NB Buffer: 0.15 M NaCl (Sigma Aldrich®), 10 mM Bicine (Sigma Aldrich®).

NP-40 lysis buffer: 20 mM tris (pH 7.5), 150 mM NaCl, 5 mM MgCl2 and 1 % NP40 (IGEPAL-CA, Sigma Aldrich®), one tablet of cOmplete inhibitor tablets (Roche, UK) and one tablet of phosStop (Roche, UK) were added to 50 ml of NP40 buffer before use.

PEG/Bicine Solution: 40 % Polyethylene glycol (PEG) (Sigma Aldrich®), 200 mM Bicine (Sigma Aldrich®).

SBEG: 1 M Sorbitol (Sigma Aldrich®), 10 mM Bicine, pH 8.35 with NaOH, 3 % PEG (Sigma Aldrich®).

TBST 1x: 10 mM tris-Cl (pH 7.5), 100 mM NaCl, 0.2 % tween.

Western blot blocking buffer: 5 % skimmed milk powder (Fluka) dissolved in TBST.

Western blot transfer buffer (1x): 240 mM tris, 190 mM glycine, 1 mM SDS, 20 % methanol.

2.1.3 Kits

BCA protein assay reagent (Thermo Scientific)

Brilliant II PCR kit (Agilent technologies)

Dual luciferase system (Promega, UK)

ECL Western blotting detection system (GE health care, UK)

Illustra GFX™ PCR DNA and Gel Band Purification Kit (GE Healthcare, Cat# 28-9034-70)

PureYield TM Plasmid Midiprep System Kit (Promega, Cat# A2492)

QIAprep Spin Miniprep Kit (Qiagen, Cat# 28704).

Verso 1-step QRT-PCR Low ROX Mix (Thermo Scientific Cat# AB4102)

2.1.4 Equipment and consumables

RC5B superspeed centrifuge (Sorvall)

Electroporation cuvette (2 mm, Cell Projects)

GenePulser (Biorad)

Fuji Medical X-Ray film (Fujifilm Europe GmbH)

MX3000-P™ real-time PCR (Strategene)

Nanodrop ND1000 (Labtech)

X-Ray Film Processor (Optimax)

Thermocycler (Techne TC512)

Plate reader (Polar star optima, BMG Biotech)

Table top centrifuge (Eppendorf 5415D)

Twin vertical electrophoresis system (Galileo, Bioscience)

UV transilluminator - Biorad Gel Doc 1000

0.45 μM nitrocellulose membranes (Amersham Biosciences, UK)

2.2 Methods

2.2.1 DNA techniques

2.2.1.1 Gateway® recombinatorial cloning

The Gateway® recombinatorial cloning system is a modified version of the bacteriophage lambda site-specific recombination (Figure 2.1). The gene of interest (GOI) is amplified by polymerase chain reaction (PCR) with primers flanking the gene-specific nucleotides with attachment B (*attB*) sites. A recombination reaction is catalysed by BP clonase enzyme to clone the amplified PCR product into an entry vector which originally contains *att*P sites. Upon recombination, the B and P sites recombine to form what is called *att*L site and the generated plasmids are called the entry clones, which contain the GOI and can be used to clone into a number of destination vectors having *att*R sites. In order to obtain the GOI into destination vector, a recombination reaction between the entry *att*L and destination *att*R site is performed using LR clonase enzyme. All the Gateway® vectors contain the coding sequence for *ccd*B gene between the *att* sites. This encodes for a toxin CcdB, which upon expression in bacteria causes cellular death allowing negative selection of clones containing the GOI (142). This method was used to clone the HPV-16 genes, the early genes E1, E2, E5, E6, E7 and late genes E4, E1^E4, L1 and L2 and some of the splice variants, E6*^E4, E1^E4*, E6*^E7*, E1^E2C necessary for this study (Table 2.5).

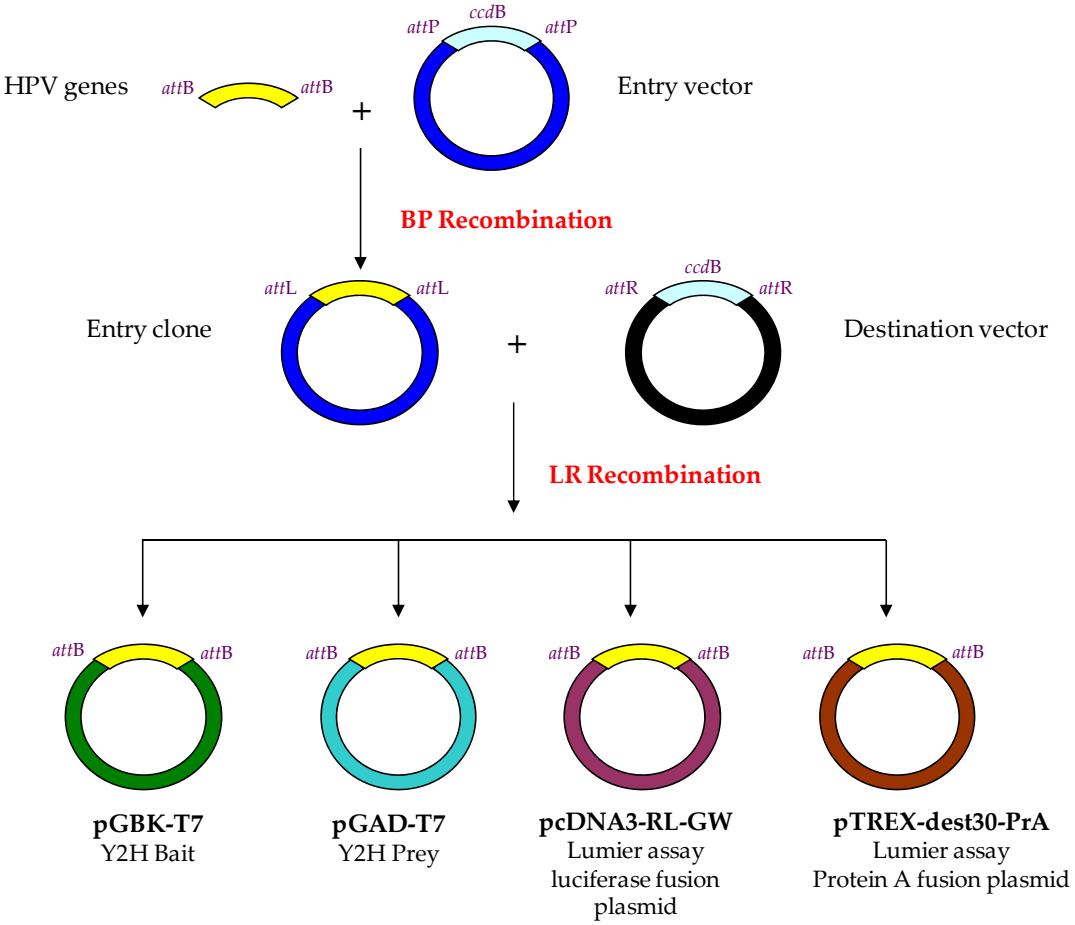

Figure 2.1: Schematic representation of Gateway® recombinatorial cloning system. The gene of interest (yellow) is PCR amplified with primers containing flanking attB sites and recombined to entry vector (blue) using BP clonase. The entry clone generated is used to shuttle the GOI into a range of destination vectors (black) by LR recombination. Some of the destination vectors used in this study are indicated.

2.2.1.1.1. Amplification of genes

The HPV-16 genes used in this study were amplified from NIBSC pBR322-HPV-16 plasmid and are listed in Table 2.5. The first round of PCR was performed with a set of designed primers comprising of about 15-18 nucleotide gene-specific sequence flanked by the internal part of the *att*B recombination site to facilitate recombination into the Gateway® entry vector and a kozak sequence CCGCC which facilitates translation of gene. The second round of PCR was performed with forward (Fwd) and reverse (Rev)

primers containing the complete *att*B sites. The primers used for PCR for different genes are listed in Appendix 1. PCR reactions were performed using conditions described in Table 2.6 with 10 μl of the first round reaction product used as a template for the second round PCR reaction. The E1-N clone had a frameshift mutation at nucleotide position 275. It was discovered that in the template of HPV-16 genome used for PCR amplification, there was a disrupted E1 gene which is consistent with published sequence (143). This frameshift mutation resulted in a stop codon at position of amino acid 101. This fragment of 101 amino acid length with 92 amino acids corresponding to E1 was denoted as HPV-16 E1-N and used for further studies. Additionally, the L1 gene of HPV-16 and E1 from HPV-18 were disrupted as the *Bam*HI site used to clone the HPV genomes into pBR322 is within the ORFs. Overlap PCR was done to clone the full-length E1 of HPV-16 (E1-FL) and HPV-16 L1 and HPV-18 E1 from pBR322-HPV-18 plasmid. Two separate first round PCR reactions were performed with Fwd and Rev-1 and Fwd and Rev-2 primers (Appendix 1). The second round PCR was performed using 5 μl products from each of the two first round PCRs as template and second round PCR primers as described in the previous section.

Gene	HPV Type	Start site	Gene length	Splice acceptor	Splice donor
E1-N	HPV-16	865	276		
E1-FL	HPV-16	865	1950		
E2	HPV-16	2755	1098		
E4	HPV-16	3332	288		
E5	HPV-16	3863	237		
E6	HPV-16	83	477		
E7	HPV-16	562	297		
L1	HPV-16	5559	1596		
L2	HPV-16	4235	1422		
E6*^E4	HPV-16	95	147	226	3357
E1^E4*	HPV-16	865	246	880	3390
E6*^E7*	HPV-16	95	165	226	743
E1^E4	HPV-16	865	279	880	3357
E1^E2C	HPV-16	1264	496	1302	3357
E1	HPV-18	914	1974		
E7	HPV-18	590	907		

Table 2.5: List of HPV genes. The start site and the length of the genes, the splice acceptor site and donor sites for the splice variants are specified in the table. The positions are given in relation to NCBI sequence K02718 for HPV-16 and X05015 for HPV-18.

PCR components	Reaction conditions
10x buffer Roche expand long template buffer 1 Fwd primer 20 pmol Rev primer 20 pmol Template DNA 20-100 ng dNTP mixture 10 mmol Expand long template enzyme mix 1.5 units	95 °C – 2 mins 95 °C – 10s 55 °C – 30s 68 °C – 1 min/kb } 15 cycles 68 °C – 7 min 4 °C forever

Table 2.6: Gateway® PCR components. PCR reaction components and conditions used for gateway® cloning are listed above.

2.2.1.1.2. Generating entry clone

PCR fragments were purified as described in Section 2.2.1.4 and purified PCR fragments were used to clone into Gateway® compatible donor vector, pDONR207. The reaction mixture consisted of 300 ng of purified PCR product, 300 ng of pDONR207, 1 µl of water and 1 µl of BP clonase® II enzyme. The reaction mixture was incubated overnight at 25 °C followed by transformation of 1 µl of the reaction mixture into electrochemically competent *E.coli* DH10β as described in Section 2.2.4.3. Colonies were screened by DNA isolation using alkaline lysis method (Section 1.2.1.7.1) and verified by restriction digestion (Section 2.2.1.6) with *Ban*II and sequencing (Section 2.2.1.1.3). A sample gel of HPV-16 genes in pDONR207 is shown in Figure 2.2**.** All human cellular genes used in this study unless otherwise specified were obtained from the MGC library in pDONR223 plasmid.

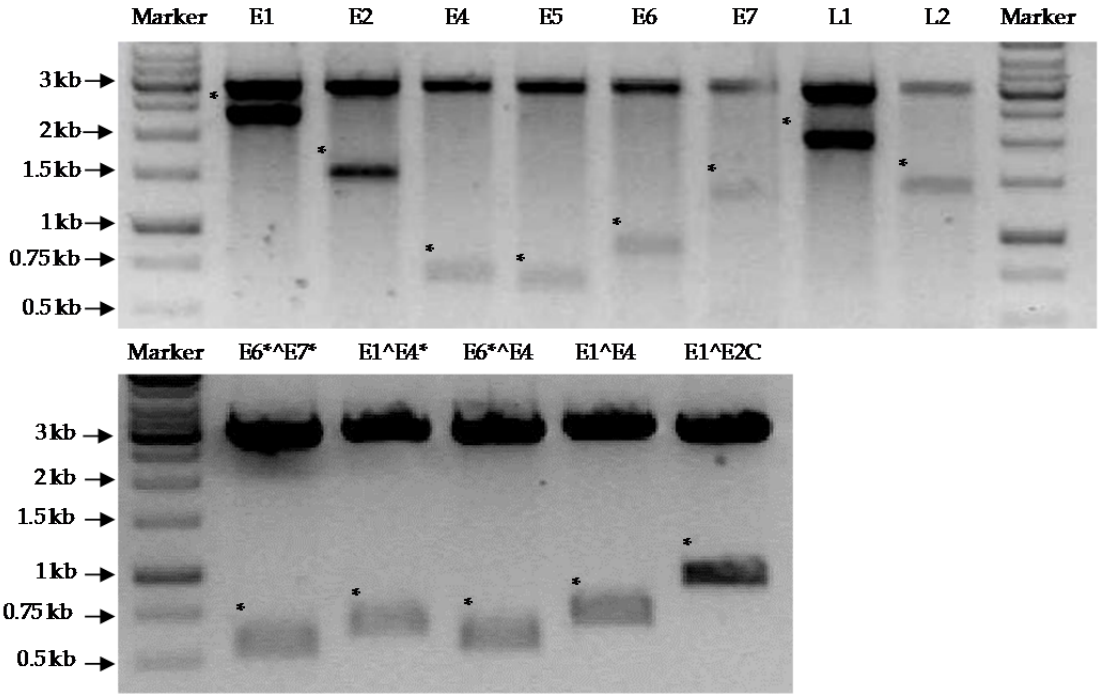

Figure 2.2: *Ban*II restriction digest of HPV-16 genes in pDONR207. Plasmid DNA was isolated from individual colonies followed by restriction digestion with *Ban*II restriction enzyme. The digestion product was separated using 1 % agarose gel, stained with SYBR safe gel stain and visualised under UV light. Gene fragments in each lane are indicated with *. A 2966 bp backbone of pDONR207 can be seen in all samples. The molecular weight markers are shown on both ends of the gels with the band sizes shown on left.

2.2.1.1.3. Sequencing

Sequencing was performed of all pDONR207 and pDONR223 genes for verification by GATC biotech, Konstanz, Germany. The sequencing primers are listed in Table 2.7. Sequencing results obtained were aligned with published sequences with the respective accession numbers using EBI Pairwise align software. Clones with silent mutations or missense mutations were considered positive.

Primer	Sequence
pDONR207 Fwd	TAACGCTAGCATGGATCTC
pDONR207 Rev	GCAATGTAACATCAGAGAT
pDONR223 Fwd	TCGCGTTAACGCTAGCATG
pDONR223 Rev	TAATACGACTCACTATAGGG

Table 2.7: Sequencing primers. The forward (Fwd) and reverse (Rev) primers used for sequencing reactions of pDONR207 and pDONR223 plasmids are listed.

2.2.1.1.4 Cloning into destination vectors

HPV genes were cloned from pDONR207 into destination vectors using LR recombination reaction. The reaction mixture consisting of 300 ng pDONR207 with gene insert, 300 ng destination vector (Table 2.1) and 1 µl of LR clonase® II enzyme was incubated at 25 °C from 1 hour to overnight depending on the size of insert. 1 µl of this reaction was transformed into chemically competent *E.coli* DH10β as described in Section 2.2.4.4. Colonies were screened by DNA isolation using alkaline lysis method (Section 1.2.1.7.1) and restriction digestion (Section 2.2.1.6).

2.2.1.2 Site-directed point mutagenesis

Alanine scanning site-directed mutagenesis was performed to generate point mutations in plasmids. Primers were designed by incorporating mutations to replace the desired amino acid with alanine. The primers for E7 and SPZ1 mutants are listed in Appendix 1. PCR amplification was done using conditions in Table 2.8. 1 µl of *Dpn*I restriction enzyme was added to the reaction after PCR and incubated for 90 mins at 37 °C to digest all template bacterial DNA. The PCR reaction was then purified as described in Section 2.2.1.4 and DNA was eluted in 20 µl ddH_2O. 5 µl of DNA was transformed into competent *E.coli* DH10β cells as described in Section 2.2.4.4. Colonies were screened by DNA isolation using alkaline lysis method (Section 1.2.1.7.1) and restriction digestion (Section 2.2.1.6) and verified by sequencing (Section 2.2.1.1.3).

PCR components	Reaction conditions:
100 ng template DNA 100 mM $MgCl_2$ 2 % DMSO 10 pmol Fwd and Rev primers 1X KOD reaction buffer 1 U KOD hotstart polymerase	94 °C for 5 mins 94 °C for 15 sec 60 °C for 30 sec 72 °C at 20 sec/KB 72 °C for 5 mins 18 cycles

Table 2.8: PCR conditions for site directed mutagenesis. The PCR reaction components and conditions for the PCR amplification of plasmids for generation of site directed mutants is shown.

2.2.1.3 Agarose gel electrophoresis

Agarose gel elexctrophoresis was performed with 1 % agarose solubilised in 1x TAE by heating in a microwave oven. SYBR® safe was added after cooling the gel solution, before pouring the gel. DNA sample was mixed with 6x loading dye and loaded on the gel. Molecular markers were added along with each set of samples and electrophoresis was performed horizontally at 80-150 V for 30-60 minutes following which the gels were illuminated with UV transilluminator for visualisation.

2.2.1.4 Purification of DNA

PCR products were purified either directly or by separation of the DNA fragment by 1 % agarose gel electrophoresis (Section 2.2.1.3). Where necessary, the DNA band of the correct size was excised from the gel. Both the PCR purification and the gel purification were performed using GFX™ PCR DNA Purification kit according to the manufacturer's instructions.

2.2.1.5 Determination of DNA concentration

The concentration and purity of DNA was determined by measuring the UV absorbance at 260 and 280 nm using the Nanodrop. The DNA concentration was

calculated with the OD at 260 nm (1 OD_{260} = 50 μg/ml dsDNA). The purity was estimated with the OD_{260}/OD_{280} ratio, with a ratio of approximately 1.8, indicating pure DNA.

2.2.1.6 Restriction digestion

Restriction digestion was performed according to the manufacturer's recommendations. In general, 1 μg DNA was digested for 2 hours with 10-20 U of restriction enzyme at 37 °C.

2.2.1.7 Plasmid DNA extraction

1.2.1.7.1. Alkaline lysis method

Individual bacterial colonies were picked from LB agar plates after transformation (Section 2.2.4.3 & 2.2.4.4) into 1.2 ml LB broth with appropriate antibiotic in 96-deep-well block and incubated overnight shaking at 250 rpm at 37 °C. The block was centrifuged at 4000 rpm for 10 minutes and the bacterial cell pellet was resuspended in 300 μl of solution I using a multi-channel pipette, lysed with 300 μl of solution II and neutralised by adding 300 μl of solution III and incubating on ice for 5 min. The blocks were centrifuged for 30 min in a pre-cooled centrifuge (4 °C) at 4000 rpm. 580 μl of isopropanol was added to the supernatant and incubated at -20 °C from 1 hour to overnight before centrifuging for 45 min at 4000 rpm in a pre-cooled centrifuge (4 °C). The pellet was washed with 500 μl of 70 % ethanol. The block was allowed to dry for about 30 min and the DNA pellet was re-suspended in 50 μl of water.

2.2.1.7.2. Small scale plasmid DNA extraction

Small scale plasmid DNA was prepared using QIAprep Spin Miniprep Kit with overnight culture of individual colonies in 5 ml LB broth with appropriate antibiotic using manufacturer's guidelines.

2.2.1.7.3. Large scale plasmid DNA extraction

Large scale plasmid DNA extraction was performed using PureYield™ Plasmid Midiprep System Kit with overnight cultures of individual colonies in 100-250 ml LB broth with appropriate antibiotic using manufacturer's guidelines.

2.2.2 RNA techniques

2.2.2.1 RNA isolation and purification

In order to extract RNA from mammalian cells, the cells were lysed using appropriate volume of TRIZOL® depending on the well type (100 µl for 96-well plate to 500 µl for 6-well plate). 1/5th of the total sample volume of chloroform was added and sample was centrifuged for 15 mins at 12 g at 4 °C. The top aqueous phase was transferred to a new tube and 2.5 V of aqueous phase 75 % ethanol, 0.1 V of 3 M sodium acetate, pH 5.2 and 20 µg glycogen were added to the aqueous solution and incubated at -80 °C for at least two hours before centrifuging for 30 min at 12 g at 4 °C. The pellets were washed twice with 75 % ethanol and dried at room temperature before resuspending in 30 µl of water by heating at 55 °C for 10 minutes.

2.2.2.2 QRT PCR

Quantitative real time (QRT) PCR was performed using Verso 1-Step Taqman QRT-PCR Low ROX Kit. Primers and probe used for QRT-PCR for SPZ1 and HRPT2 are listed in Table 2.9.

.

Primer/ Probe	Sequence
SPZ1 Fwd primer	TTCCAAACCCAGCCAAATAA
SPZ1 Rev primer	TGGCTCAGTTTCTTCACCTG
SPZ1 probe	UPL #78
HRPT2 Fwd primer	TGACCTTGATTTATTTTGCATACC
HRPT2 Rev primer	CGAGCAAGACGTTCAGTCCT
HRPT2 probe	UPL #73

Table 2.9: Sequences of primers and probes used for QPCR analysis. The sequences of DNA primers for qPCR analysis of SPZ1 and HRPT2 and the UPL probe numbers used are listed.

PCR components	Reaction conditions:
0.1 µl Verso Enzyme Mix 1 µM Forward Primer 1 µM Reverse Primer 0.5 µl Enhancer 20 ng Template RNA 5 µl 1-Step QPCR low ROX Mix (2x) Upto 10 µl with water	95 °C for 10 mins 95 °C for 30 sec 60 °C for 1 min } 40 cycles

Table 2.10: QPCR conditions. The PCR reaction components and conditions for the QPCR amplification of RNA are shown.

A standard curve analysis was performed using Verso 1-Step QRT-PCR SYBR® Green Low ROX Kit and conditions as described in Table 2.10 to determine the amplification efficiency of the primers used. The efficiency was calculated according to the Ct values, obtained from ten-fold serial dilution of RNA template and efficiency between 90 % and 110 % was considered ideal. The efficiency obtained for SPZ1 was 111.4 % and HRPT2 was 113.2 % (Figure 2.3). A dissociation curve analysis was performed to determine specificity of binding of the primer pair and specific binding was seen by both primer pairs. The dissociation curves indicate specific binding of the primers (Figure 2.4).

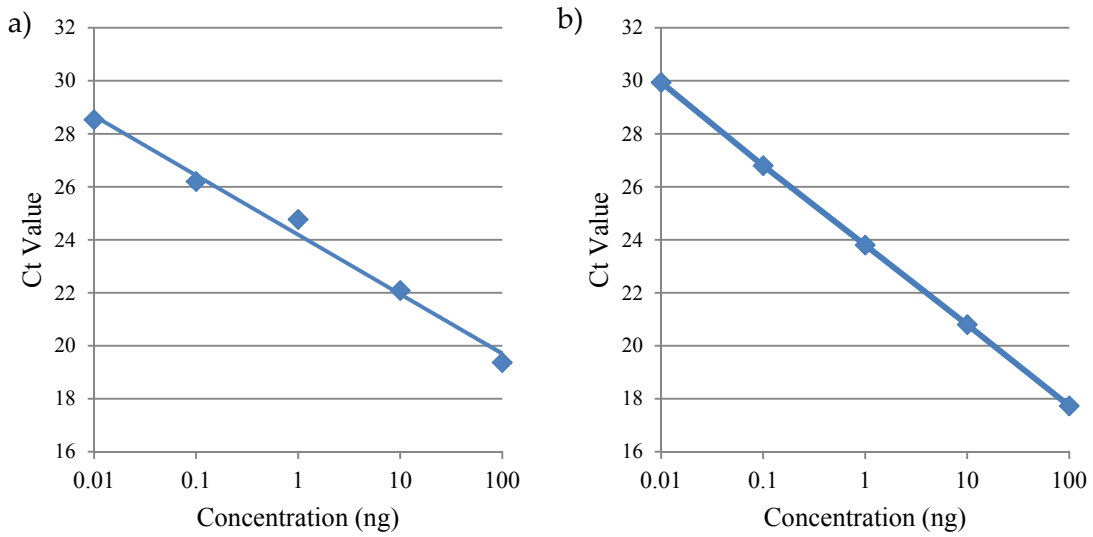

Figure 2.3: QPCR Standard curves. Standard curves were measured for ten-fold dilutions of primer pairs used for (a) SPZ1 and (b) HRPT2. The slope of the curves for SPZ1 is 111.4 % and HRPT2 is 113.2 %. Each dilution was run in duplicates and the analysis was performed using MxPro software.

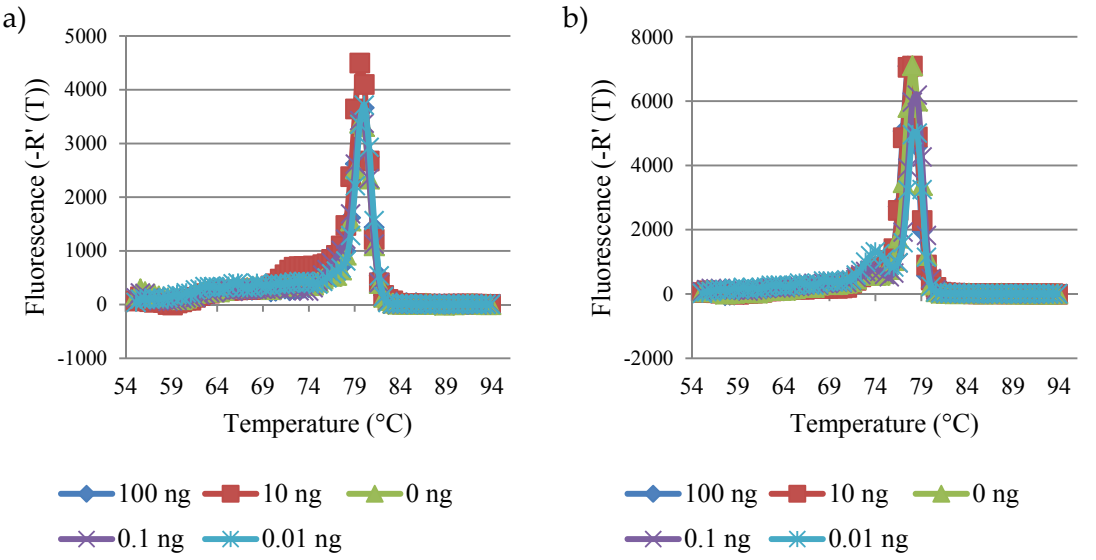

Figure 2.4: Dissociation curves for QPCR primer pairs. Dissociation curves for ten-fold dilutions of primer pairs used for (a) SPZ1 and (b) HRPT2. Each dilution was run in duplicates and the analysis was performed using MxPro software.

2.2.3 Protein techniques

2.2.3.1 Preparation of protein extracts for western blot analysis

Cells were washed once with PBS before being lysed in NP40 lysis buffer on ice for 30 minutes. The cell lysates were then centrifuged for 10 minutes at 1000 rpm and 4 °C to remove debris. The supernatant was resuspended in 2x SDS protein sample buffer and boiled for 10 minutes at 95 °C and analysed by SDS-PAGE.

2.2.3.2 Quantification of protein

Protein was quantified using BCA assay kit according to manufacturer's guidelines. Absorbance was measure and protein quantified using a polar star plate reader.

2.2.3.3 Co-immunoprecipitation

Cell lysates in NP40 were measured when necessary and lysates were pre-cleared with 50 µl of pre-equilibrated protein G-Sepharose beads by incubating in a over-head rotator for 1 hour at 4 °C followed by centrifugation at 2000 g. The supernatant was divided into two equal parts and used to precipitate with 1 µg of each antibody (anti-c-MYC for baits and anti-HA for preys) with 50 µl protein G-Sepharose beads. Beads were washed three times with ice-cold NP-40 buffer and were resuspended in 2x SDS protein sample buffer. Samples were boiled for 10 minutes at 95 °C and directly analysed by SDS-PAGE.

2.2.3.4 SDS-PAGE

Gel electrophoresis was performed with gels using a twin vertical electrophoresis system with 10-15 % resolving gel and 5 % stacking gel. The resolving gels were prepared with acrylamide mix to the desired concentration, 375 mM tris (pH 8.8) and 0.03 % SDS. Prior to pouring the gel, 0.03 % ammonium persulfate (APS) and TEMED were added, mixed and, after pouring, the gel was overlaid with isopropanol. After

polymerisation, the isopropanol was removed and the stacking gels were prepared with 5 % acrylamide mix, 125 mM tris (pH 6.8) and 0.01 % SDS. Prior to pouring the gel 0.01 % APS and TEMED were added. The stacking gel solution was poured on top of the resolving gel and a comb was fixed. After polymerisation, the glass plates containing the gel were assembled in the gel electrophoresis apparatus. Samples were loaded on the gel together with a protein ladder. Separation was performed at 150 V for 1-3 hours.

2.2.3.5 Western blot

Proteins were transferred to nitrocellulose membranes using the Trans-Blot semi dry Transfer Cell (Bio-Rad, UK). A sandwich was formed with all layers pre-soaked in transfer buffer: two layers of filter paper (Whatman, UK), a layer of nitrocellulose membrane, SDS-PAGE gel and two layers of filter paper on the platinum anode. The air bubbles were removed by rolling a pipette over the stack and subsequently the cathode was placed onto the stack followed by the safety cover. The transfer was performed at 15 V for one hour.

The membrane was blocked by incubation in blocking buffer from 1 hr at room temperature to overnight at 4 °C. The incubation with primary antibody was performed in blocking buffer. Three, ten minute washes were performed with TBST buffer followed by incubation with the secondary antibodies for one hour in blocking buffer. Three, ten minute washes were performed with TBST buffer. Proteins were detected using the ECL Western blotting detection system according to the manufacturer's instructions. The membranes were exposed to X-ray film for different exposure times and films were developed using X-Ray Film Processor.

2.2.4 Bacterial techniques

2.2.4.1 Preparation of chemically competent *E.coli* DH10β

1 litre LB-broth was inoculated with 5 ml overnight culture of a single colony from a freshly streaked LB-agar plate and incubated at 37 °C shaking at 250 rpm until an OD_{600} of 0.5 was reached. Cell growth was arrested by swirling vigorously on ice for 20 minutes following which cells were pelleted in a precooled centrifuge at 4000 g for 10 minutes. Cell pellets were washed twice with 100 mM $CaCl_2$. The cell pellet was then resuspended in 3-6 ml of 100 mM $CaCl_2$ with 15 % glycerol. Transformation efficiency was measured by transforming 1 ng of undigested plasmid and calculating the number of colonies per μg of DNA

2.2.4.2 Preparation of electrocompetent *E.coli* DH10β

1 litre 2YT was inoculated with 10 ml overnight culture of a single colony from a freshly streaked LB-agar plate and incubated at 37 °C shaking at 250 rpm until an OD_{600} of 0.5 was reached. Cell growth was arrested by swirling vigorously on ice for 20 minutes following which cells were pelleted in a pre-cooled centrifuge at 4000 g for 10 minutes. Cell pellets were washed once with water and once with 10 % glycerol and then resuspended in 3-6 ml of 10 % glycerol and immediately frozen in liquid nitrogen or dry ice. Transformation efficiency was measured by transforming 1 ng of undigested plasmid and calculating the number of colonies per μg of DNA.

2.2.4.3 Transformation of electrocompetent *E.coli*

1-2 μl of reaction mixture was mixed with 50 μl thawed electrochemical DH10β competent cells. This mixture was then transferred to an electroporation cuvette. An electric pulse of 2.5 kV was provided to the cells followed by recovery of cells at 37 °C in 500 μl LB media for one hour shaking at 1200 rpm. 250 μl of the culture was plated on LB-agar plates with the appropriate antibiotic. The plates were incubated overnight

in a dry incubator at 37 °C. Colonies were picked in appropriate volume of LB media with antibiotics for plasmid DNA extraction.

2.2.4.4 Chemical transformation of competent *E.coli*

1-2 µl of reaction mixture was mixed with 50 µl thawed competent DH10β cells and incubated on ice for 30 minutes. A heatshock of 42 °C was given in a waterbath for 45 sec followed by incubation on ice for 2 minutes. Cells were recovered by incubation at 37 °C in 500 µl LB media for one hour shaking at 1200 rpm. 250 µl of the culture was plated on LB-agar plates with the appropriate antibiotic. The plates were incubated overnight in a dry incubator at 37 °C. Colonies were picked in appropriate volume of LB media with antibiotics for plasmid DNA extraction.

2.2.5 Yeast techniques

2.2.5.1 Preparation of competent yeast cells

Two strains of yeast *Saccharomyces cerevisia* were used routinely, AH109 (mating type a) and Y187 (mating type α). 250 ml of fresh YPD was inoculated with the appropriate amount of overnight culture of yeast strain to an OD_{600} value of 0.15 and incubated at 30 °C shaking at 250 rpm till the OD_{600} of 0.6 was reached. Cells were pelleted by centrifuging at 2000 g for 5 minutes at room temperature, washed once in SBEG and resuspended in 5 ml SBEG and stored at -80 °C until use.

2.2.5.2 Transformation of competent yeast cells

1 µg plasmid DNA was added to 100 µl of the appropriate competent yeast. 750 µl of PEG/Bicine solution was added followed by one hour incubation at 30 °C shaking at 900 rpm. Heat-shock was given at 45 °C for 5 min. Cells were pelleted by centrifuging for 2 min at 3000 rpm. Pellet was washed in 1 ml NB buffer by centrifuging for 5 min at 3000 rpm. Cells were resuspended in 200 µl NB buffer which was plated on SD-agar

plates lacking the appropriate selective amino acid. Plates were incubated at 30 °C for 3 days till colonies appeared.

2.2.5.3 Protein extraction from yeast cells

A 5 ml overnight culture of transformed yeast was prepared in the appropriate media by inculating a single yeast colony. The overnight culture was used to inoculate 50 ml YPD and incubated shaking at 250 rpm at 30 °C till an OD_{600} of 0.4-0.6 was reached. The cultures were then chilled on ice and centrifuged at 1000 g for 5 mins. The cell pellet was washed in water. The total volume of the culture was multiplied with the OD_{600} to obtain OD units and protein was extracted by Urea/SDS method according to instructions Clontech manual. In short, the cell pellet was resuspended on pre-warmed (60 °C) yeast complete cracking buffer (100 µl per 7.5 OD units (For example, for 33 total OD_{600} units of cells, 0.44 ml of cracking buffer was used). 80 µl of glass beads (425–600 µm, Sigma) was added per 7.5 OD units and samples were boiled at 70 °C for 10 minutes followed by vigorous vortexing for 1 minute. The samples were then centrifuged to remove debris and supernatents were collected. The pellets were further boiled at 100 °C for 5 minutes, vortexed and centrifuged at 14,000 rpm for 5 min. The remaining supernatant was combined with the remaining supernatant and protein was quantified (Section 2.2.3.2) and used for western blot analysis (Section 2.2.3.4 and 2.2.3.5)

2.2.5.4 Yeast two-hybrid screen– Direct protein interaction

Direct yeast two-hybrid screen was done to test for interactions between two proteins. Plasmids encoding bait proteins were transformed into Y187 and prey proteins were transformed into AH109 and grown on SD-agar plates with appropriate selective media (SD-L for preys and SD-W for baits). Yeast colonies were mated on YPDA agar plate or SD-LW/5% YPDA broth by mixing each bait with each prey individually and incubating from 5 hours to overnight at 30 °C. The colonies were restreaked on SD-LW

agar plates or transferred into SD-LW broth and incubated at 30 °C for 2 days for selection of diploids. Colonies were then restreaked onto SD-LWH agar plates or transferred to SD-LWH broth and incubated at 30 °C for 6 days for selection of interactions. An inhibitor of interaction 3-Amino-1, 2, 4-triazole (3-AT) was used in increasing concentrations (0 mM, 1 mM, 2.5 mM, 5 mM and 10 mM) to competitively inhibit the interaction. Auto-activation was tested for every bait and prey by testing against empty prey or bait. Interaction was detected by growth on agar plate or fluorescence measurement in liquid culture. A substrate 4-methylumbelliferyl-β-xylobioside (4-MuX) was added to SD-LWH broth to measure fluorescence readout (excitation at 365nm; emission at 448nm).

2.2.5.5 Yeast two-hybrid screen– Library screening

In order to identify new interacting partners for proteins, yeast two-hybrid library screen was performed. Plasmid DNA expressing genes as baits were transformed into AH109 and prey libraries were obtained in Y187.

2.2.5.4.1. Pre-screen

15 ml of appropriate SD broth was inoculated with baits to be tested and prey library to an OD of 0.1 and incubated overnight at 30 °C shaking at 160 rpm. After overnight incubation, the OD_{600} of the cultures were measured and volume equivalent to an OD_{600} value of 12 each of bait and prey cultures were mixed and pelleted at 2000 g for 2 minutes followed by incubation in 25 ml of YPDA with 20 % PEG 6000 at 30 °C shaking at 100 rpm for exactly 3 hours. Cells were further pelleted and resuspended in 10 ml SD-LWH. A 1/100 dilution of this was plated on SD-LW plates and incubated at 30 °C for 3 days to confirm the formation of diploids. From the remaining cell suspension, 1 ml was added to 22 ml of detection media (SD-LWH, 5 µl/ml pen-strep, 50 µM MuX) supplemented with a range of 3-AT (0 mM, 1 mM, 2.5 mM, 5 mM and 10 mM), 200 µl of which was added to each well of a 96-well plate and incubated for 6 days at 30 °C.

Therefore for each interaction, seven 96-well plates were prepared. Interactions were detected by visually detecting individual colonies or measuring fluorescence readout (excitation at 365nm; emission at 448nm). A single colony or high fluorescence readout in a well indicated a single interaction. Interactions at each 3-AT were counted and a 3-AT concentration which gave roughly 10 single colonies per 96-well plate was used for the large scale screen.

2.2.5.4.2. Large scale screen

Yeast expressing bait and prey proteins were grown and mated as described in Section 2.2.5.4.1 for pre-screen. The mated cell suspension was then divided equally into ten 96-well plates containing interaction detection media (SD-LWH, 5 µl/ml pen-strep, 50 µM MuX and selected 3-AT concentration). Plates were incubated for 6 days at 30 °C followed by fluorescence measurement. All positive single colonies were picked into 96-well plates and transferred to SD-LWH agar plates using 96-well stamp and incubated for 3 days at 30 °C.

2.2.5.4.3. Colony PCR

An inoculum from the colonies was lysed in either 0.25 % SDS or 0.02 M NaOH at 95 °C for 10 minutes and centrifuged for one minute at 1000 g. 5 µl of supernatant was used as template for PCR using BioMix™ red Taq polymerase or NEB Taq polymerase using primers and conditions shown in Table 2.11 and Table 2.12. PCR samples were verified by agarose gel electrophoresis. All samples in which a single band of amplified DNA was seen, 20 µl of PCR reaction was sent for sequencing using the primers– pACT2- FP.

Primer	Sequence
Oligo 136	cta gag gga tgt tta ata cca cta caa tgg
Oligo 137	ggt tac atg gcc aag att gaa act tag agg
Oligo 80	tgt tta ata cca cta caa tgg atg atg
Oligo 81	cat aaa aga agg caa aac gat g
pACT2-FP	gat gat gaa gat acc cca c

Table 2.11: Primers for Y2H screen. Primers used for colony PCR and sequencing of prey genes to identify interactors in Y2H library screen.

	First Round PCR	Second Round PCR
Reaction conditions	2.5 µl NEB 10x reaction buffer 0.5 µl dNTPs (10 mM) 1 µl oligo 136 (10 µM) 1 µl oligo 137 (10 µM) 5 µl lysate 0.125 µl NEB Taq polymerase 9.875 µl water	5 µl NEB 10x reaction buffer 1 µl dNTPs (10 mM) 2 µl oligo 80 (10 µM) 2 µl oligo 81 (10 µM) 2 µl DNA template 0.25 µl NEB Taq polymerase 37.75 µl water
PCR program	95 °C – 5 mins 95 °C – 30s 55 °C – 1 min 30s — 26 X 72 °C – 3 min 30s 72 °C – 7 min 4 °C forever	95 °C – 5 mins 95 °C – 30s 55 °C – 1 min 30s — 20 X 72 °C – 3 min 30s 72 °C – 7 min 4 °C forever

Table 2.12: PCR reaction conditions for Y2H. Reaction components and program for PCR amplification of interaction partners in Y2H.

2.2.6 Mammalian cell culture

2.2.6.1 Maintenance of cell lines

All cell lines were maintained in incubators at 37 °C and 5 % CO_2. Cultures were passaged when they reached 90-95 % confluency by washing with PBS and treating with trypsin/EDTA solution at 37 °C till all cells were detached from the flask. Cells were recovered by adding complete growth media and centrifuged at 1000 rpm for 10 minutes in a benchtop centrifuge. The cell pellets were resuspended in growth medium

and counted by use of a haemocytometer (Section 2.2.6.4) and passaged into new flasks in the ratio of 1:3–1:5 or seeded as required for experiments.

2.2.6.2 Freezing of cell lines

Cells were trypsinised and counted as described in Section 2.2.6.4. Cells were frozen at a density of 1 x 10^7 cells/ ml in pre-cooled freezing media (70 % growth media, 20 % FCS and 10 % DMSO) in sterile freezing ampoules (Nunc, UK) at a density. Cells were transferred to a cryopreservation box (Mr Frosty, Nalgene) and gradually frozen overnight at -80°C and then transferred into liquid nitrogen storage tank.

2.2.6.3 Thawing of frozen cell lines

Frozen ampoules were thawed rapidly by warming in a 37 °C water bath. Thawed cells were transferred into 15 ml tubes and recovered by adding growth media slowly and centrifuging for 1000 rpm for 10 minutes. Cell pellet was then suspended in complete growth media and grown in cell culture flasks.

2.2.6.4 Counting of cells

Cells were trypisinised and concentrated in 10 ml appropriate media and 10 µl of live cells were added into a slide chamber (HYCOR: KOVA, Cat# 87144) and the number of cells in three squares was counted under a microscope at 10x magnification. The number of cells per ml was calculated as follows:

Cells/ml = average number of cells per square x 1000

2.2.6.5 Transfection of plasmids into cells

2.2.6.5.1 Calcium phosphate transfection

Calcium phosphate transfection into 10 cm dishes was done as follows. 6 x 10^5 to 2 x 10^6 cells were seeded one day prior to transfection and incubated at 37 °C. DNA to be transfected was mixed with 50 µl 2.5 M $CaCl_2$ and made upto a volume of 500 µl with 0.1x TE. The DNA-$CaCl_2$ mixture was dropwise added on a vortex into a bijoux containing 500 µl of 2x HBS and incubated at room temperature for 20 minutes. The transfection mix was added to the cells and incubated at 37 °C. Transfection into different sizes of tissue culture dishes were done by scaling down the reaction volumes.

2.2.6.5.2 Lipid transfection

A range of lipid transfection reagents were used according to manufacturer's instructions.

2.2.6.6 Co-immunoprecipitation

2 x 10^5 HEK293 cells were seeded a day prior to transfection in 10 cm dishes. MYC and HA N-terminal fusion proteins (baits and preys respectively) were used for co-immunoprecipitation. Since the bait and prey plasmids have a T7 bacteriophage promoter, cells were infected with recombinant vaccinia virus (NIH AIDS repository) expressing T7 polymerase before transfection of plasmids at an MOI of 10 in DMEM with 1 % FCS. The virus was removed after one hour and complete media was replaced. 10 µg each of plasmids was transfected by calcium phosphate transfection. After 48 hours, cells were lysed with 2 ml NP40 lysis buffer per 10 cm dish on ice for 30 minutes. The lysates were centrifuged for 10 minutes at 1000 g at 4°C to remove debris and the supernatant was pre-cleared with 50 µl of pre-equilibrated protein G-Sepharose beads by shaking for 1 hour. The lysates and beads were then centrifuged

and the supernatant was collected and divided into two parts. The proteins were immunoprecipitated from the supernatant by adding 1 μg of the anti-HA antibody or the anti-c-Myc antibody with 50 μl of protein G-sepharose beads and incubating overnight shaking at 4°C. The beads were then washed three times with ice-cold NP-40 buffer and were resuspended in 2x laemmli buffers. Samples were boiled for 10 minutes and directly analysed by SDS-PAGE.

2.2.6.7 Immunofluorescence

1 x 10^5 cells were grown in 8-well culture glass slide and transfected with desired plasmid. 48 hours post transfection, cells were washed thrice with PBS and fixed with 4 % PFA for 15 minutes at room temperature. Cells were further washed thrice with PBS and incubated with 50 mM NH_4CL for 10 minutes, washed twice with PBS, permeabilised with 50 μl of 0.5 % Triton X-100 for 3 minutes and washed twice with PBS. Cells were then blocked by immunofluoresence blocking buffer for one hour at room temperature, then the cells were stained overnight with 1/100 primary antibody in antibody dilution buffer. Cells were washed 3 times with PBS and then incubated for 1 hour with 1/500 secondary fluorescent antibodies at room temperature in dark. Cells were washed with PBS three times and mounted with Prolong Gold Anti-fade reagent with DAPI and examined using LEICA SP5 confocal microscopy.

2.2.6.8 Dual luciferase reporter assay

The dual luciferase reporter assay was performed using the Dual luciferase reporter kit (Promega). Cells were plated on cell culture dish as necessary for the assay one day prior to transfection. Transfection reactions were prepared using the desired volumes of DNA for each experiment. 10 ng of pRL-TK expressing renilla luciferase was transfected with each sample. 48 hours post transfection; cells were washed and lysed with 1x Passive lysis buffer for 15 mins at room temperature. 20 μl of cell lysate was transferred into 96-well black plates. 30 μl of LARII reagent was added to each well

and relative luciferase units measured on the plate reader on the luminescence setting. After the plate was read, 30 µl of Stop and Glo reagent was added to each well to quench the firefly luciferase activity and read again on luminescence settings to measure Renilla luciferase activity. Relative luciferase activity was calculated by normalising the firefly luciferase value to that of the Renilla luciferase per sample.

2.2.6.9 LUMIER Assay

2.2.6.9.1 DKFZ,Heidelberg

Luminescence based Mammalian IntERactome mapping (LUMIER) assay was performed in mammalian HEK293 cells in DKFZ, Heidelberg by Kerstin Mohr. 1 x 10^4 cells were seeded per well in 96-well plate a day prior to transfection. 12 ng of each plasmid expressing fusion proteins with N- terminal *Staphylococcus aureus* protein A tag or *Renilla reniformis* luciferase tag are transfected using 0.05 µl lipofectamine 2000 (Invitrogen). Cells were lysed 48 hours post transfection using 10 ul ice cold lysis buffer containing sheep-anti-rabbit IgG-coated magnetic beads on ice for 30 mins. 100 µl washing buffer (PBS, 1 mM DTT) was added per well and transferred into Greiner white flat bottom plate. A 1/10 dilution of the lysate was used for measurement of baseline activity of luciferase. The remaining lysate with beads were washed 6 times with washing buffer. Luciferase activity was measured using 2.5 M coelenterazine in renilla assay buffer as substrate. Negative controls were wells transfected with the plasmid expressing the luciferase fusion protein and a vector expressing two copies of protein A. For each sample, four values were measured: the luciferase present in 10% of the sample before washing ("input"), the luciferase activity present on the beads after washing ("bound"), and the same values for the negative controls ("input nc" and "bound nc"). Normalized interaction signals were calculated as follows:

Log (bound)/log (input) – log (bound nc)/log (input nc).

Normalized interaction signals were z-transformed by subtracting the mean and dividing by the standard deviation. The mean and standard deviation were calculated from large datasets of protein pairs which were not expected to interact, i.e. from negative reference sets.

2.2.6.9.2 Modified LUMIER assay

Luminescence based Mammalian IntERactome mapping (LUMIER) assay was also performed be me in the laboratory with modification. 1 x 10^4 cells were seeded per well in 96-well plate a day prior to transfection. 12 ng of each plasmid expressing fusion proteins with N-terminal *Staphylococcus aureus* protein A tag or *Renilla reniformis* luciferase tag are transfected using 0.05 µl lipofectamine 2000 (Invitrogen). Cells were lysed 48 hours post transfection using 10 ul ice cold lysis buffer containing sheep-anti-rabbit IgG-coated magnetic beads on ice for 30 mins. 100 µl washing buffer (PBS, 1 mM DTT) was added per well and transferred into Greiner white flat bottom plate. A 1/10 dilution of the lysate was used for measurement of baseline activity of luciferase. The remaining lysate with beads were washed 6 times with washing buffer. Luciferase activity was measured using 2.5 M coelenterazine in PBS/5M NaCl as substrate. Negative controls were wells transfected with the plasmid expressing the luciferase fusion protein and a vector expressing two copies of protein A. For each sample, four values were measured: the luciferase present in 10% of the sample before washing ("input"), the luciferase activity present on the beads after washing ("bound"), and the same values for the negative controls ("input nc", and "bound nc"). Normalized interaction signals were calculated as follows:

(bound/input) sample/ (bound/input) nc

Normalized interaction signals were z-transformed by subtracting the mean and dividing by the standard deviation. The mean and standard deviation were calculated from the complete dataset of all protein pairs tested in this study.

2.2.6.10 HPV Replication Assay

Replication assays were done in Morgan lab under the supervision of Mary Donaldson. 6 x 10^5 HEK293T cells were seeded one day prior to transfection and incubated at 37 °C. Plasmids expressing pOriM, HPV-16 E1, HPV-16 E2 and HPV-16 E7 were transfected at concentrations as mentioned using calcium phosphate. Cells were washed four days post-transfection and lysed *in situ* using HIRT buffer. The lysates were transferred into eppendorf tubes containing 5 M NaCl and incubated at 4 °C overnight. The lysates were cleared by centrifuging at 13000 g for 30 min at 4 °C and extracted by phenol-chloroform twice. DNA was precipitated using 100 % ethanol and 40 µl 3 M sodium acetate to each tube and incubating at -20 °C for 2 hours and centrifuging at 13000 g for 30 min at 4 °C. Samples were then desalted with 70 % ethanol and DNA was pelleted. DNA pellets were dried on heat block at 70 °C for 1 minute resuspended in 20 µl ddH2O. DNA was digested overnight with *Dpn*I at 37 °C followed by digestion with *Exo*III at 37 °C for 90 minutes. Samples were heat-inactivated at 70 °C for 30 minutes.

5 µl of DNA was used in QPCR reaction using Brilliant II QPCR kit using primers and probe as described in Table 2.13 and reaction conditions as described in Table 2.14. A standard curve was performed seven 10-fold dilutions (100 pg to 0.0001 pg) of pOri-M plasmid. 100 pg of DNA on the standard curve equated to 1.8 x 10^7 viral copies and the lowest dilution of 0.0001 pg DNA equated to 1.8 viral copies. Standard curves were performed in duplicates, a non-template control in quadruplicates and each sample in triplicates. The qPCR reaction was performed using ABI 7500 machine and the amount of pOriM in each sample was calculated against the standard curve using the Applied Biosystems 7500 sequence detection systems version 1.2.2 software.

Primer	Sequence
Fwd primer	atcggttgaaccgaaaccg
Rev primer	taacttctgggtcgctcctg
DNA probe	5' FAM - accaaaagagaactgcaatgtttcaggatcc-TAMRA

Table 2.13: Primers used in HPV replication assay. Sequences of primers and probe used for amplification of pOriM in HPV replication assay.

PCR components	Reaction conditions:
2x Mastermix 12.5 µl Fwd primer 25 pmol Rev primer 25 pmol Template DNA 5 µl DNA probe 100 nM ddH2O – 6 µl	95 °C – 10 mins 95 °C – 30 s 60 °C – 1 min } 40 cycles

Table 2.14: PCR reaction for HPV replication assay. Reaction components and conditions for qPCR amplification pOri-M in HPV replication assay.

2.2.6.11 Amplification of modified vaccinia virus Ankara

Modified vaccinia virus Ankara (MVA) was used for co-immunoprecipitation in Section 2.2.3.3 . Forty-six T-175 tissue culture flasks of BHK-21 were infected with crude stock of MVA at an MOI of 0.5 for 2 hours in pen-strep free DMEM (5 % FCS). Fresh complete medium (10 % FCS and 1 % penstrep) was added to the flasks and incubated for 2-3 days at 37 °C till a cytopathic effect of 70 %-80 % was visible. The flasks were frozen at -80 °C overnight. The flasks were thawed and when ice layer loosened, flasks were shaken forcefully so that ice layer lyses cells. The contents of the flasks were pooled into sterile 250 ml centrifuge bottles and centrifuged at 16000 g for 90 min. The pellets were resuspended in total of 50 ml 10 mM tris resulting in crude stock of virus. The crude stock was freeze thawed three times followed by sonication for 4 x 15 sec. 15 ml of 36 % sucrose was added into six 35 ml centrifuge tubes and 15

ml of virus suspension was slowly pipetted and centrifuged for 90 min at 70000 g. Each pellet was resuspended in 0.5 ml 1 mM tris and aliquoted in 100 µl aliquots.

Chapter 3:

Intra-viral interactions of HPV

3.1 Introduction

The yeast two-hybrid system is a useful technique in determining direct binary interactions between proteins. At a whole genome level, interactome studies for complete protein interactions for several eukaryotes have been performed over the years, which have provided valuable insights into understanding their life cycle. These include *Campylobacter jejuni* (144), *Saccharomyces cerevisiae* (145), *Caenorhabditis elegans* (146), *Drosophila melanogaster* (147), *Plasmodium falciparum* (148), plants (149) and *Homo sapiens* (150,151).

Analysis of intra-viral protein interactions (interactions between the proteins of a virus), have been reported for several viruses including SARS coronavirus (151), *E.coli* bacteriophage (152), Vaccinia virus (153), Hepatitis C virus (154), Varicella zoster virus (VZV), Kaposi's sarcoma herpesvirus (KSHV) (155), Epstein-Barr virus (EBV) (156)(141), Cytomegalovirus (CMV) (141) and Herpes simplex virus (HSV-1) (141)(157). In addition, on a non-genomic level, the discovery of binary interactions between a large number of viral proteins has been attributed to Y2H, including some in HPV.

Although HPV has a small number of proteins, the interactions that occur between the viral proteins play a very important role. The interactions between the HPV proteins E1 and E2 are essential for the replication of the viral episome. Y2H was used to identify the interaction domains on these proteins to N-terminal 190 amino acids of HPV-16 E2 and the C-terminal 229 amino acids of E1 (158). Additionally, Y2H led to the discovery of the dimerization domain of HPV-16 E7 indicating that this interaction is dependent on the CxxC domain in the C-terminal of E7 (136). Similar studies with HPV-11 E1^E4 protein led to the discovery of its dimerization (159). *In-vitro* binding assays showed that E2 causes repression of E7 activity by direct interaction (160), binding of E1^E4 to E2 leads to stabilisation of E2 (161) and direct binding of L2 protein

to E2 causes transcriptional repression, but not a reduction in replication mediated through direct binding of E2 (162).

Although some studies have looked into individual interactions between proteins of HPV, to date there is no published evidence of a complete interactome study of the HPV proteins at a genome-wide level. The aim of the work presented in this Chapter is systematically analyse the binary interactions between HPV proteins using the Y2H system and to validate these interactions by LUMIER assay. A further aim was to investigate the biological relevance of novel interactions.

3.2 Results

3.2.1 HPV intra-viral Y2H screen

In order to identify new intra-viral interactions of HPV proteins, a genome-wide Y2H screen was performed under the supervision of Dr Susanne Bailer in Max von Pettenkofer Institute, Munich. All the baits and prey proteins of HPV-16 E1, E2, E4, E5, E6, E7, L1, L2, E1^E4, E1^E4*, E6*^E4, E6*^E7*, E1^E2C and HPV-18 E1 in the bait form generated in Section 2.2.1.1 were used to test for interactions using Y2H assay. In order to check for auto-activation of the GAL4 promoter in the Y2H system, all HPV baits were tested against the empty prey protein (expressing only GAL4 activation domain) and all HPV preys with empty bait protein (expressing only GAL4 DNA-binding domain) as described in Section 2.2.5.4. In short, haploid yeast strains Y187 (mating type α) and AH109 (mating type a) were transformed with plasmids expressing the bait and the prey proteins, respectively. For each pairwise interaction, the two strains, which are of opposite mating types were mated by mixing together and diploids were selected. The diploids were then transferred to media lacking amino acid histidine, one of the reporters of Y2H system but supplemented with 0 to 5 mM 3-AT (which is inhibitor of histidine biosynthesis) and 4-Mux (the substrate necessary to detect fluorescence readout). If there was interaction, histidine biosynthesis occurred which

enabled the yeast to grow in media devoid of histidine. Also, upon interaction α-galactosidase was produced. The activity of α-galactosidase was measured by the fluorescence generated by degradation of the 4-Mux substrate (Figure 3.1).

Bait E2 and prey L2 interacted with empty prey and empty bait, respectively. These two proteins were auto-activating in the assay and removed from further analysis. Bait L2 showed a weak level of auto-activation which could be blocked by the use of low concentration (1 mM) of 3-AT.

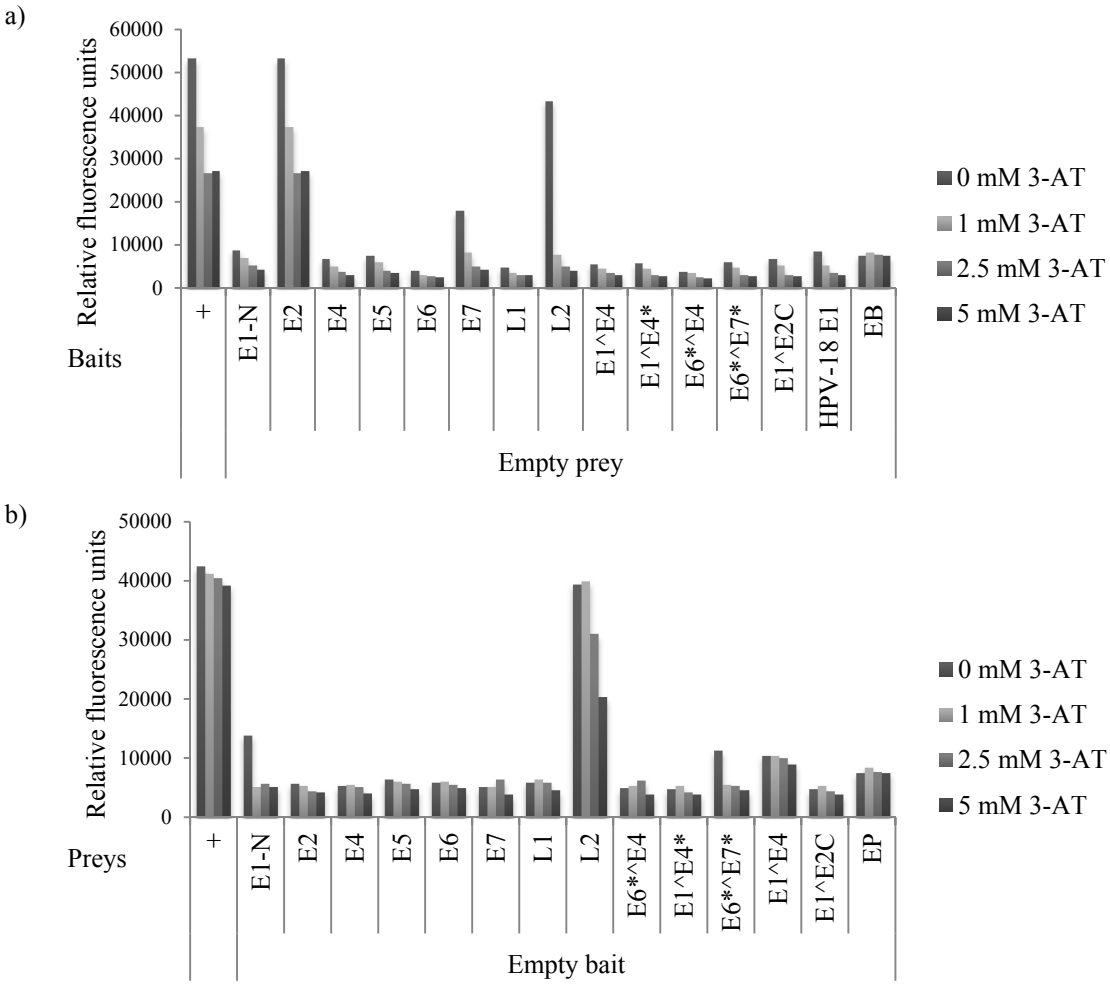

Figure 3.1: Auto-activation by HPV bait and prey proteins. HPV (a) baits and (b) preys were tested for auto-activation against empty prey and empty bait respectively. A known interaction between HSV-1 UL34 and UL31 was used positive control (+) and interaction between empty bait and empty prey was used as negative control. Relative fluorescence units were measured for four different 3-AT concentrations (0 mM, 1 mM, 2.5 mM, 5 mM) and plotted against Y-axis.

To test for interactions between the viral proteins, the Y2H assay was performed as described in Section 2.2.5.4. In total, 210 pair-wise interactions were tested and growth of colonies was determined visually. Successful mating was confirmed by growth on diploid selection plates. Growth on interaction detection plates confirmed an interaction between the two proteins. Five interactions were detected (Figure 3.2): (i) between E7 bait and E1-N prey; (ii) HPV-18 E1 bait and E1-N prey; (iii) E7 bait and prey; (iv) E1^E2C bait and E2 prey; and (v) HPV-18 E1 bait and E2 prey.

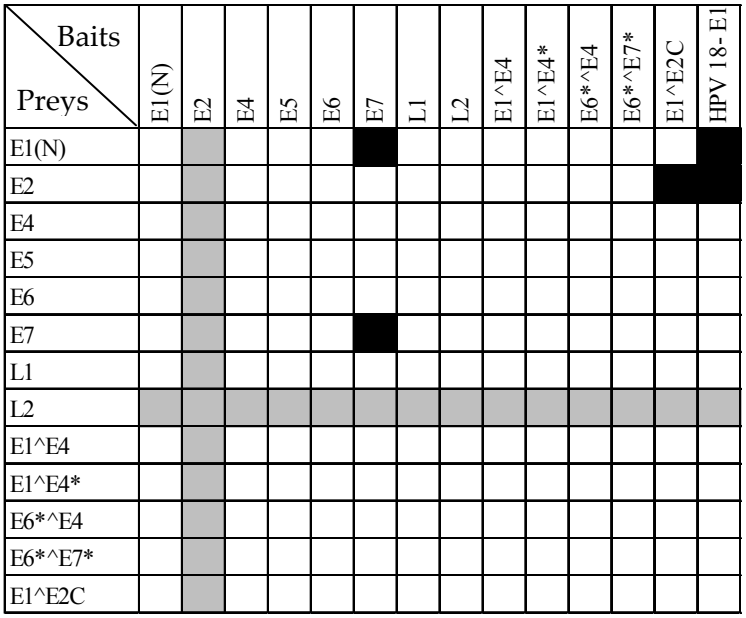

Figure 3.2: Identification of HPV intra-viral interactions by Y2H. HPV proteins were tested for interaction with each other. The baits are shown along the columns and preys are shown across in rows. The identified interactions are indicated by black squares and auto-activation is shown in grey.

3.2.2 Validation of interactions by LUMIER assay

Due to the possible occurrence of false positive interactions, it is crucial to confirm the identified interactions in a mammalian expression system. All the interactions identified by Y2H were therefore tested in LUMiniscence based Mammalian Interactome (LUMIER) assay. This assay was performed by Kerstin Mohr as part of a

collaboration with Dr. Manfred Koegl, German Cancer Research Centre, Heidelberg, Germany as described in Section 2.2.6.9.1.

Plasmids expressing fusion proteins with N-terminal *Staphylococcus aureus* protein A tag (pTREX-dest30-PrA) or *Renilla reniformis* luciferase tag (pcDNA3-RL-GW) were transfected into HEK293 cells and lysed 48 hours post transfection. A known interaction between JUN and FOS proteins was used as positive control and a z-score of >1 was considered as a weak interaction and >1.5 as a strong interaction (Figure 3.3).

Interactions between E7 and E1-N; E2 and HPV-18 E1; E7 and E7; and E2 and E1^E2C gave a z-score >1.5 ranging from 1.8 to 3.4 confirming that these interactions are genuine. However, z-score of -0.5 was detected for HPV-16 E1-N and HPV-18 E1 suggesting that this might be a false positive interaction.

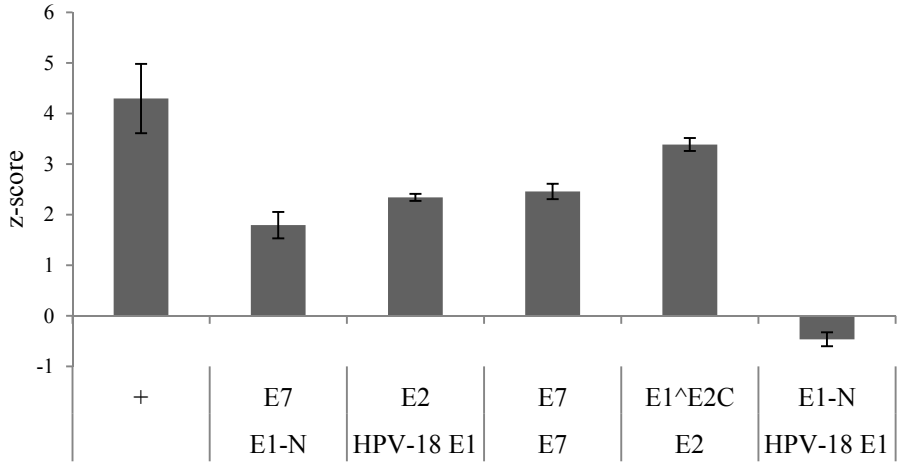

Figure 3.3: Confirmation of Y2H interactions by LUMIER assay. Protein interactions were tested by LUMIER and observed luminescence is presented as z-score. A known interaction between JUN and FOS was used as positive control (+). Error bars represent standard deviation of triplicates in one representative experiment. z-score >1 represents positive interaction.

3.2.3 Confirmation of the interaction between E7 with E1

Among the interactions identified in the Y2H screen, a novel interaction between E7 and E1-N was discovered. The original intra-viral screen was performed using HPV-16

E1-N containing the N-terminal 92 amino acids. In order to identify if the full-length E1 (E1-FL, aa 1-648) interacts with E7, a direct Y2H screen was performed as described in Section 2.2.5.4. Both full-length and the N-terminal E1 interacted with E7 with similar affinities, suggesting that the N-terminal 92 amino acids of E1 are necessary and sufficient for the interaction with E7 (Figure 3.4).

To check if this interaction also occurs in HPV-18, Y2H was performed with E7 bait and E1 prey from HPV-18. Whilst an interaction was observed between these two proteins, it was weaker and could be reduced with increasing amounts of inhibitor 3-AT suggesting that the interaction is not as strong in HPV-18 as it is in HPV-16 (Figure 3.4).

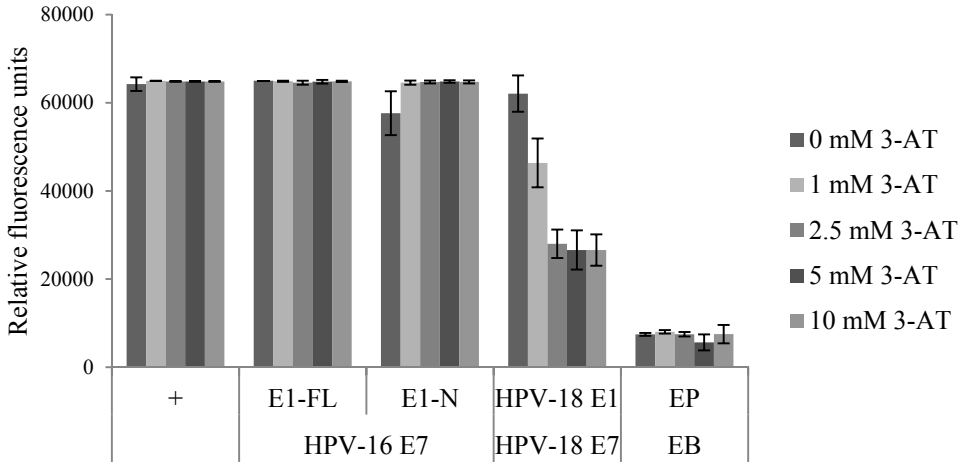

Figure 3.4: Interaction between E1 and E7. Interactions between E7 bait and E1-N and E1-FL of HPV-16 along with E1 and E7 from HPV-18 were performed. A known interaction between MYC and MAX proteins was used as positive control (+) and interaction between empty bait (EB) and prey (EP) protein was used as negative control. Relative fluorescence units were measured for five different inhibitor 3-AT concentrations (0 mM, 1 mM, 2.5 mM, 5 mM and 10 mM). Error bars represent standard deviation of quadruplicates in one representative experiment.

Co-immunoprecipitation experiments were performed to confirm the interaction between HPV-16 E1 with E7 in mammalian system. Plasmids expressing E7 bait (N-terminal MYC tag fusion) and E1-FL prey (N-terminal HA tag fusion) were transfected into HEK293 cells. Since the plasmids contain a T7 promoter, the cells were infected

with a modified vaccinia virus Ankara (Section 2.2.6.11) to induce the expression of T7 driven promoters. The proteins were co-immunoprecipitated as described in Section 2.2.6.6. Expression of both E1 and E7 was confirmed by blotting immunoprecipitated samples with anti-HA and anti-MYC antibodies respectively (Figure 3.5). Unspecific binding was ruled out by testing both E1 and E7 with empty bait and empty prey respectively. The small molecular weight (~20 kDa) and low expression E7 made it difficult to visualise by western blot. However, despite the low concentrations of E7, it was sufficient to co-immunoprecipitate E1-FL.

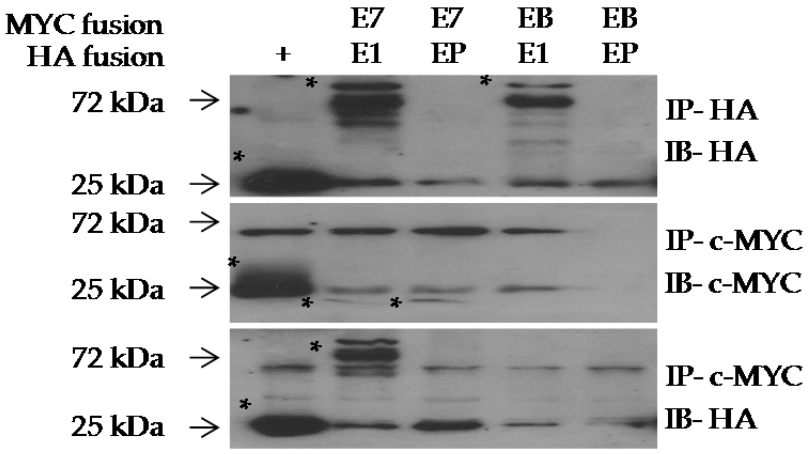

Figure 3.5: Validation of E1-E7 interaction by co-immunoprecipitation. Cell lysates immunoprecipitated (IP) with either anti-MYC or anti-HA antibodies were lysed with 2x Laemmlli buffer, separated on 15 % polyacrylamide gels and immunoblotted (IB) with either anti-MYC or anti-HA antibody as indicated on the right. A known interaction between MYC and MAX proteins was used as positive control (+) and empty bait (EB) and empty prey (EP) were used as negative control. Unspecific binding was ruled out by testing both E1 and E7 with empty bait and empty prey respectively. The heavy and light chains of anti-MYC and anti-HA antibodies can be seen. Specific bands corresponding to MYC, MAX, E1 and E7 are indicated with *. The molecular weights are shown on the left.

3.2.4 Mapping of interaction domains

3.2.4.1 Mapping of interaction domains by deletion mutagenesis

In order to identify the E1 binding site on E7, six deletion mutants of HPV-16 E7 were generated spanning the different domains of E7 (Figure 3.6a and b). The cloning of these fragments into pGBK-T7 was done under my supervision by an intern student,

Annette Murr. The domains were PCR amplified from pDONR207 E7 template using sequence-specific primers (Appendix 1) and recombined into pDONR207. The clones were sequence-verified and recombined into pGBK-T7 using Gateway® technology as described in Section 2.2.1.1. Expression of E7 deletion mutants in yeast was confirmed by western blot with an anti-MYC antibody (Figure 3.6c). It has previously been shown that pGBK-T7 plasmid on its own expresses a protein of 21 kDa which contains the GAL-4 DNA-binding domain (163). The molecular weight of HPV-16 E7 is 21 kDa. The fusion protein pGBK-T7 with E7 was expected to have a molecular weight of 42 kDa and all deletion mutants were correspondingly lower molecular weight that the wild-type E7. All the proteins were expressed in yeast except the E7 M1 protein, which was therefore removed from further analysis.

a)

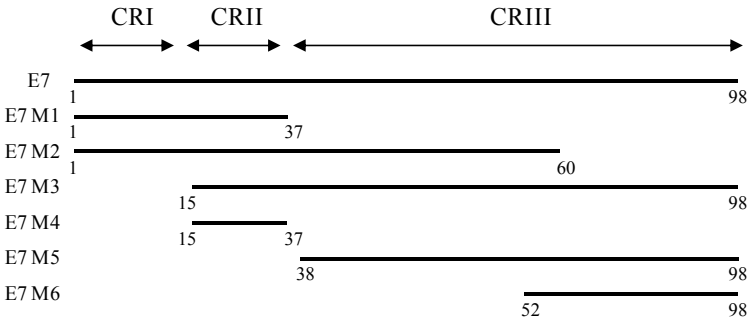

b)

Fragment	amino acids	E7 domains
E7	1-98	Full-length
E7 M1	1-37	CRI and CRII
E7 M2	1-60	CRI, CRII and N-terminal part of CRIII
E7 M3	15-37	CRII
E7 M4	15-98	CRII and CRIII
E7 M5	38-98	CRIII
E7 M6	52-98	C-terminal part of CRIII

c)

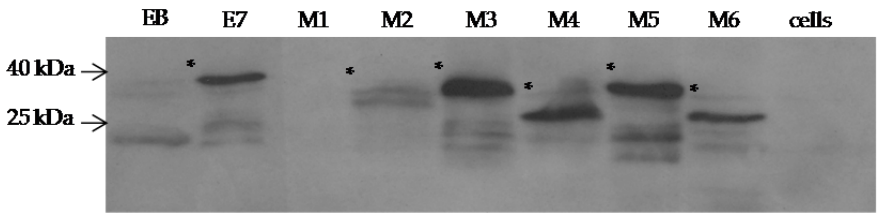

Figure 3.6: Deletion mutants of E7. a) Schematic representation of E7 deletion mutants. Full-length E7 is shown at the top and the mutant fragments below. The numbers correspond to the start and end amino acids. b) The amino acids and domains spanned by each E7 deletion mutant are listed in the table below. c) 1 mg of protein from Y187 cells was separated by 15 % polyacrylamide gel and western blot was performed. Protein extracted from Y187 cells (cells) and cells transformed with empty bait plasmid (EB) were used as negative controls and wild-type E7 protein was used as positive control. The E7 proteins are highlighted with *. The molecular weights are indicated on the left.

The interaction of E7 and retinoblastoma gene (RB), a cellular tumour suppressor protein is well documented (Section 1.2.8.1). The LxCxE domain in the CRII region (164) and the zinc finger CxxC domain in CRIII region (165) both independently interact with RB, and the affinity of the interaction is increased in the presence of both domains. In order to check whether the deletion mutants generated retained their

conformation and biological function, their interaction with RB was tested. RB was cloned into pGAD-T7 and Y2H was performed to determine the ability of the deletion mutants to interact with it as described in Section 2.2.5.4. The relative fluorescence units of E7-RB interaction, performed in parallel as positive control was arbitrarily set to 100 and all interactions were measured as a percentage of this interaction (Figure 3.7).

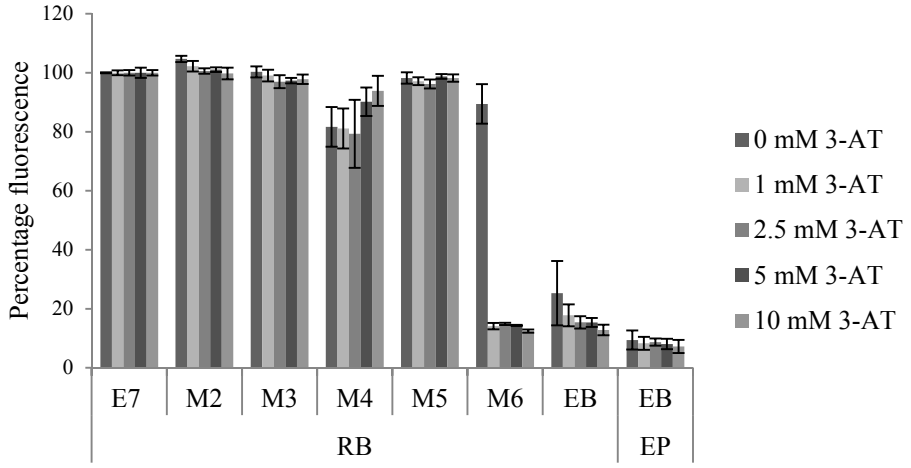

Figure 3.7: Interaction of E7 deletion mutants with RB. Interaction between E7 deletion mutants and RB was tested using Y2H. Relative fluorescence units were measured for five different 3-AT concentrations (0 mM, 1 mM, 2.5 mM, 5 mM, 10 mM). All interactions were normalised to positive control of wild-type E7 and RB (arbitrarily set to 100) for each 3-AT. Interaction between RB and empty bait (EB) and empty bait and empty prey (EP) was performed as negative control. Error bars represent standard deviation of quadruplicates in one representative experiment.

All E7 mutants that possess the CRII domain (M2, M3, M4) retain close to 100 % interaction with RB including M4 which contains only CRII domain in agreement with literature (164). M5 which lacks the CRII domain but contains the CxxC zinc-binding domain still maintains the ability to interact with RB. However, M6 which does not have either of the two domains fails to interact with RB. These results indicate that the deletion of functional domains CRI and CRIII does not disrupt the interaction of E7 with RB.

The E7 deletion mutants were tested in Y2H for interaction with E1-FL and E1-N (Figure 3.8). Deletion mutants M2, M5 and M6 retained the same level of interaction with E1 as wild-type E7. Removal of CRI domain on M3 resulted in a moderate reduction of interaction affinity (60 % interaction compared to wild-type). Removal of both CRI and CRIII domains in M4 had the most significant effect on interaction, reducing it to 30 % compared to the wild-type. However, removal of CRI did not have much effect in M5 or M6 indicating that this domain is not vital for the interaction. The CRII domain alone in M4 was unable to interact with E1 which suggests that CRII domain is also not sufficient for this interaction. Within the CRIII domain, the overlapping region among the three mutants M2, M5 and M6 is a region between 52 and 60 amino acids which might be the putative interaction domain. Although deletion mutant M3 contains the domain, the moderate reduction in interaction affinity might indicate that there are additional domains which might be necessary for stabilising this interaction. The interaction affinities for all the mutants were similar with E1-FL and E1-N indicating that the N-terminal 92 amino acids of E1 are sufficient for this interaction.

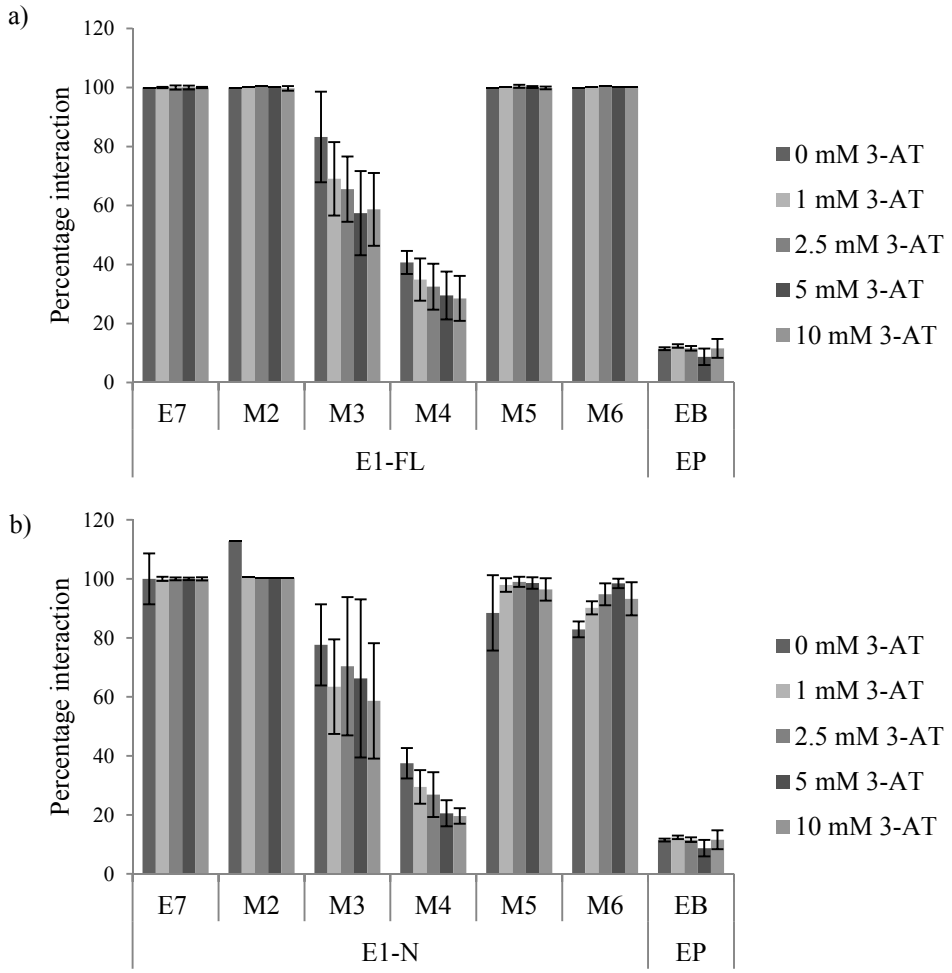

Figure 3.8: Interaction of E7 deletion mutants with E1. The E7 deletion mutants were tested for interaction with a) E1-FL and b) E1-N using Y2H. Relative fluorescence units were measured for five different 3-AT concentrations (0 mM, 1 mM, 2.5 mM, 5 mM, 10 mM). All interactions were normalised to positive control of wild-type E7 and E1-FL or E1-N (arbitrarily set to 100) for each 3-AT. Interaction between empty bait (EB) and empty prey (EP) was performed as negative control. Error bars represent standard deviation of quadruplicates in one representative experiment. For interaction data of E7 and E1-FL, M2 and E1-FL, M5 and E1-FL, M6 and E1-FL, E7 and E1-N, and M2 and E1-N, standard deviation was found to be zero or very low.

3.2.4.2 Mapping of interaction domains by point mutagenesis

The main interaction domain of E1 on E7 as indicated in Section 3.2.4.1 is between amino acids 52 and 60 which contain a zinc-binding CxxC motif at position 58-61. In order to investigate the role of this domain in E1 binding, point mutations of amino acids between 51 and 61 corresponding to HYNIVTFCCKC to alanine were performed by alanine scanning site-directed mutagenesis as described in Section 2.2.1.2. A total of eleven mutants were generated and denoted as H51A, Y52A, N53A, I54A, V55A, T56A, F57A, C58A, C59A, K60A, and C61A. Using pDONR207 HPV-16 E7 as template, PCR was performed to amplify the plasmid with primers containing the desired mutation (Appendix 1) and then recombined into pGBK-T7 for Y2H.

To check the expression of these deletion mutants, plasmids were transformed into yeast strain Y187. The expression of these proteins was detected by western blot using an anti-MYC antibody (Figure 3.9). All the site-directed mutants of E7 expressed a protein with a size around 42 kDa. A band corresponding to about 21 kDa was seen in all samples including pGBK-T7 but excluding untransformed cells. Small variation was seen in size of E7 C59A and C61A as compared to wild-type E7 possibly due to change in the phosphorylation of the protein or folding due to the mutation. In C61A two bands are seen, which might correspond to the monomeric and dimeric form of E7.

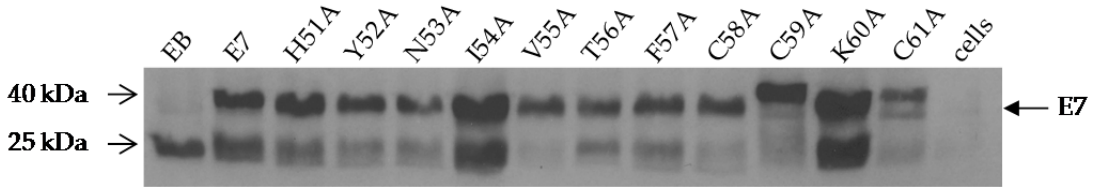

Figure 3.9: Expression of E7 point mutants in yeast. Western blot image of E7 site-directed mutants expressed in yeast strain Y187. 1 mg of total yeast protein extract was separated on 15 % SDS-PAGE, transferred to nitrocellulose membrane and blotted with 1:1000 anti-MYC primary and 1:3000 HRP conjugated secondary antibody. As controls, protein from untransformed and pGBK-T7 transformed yeast was included. Molecular weight marker is shown on the left.

In order to confirm the functional activity of the E7 mutants, they were tested for interaction with RB (Figure 3.10a). All the point mutants interacted with RB with similar affinity to wild-type E7 except C61A where a moderate reduction (70 % compared to wild-type interaction) was seen. As previously performed, the mutants were tested for interaction with E1-FL. It can be seen from Figure 3.10b that mutation of the cysteine residues at position 58, 59 and 61 into alanine reduces the ability of E7 to interact with E1. This assay suggests that the zinc-binding domain CCKC of E7 is involved in its interaction with E1.

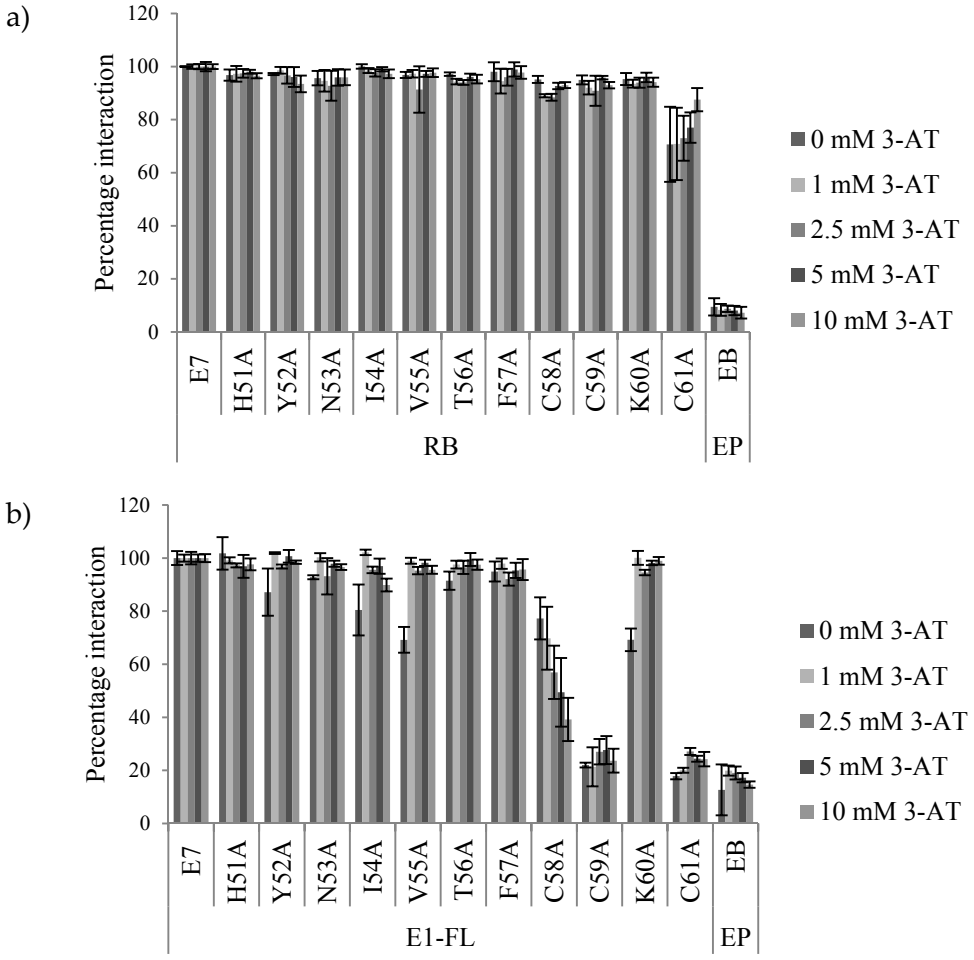

Figure 3.10: Interaction of E7 point mutants with RB and E1-FL. The E7 point mutants were tested for interaction with a) RB and b) E1-FL using Y2H. Relative fluorescence units were measured for five different 3-AT concentrations (0 mM, 1 mM, 2.5 mM, 5 mM, 10 mM). All interactions were normalised to positive control of wild-type E7 and Rb or E1-FL (arbitrarily set to 100) for each 3-AT. Interaction between empty bait (EB) and empty prey (EP) was performed as negative control. Error bars represent standard deviation of quadruplicates in one representative experiment.

3.2.5 E7 suppresses E1-induced replication

The E1 protein is a viral replication factor necessary for HPV episomal replication. The N-terminal region of E1 is necessary for its interaction with histone (166). Since this study identified that the N–terminal 92 amino acids were necessary and sufficient for its interaction with E7, it was hypothesized that E7 may play a role in replication. In order to test this hypothesis, transient replication assays were performed as described in Section 2.2.6.10 under the guidance of Dr Mary Donaldson in Prof Iain Morgan's laboratory in the Centre for Virus Research (CVR), Glasgow University. 293T cells were co-transfected with a plasmid containing the HPV-16 pOriM and plasmids expressing HPV-16 E1 and E2. The effect of E7 on replication was tested by transfecting wild-type E7 (WT) or mutants C58A, C59A or C61A as indicated. The amplified pOriM was then detected by QPCR (Figure 3.11). The E7 protein caused a 50 % reduction in episomal replication suggesting that E7 plays an inhibitory role in episomal replication. Interestingly, the mutants of E7 unable to interact with E1, C58A and C61A led to a three-fold and a two-fold increase respectively, whereas C59A does not have any effect on episomal replication.

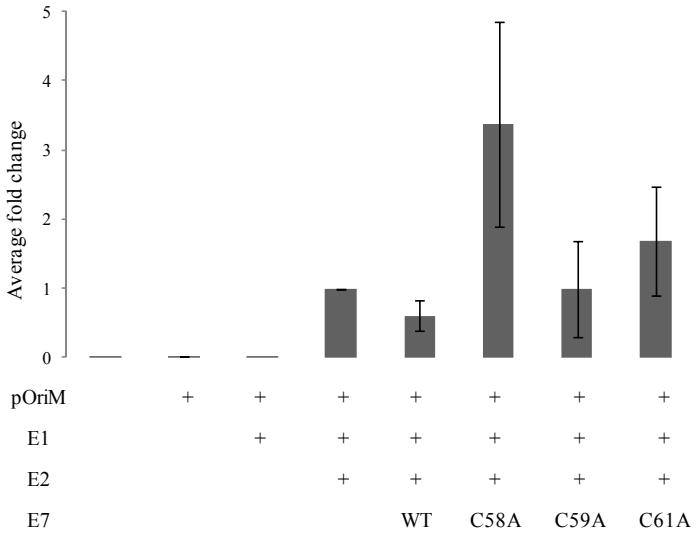

Figure 3.11: E7 reduces HPV replication in transient HPV replication assay. 293T cells were co-transfected with 100 pg of plasmid containing the HPV-16 origin of replication (pOriM) and plasmids expressing HPV-16 E1 (1 μg) and HPV-16 E2 (10 ng) along with 1 ng of wild-type (WT) E7 or C58A, C59A or C61A. The amplified pOriM was then detected by QPCR. Copy number of each sample was calculated using a standard curve of pOriM plasmid and normalised to copy number of samples transfected with E1 and E2 (set to 1). Data shown is an average of three independent experiments.

3.3 Discussion

3.3.1 Intra-viral Y2H screen

Genome-wide Y2H analysis for several large DNA viruses such as herpesviruses has provided vital insights into their biology. A similar approach was used here to identify interactions between the HPV proteome. The HPV genes were cloned into bait and prey plasmids and screened for interactions against each other. Proteins fused to the DNA-binding domain are sometimes known to auto-activate and, in this Y2H screen, E2 bait was auto-activating up to an inhibitor (3-AT) concentration of 5 mM in agreement with previous reports which have either used mutants of E2 (which lack the ability to auto-activate) (56) or performed Y2H screens using E2 bait from different HPV types such as HPV-5 E2 with much higher concentrations of inhibitor of about 25

mM 3-AT (167). Less frequently, proteins fused to GAL4 activation domains such as L2, can show auto-activation. Therefore, E2 bait and L2 prey were not used for further Y2H assays.

The Y2H screen identified five interactions between HPV proteins, which are: (i) E7 bait and E1-N prey; (ii) HPV-18 E1 bait and E1-N prey; (iii) E7 bait and prey; (iv) E1^E2C bait and E2 prey, and (v) HPV-18 E1 bait and E2 prey. Of these interactions, all were validated by LUMIER assay except HPV-18 E1 bait and E1-N prey. The results obtained confirm previously published interactions between E1 and E2 (158), dimerization of E7 (136) and interaction between E2 and E1^E2C, which can be attributed to the dimerization of E2 protein (47). Although the interaction between HPV-16 E1-N and HPV-18 E1 was seen in Y2H, it couldn't be validated by LUMIER which suggests that it is false positive interaction. The C-terminal domain of E1 is necessary for the dimerization of E1 (168), which is lacking in the HPV-16 E1-N used in the study. As the false positive rate of Y2H is quite high, it is quite likely that this is an artefact detected by the system. However, in this study the false positive rate of 20 % is within the limits seen in other publications (138).

Some of the previously known interactions were not identified in this study, which can be attributed as false negatives in this study, such as E7 and E2, E1^E4 and E2, L2 and E2 were not identified in this system. This could also be due to the fact that E2 bait was auto-activating. Additionally, interactions of E4, E6, L1 and L2 proteins were not seen in this assay. There are several limitations of Y2H which are also listed in Table 1.3**.**

1) Error in cloning of the plasmids which could result in the loss of expression of the protein. While the HPV gene with plasmid was sequence verified, the fused GAL4 DNA binding domains were not verified. A further check of this will be useful to perform. The expression of the proteins can further be tested by western blot analysis.

2) Error in the folding of proteins. As the yeast system is used where post translational modifications do not occur, it is possible that the proper folding of the viral proteins did not occur (169). This can be tested by testing the proteins for interactions with known interacting partners.

3) Expression of fusion proteins might mask the interaction domain. It is therefore useful to test N terminal and C terminal fusion proteins and to test individual proteins as 'baits' and 'preys' (170).

3.3.2 The E1-E7 interaction

This interaction between E1 and E7 was further confirmed with full-length E1 (E1-FL) and also using E1 and E7 from HPV-18 and validated using LUMIER and co-immunoprecipitation assay. It is interesting to note that preliminary evidence in Y2H indicates that the affinity of E1-E7 interaction is higher in HPV-16 as compared to HPV-18 where it can be inhibited by increasing amounts of 3-AT. Although HPV-16 and HPV-18 are both high-risk types, there are some differences between the two types, for example, HPV-18 is ten-fold more potent in keratinocyte transformation than HPV-16 (171). Further experiments to confirm the differences in affinities might shed light on the differences between the two high-risk types. It would also be interesting to check whether this interaction occurs in other HPV types including low-risk types such as -6, -11 and whether there are any differences in affinities which could lead the differences in the oncogenic potential of the virus.

Although a clear role for the N-terminus domain is unknown, this region in E1 can bind histones and is required for viral episomal replication initiation and elongation (166). Mutants lacking the N-terminal regions have been shown to be less effective in replication (172). The initial Y2H screen used E1-N which contains the N-terminal 92 amino acids which is sufficient for interaction with E7 as confirmed by LUMIER assay. The CRII domain along with CRIII domain of E7 are largely necessary for RB binding

and abrogation of E2F-mediated cell cycle control (Figure 1.6) (173). The CRIII domain has two zinc-binding CxxC motifs separated by 29-30 amino acids which are necessary for dimerisation and protein stability of E7. It has been shown previously that mutation of these zinc-binding motifs decrease protein stability and impairs transformation (174,175).

In order to map the interaction domains of E1 on E7, six deletion mutants spanning the three regions of E7 were generated. Western blot analysis of protein expression indicated that all mutants except M1 (containing 1-37 amino acids) were expressed in yeast. Although the reason for this is unknown some possible explanations are: (i) improper folding of the M1 protein; (ii) fault in cloning the gene; (iii) a mutation in the MYC epitope of the fusion protein. All the mutants except M8 which lacked CRII domain and first fifteen amino acids of CRIII were able to interact with RB indicating that deletion of functional domains did not alter the functional interactions of the mutants ((164,165,176). The region between 52-60 amino acids containing the first CCKC domain was identified as necessary for interaction with E1.

Point mutations within the region of 51-61 amino acids were generated and expression was verified by western blot analysis. Of the eleven mutants generated, two (I54A and K60A) show much higher stability as seen by the denser band on the gel and two (C59A and C61A) showed slight change in molecular weight as compared to the wild-type. In C61A, two distinct bands possibly corresponding to monomeric and dimeric form of the protein were seen. All the point mutants however, retained their ability to bind to RB confirming that they are functionally active. Upon testing interaction with E1, it was confirmed that mutation of C59A and C61A residues abrogated the E1-E7 interaction and mutation in C58A resulting in partial reduction in interaction. Mutation in any of the three cysteine residues of the CCKC domain causes an abrogation of interaction confirming that this domain plays an important role in the E1-E7 interaction.

3.3.3 Role of E7 in HPV episomal replication

Transcient replication assays performed to look at the effect of E7 on E1-mediated replication showed that wild-type E7 caused a 50 % reduction in replication (Figure 3.11). Interestingly, mutants C58A and C61A cause a three-fold and two-fold increase in replication whereas C59A shows no difference. This indicates that E7 is able to cause episomal reduction by direct binding to E1 and in the absence of this binding, no reduction is seen. It is known that E7 interacts with E2 and the CRIII region particularly amino acids 79-83 is necessary for this interaction (160), so it is possible that E7 interacts with E1 and E2 in the replication. The formation of a complex of E7 with both E1 and E2 potentially induces repression of viral replication. The mutants which do not bind to E1 but possibly retain their ability to interact with E2, cause an increase in replication. Alternatively, E7 might inhibit interaction of E1 with cellular factors such as DNA polymerase alpha primase (177) or topoisomerase I (178) which are necessary for replication causing a reduction which the mutants are unable to do. Future work will involve investigation of this mechanism.

At a functional level in raft culture systems, infection with HPV lacking E7 protein showed reduced viral genome replication (179), implying a role of E7 in replication. In our assay, where the cells are in a non-infected state, we see a reduction in replication in the presence of E7. Owing to the nature of HPV replication in differentiating layers of epithelium, it is possible that E7 plays a repressor role in the basal layers of epithelium where a low copy number of HPV genomes need to be maintained as compared to upper layers of epithelium where it could play an activator role. Further work needs to be done to elucidate this role in detail.

3.3.4 Possible role of E1-E7 interaction

Apart from the suspected role of E7 in replication, there are several possible roles for the E1-E7 interaction in the HPV life cycle and pathogenesis. The C-terminus zinc-

binding domain of E7 is necessary for interaction with several cellular proteins including AP1 (180) and TBP (181) necessary for maintainance of cell cycle. Interaction of E1 may competitively inhibit these interactions resulting in repression of E7 activity. The E1 and E2 proteins are transcriptional repressors of viral genes. Mutation of either E1 or E2 causes an increase in immortalisation of HPV infected cells (48). This, along with the fact that E2 causes repression of E7 by direct binding (160) indicates a similar role for E1 in inhibition of E7-mediated cellular transformation and immortalisation.

Future experiments will be directed towards further understanding the role of E7 in replication using mutant E7 unable to interact with E1 in raft culture studies. Inhibition studies to check if the E1-E7 interaction competes with any cellular binding partners of E1 will be interesting to look into. Also, transformation assays (182) can be performed to understand the effect of E1 on the transforming ability of E7. Elucidation of the biological relevance of E1-E7 interaction will provide insights into better understanding of the viral life cycle.

Chapter 4:

Inter-viral Y2H analysis between HPV-16 and HSV-1 proteins

4.1 Introduction

Herpes simplex virus (HSV) belongs to the family of *alphaherpesviridae* and has two serotypes HSV-1 and HSV-2. The two viruses have 85 % sequence homology and although historically it was believed that HSV-1 infected oral mucosa and HSV-2 infected genital mucosa, in the past 15 years, the perception has changed. About half of the genital infections in developed countries have now been attributed to HSV-1 (183). Both serotypes are considered ubiquitous and capable of causing genital infections.

HSV has a large dsDNA circular genome of about 152 Kb (Figure 4.1). The genome is divided into: (i) a nine Kb long repeat (R_L) region, which codes for early regulatory proteins and promoter regions of the latency associated transcripts (LAT); (ii) a 108 Kb long unique region (U_L) coding for atleast 56 UL proteins; (iii) a 6.60 Kb short repeat (R_S) region; and (iv) a 13 Kb unique short region (U_S) that encodes 12 US proteins (42).

Figure 4.1: HSV-1 genome organisation. Linear form of HSV-1 genome showing the two unique regions (UL) and (US). The RL and RS regions are highlighted with blue and red square boxes respectively. Figure recreated from reference (128).

Several studies have shown that HSV might act as a co-factor in cervical carcinogenesis. Most of the evidence to date has come form sero-epidemiological studies (Section 1.4), however, molecular studies designed to understand the interplay between the viruses are lacking. The susceptibility of female genital epithelium to HSV-1 and HSV-2 has been shown in ex vivo studies conducted on epithelial cells (184–186), there is no evidence suggesting that HPV and HSV-1 co-infect the same cells. Infection of HSV-1 and HSV-2 is shown to cause multinuclear giant ell formation and damage the cervical mucosal epithelial cells and is suggested to increase susceptibility

to HIV-1 infection (186). However no studies have looked into co-infection of HPV and HSV in the same cell or even a simultaneous infection of the two viruses.

Apart from the supportive role of HSV in increasing susceptibility to HPV infection, there are also studies that show a possible role of HSV-1 in the repression of HPV and its carcinogenesis. These include (i) a reduction in the HPV-18 gene expression with HSV-1 infection in HeLa cells (187); (ii) down-regulation of HPV-16 E7 by antisense RNA against HPV-16 E7 expressed from HSV modified vectors (188); and a reduction of HPV gene transcription with co-infection of both HPV-11 and HSV-2 (189).

Interest in HSV-1 in the context of cervical cancer has increased in the past few years as a therapeutic strategy. HSV-1 is a good candidate oncolytic virus in therapy of oral cancers in mouse models (190). HSV-1 infects some tumour cells and activates apoptotic pathways leading to the lysis of cells. In addition, cells of breast, colon, brain and cervical tumours have been shown to be susceptible to HSV-1 dependent apoptosis (191). A modified HSV-1 virus with LCR of HPV-16 was shown to be more effective in targeting and lysing HPV infected tumours in oral cavity (192). An adenoviral vector expressing fusion protein of HSV-1 VP22 and HPV E2 was able to induce apoptosis in cancerous cells (193). Recently, a multiplex PCR for screening of patients with HPV-16/18 and HSV-1/2 has been proposed to improve diagnostic reliability (194).

It is therefore important to understand both the mechanism by which HSV acts as a co-factor of cervical carcinogenesis and whether it can be used in therapy. While the study of molecular effects of co-infections is harder to study, it was hypothesised that identification of direct protein interactions, if any, between the two viruses will give an understanding of the interplay between the viruses. The aim of the work presented in this chapter is to identify any interactions between HPV and HSV at proteome level. A genome-wide Y2H screen between proteins of the two viruses was performed to

identify novel interactions and these interactions were validated by biochemical assays in mammalian cell system.

4.2 Results

4.2.1 Identification of protein interactions

A yeast two-hybrid screen was performed between proteins of HPV and HSV-1 in order to identify interactions under the supervision of Dr Susanne Bailer in Max von Pettenkofer Institute, Munich. A previously generated library of HSV-1 proteins containing full-length and fragments of 108 baits in Y187 and 106 preys in AH109 was used in this assay (141). The complete list of HSV-1 protein used is shown in Appendix 2. All the HPV bait proteins were expressed in yeast strain Y187 and the prey proteins in AH109 as described previously in Section 2.2.5.4. All the HPV proteins were previously tested for auto-activation (Figure 3.1) and E2 bait and L2 prey were omitted from the test. Similarly, all HSV-1 baits and preys were tested to identify auto-activation. Auto-activation was seen by five HSV-1 baits UL5, UL21, UL26.5, US8B, RL2 exon2 (Figure 4.2). Alternatively, none of the HSV-1 preys appeared to auto-activate in this assay.

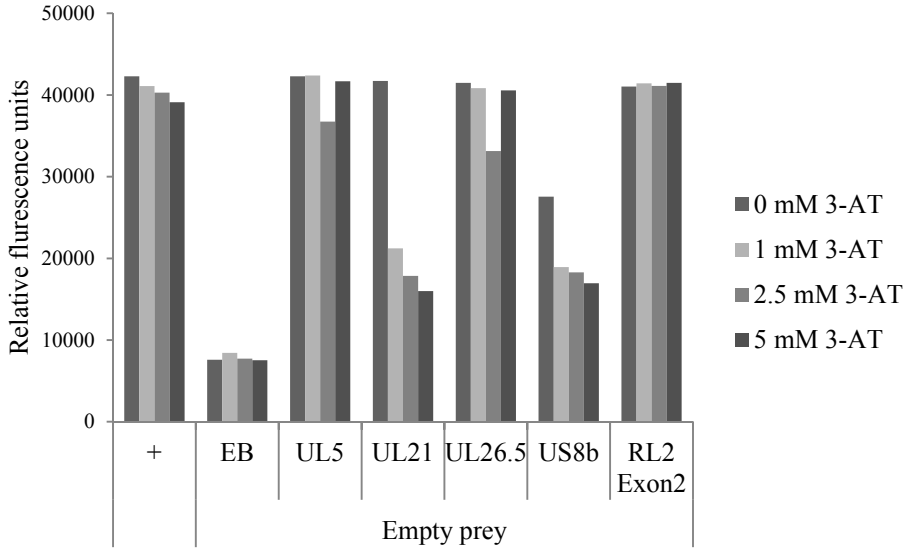

Figure 4.2: Auto-activation of HSV-1 genes. HSV-1 baits were tested for auto-activation against empty prey and empty bait respectively. A known interaction between HSV-1 UL34 and UL31 was used positive control (+) and interaction between empty bait and empty prey was used as negative control. Relative fluorescence units was measured for four different 3-AT concentrations (0 mM, 1 mM, 2.5 mM, 5 mM) and plotted against Y-axis. For simplicity, only interactions where auto-activation was seen are shown.

A total of 2568 interactions were tested between HPV and HSV-1 proteins. Any interaction where relative fluorescence activity was at least double than the relative empty bait–empty prey activity at a 3-AT inhibitor concentration of at least 2.5 mM was considered positive. Seventeen interactions were identified between the two viral proteomes (Figure 4.3), four interactions with HPV-16 E1-N which are with UL25, US3, US5A and US9A; one with E2, US10; two with E7, US1 and US3 and one with HPV-18 E1, RL1. Interaction of UL48 of HSV-1 was seen with HPV splice variants E6*^E4 and E1^E4* indicating that UL48 might have interacting domain within the E4 ORF. Interestingly, the interaction of RS1a, RS1b and RL1 was seen with E1^E4, E1^E2C. E1^E2C also interacted with US1 (Table 4.1).

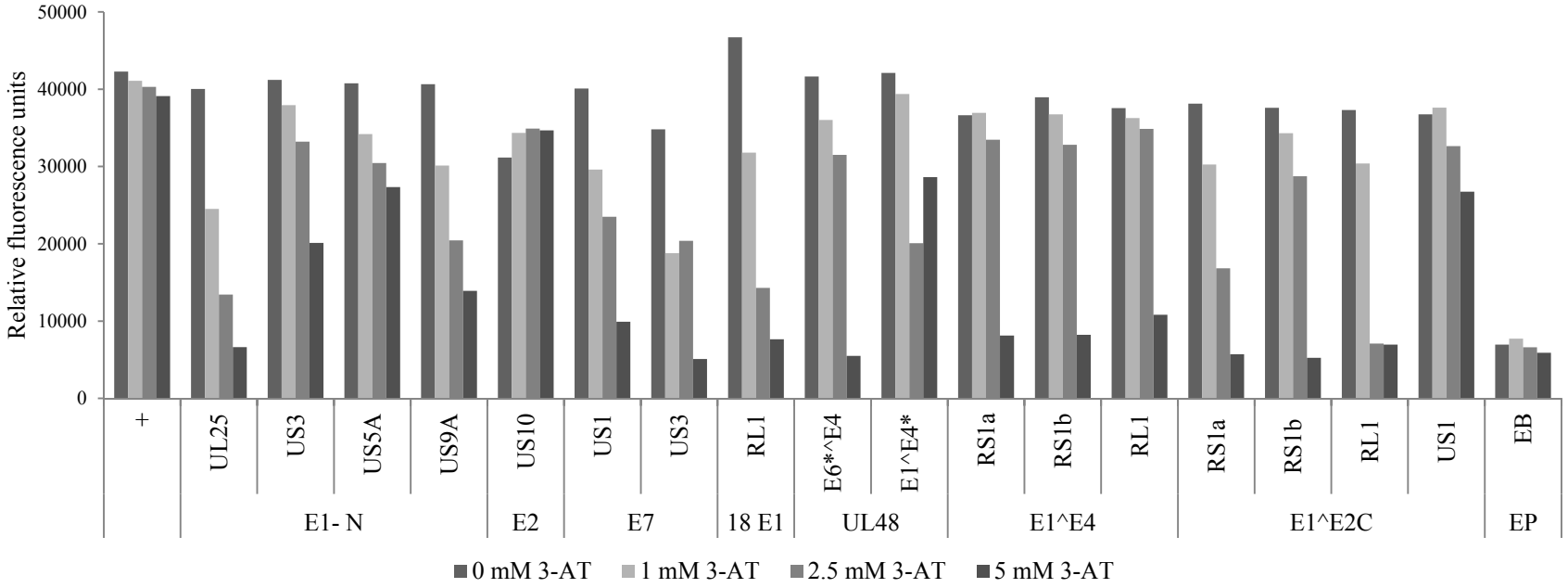

Figure 4.3: Interactions between HPV and HSV-1 proteins in Y2H assay. HPV proteins and splice variants were tested for interaction with HSV-1 library by Y2H. A known interaction between HSV-1 UL34 and UL31 was used positive control (+) and interaction between empty bait and empty prey was used as negative control. Relative fluorescence units were measured for four different 3-AT concentrations (0 mM, 1 mM, 2.5 mM, 5 mM) and plotted against Y-axis.

HPV protein	HSV-1 protein
HPV-16 E1-N	UL25
HPV-16 E1-N	US3
HPV-16 E1-N	US5A
HPV-16 E1-N	US9A
HPV-16 E2	US10
HPV-16 E7	US1
HPV-16 E7	US3
HPV-18 E1	RL1
HPV-16 E6*^E4	UL48
HPV-16 E1^E4*	UL48
HPV-16 E1^E4	RS1a
HPV-16 E1^E4	RS1b
HPV-16 E1^E4	RL1
HPV-16 E1^E2C	RS1a
HPV-16 E1^E2C	RS1b
HPV-16 E1^E2C	RL1
HPV-16 E1^E2C	US1

Table 4.1: Interactions between HPV and HSV-1 proteins in Y2H. The table represents the seventeen interactions identified between the two viral proteins using the yeast two-hybrid assay.

4.2.2 LUMIER assay

In order to validate a subset of interactions detected by Y2H, LUMIER assay was performed as described in Section 2.2.6.9.1. Out of the ten HSV-1 proteins that interacted with HPV proteins, cDNA clones for only seven were available in pRL-GW and pTREX-dest-PrA plasmids, US1, US3, US5A, US9A, US10, UL25 and UL48. The ten interactions of these proteins were tested (Figure 4.4). None of the ten interactions were found positive in this assay. The seven interactions that could not be tested for validation are interactions of RL1 with HPV-18 E1, E1^E4 and E1^E2C and interactions of RS1a and RS1b both with E1^E4 and E1^E2C which could not be performed due to unavailability of the RL1, RS1a and RS1b cDNA clones.

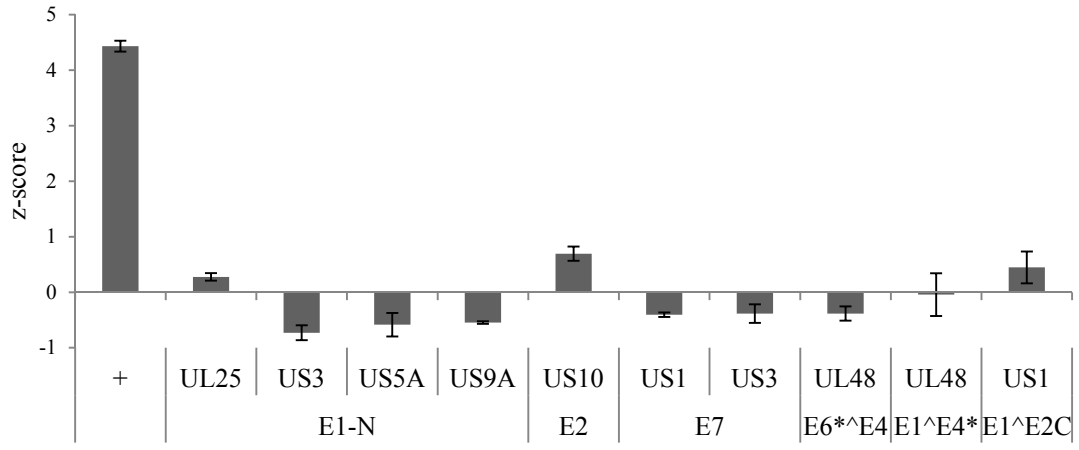

Figure 4.4: Confirmation of Y2H interactions using LUMIER assay. Protein interactions were tested by LUMIER and observed luminescence is presented as z-score. A known interaction between JUN and FOS was used as positive control (+). Error bars represent standard deviation of triplicates in one representative experiment. Z-score >1 represents positive interaction.

4.3 Discussion

HPV and HSV viruses have for long been thought to be co-factors in cervical cancer. While most of the data towards this comes from serological evidence and presence of HSV DNA and anti-HSV antibodies in cervical cancer patients, there have been few studies which attempt to understand the interplay between these two viruses at molecular level. Some studies have addressed this issue by looking at HPV transcription levels in the presence of HSV viral infection or the level of transcription of HSV genes in the context of over-expression of HPV proteins (187). However, the interplay between the two viruses at a proteomic level remains difficult to elucidate. The inter-viral Y2H assay in this study was performed with a library of full-length and fragments of HSV-1 proteins and the HPV proteins. It was very interesting to find seventeen interactions between the proteins of the virus which are listed in Table 4.1.

HSV-1 US3 is a multifunctional serine/threonine kinase that plays a role in several processes including egress of virus particles from the nucleus, modulation of the actin cytoskeleton, inhibition of apoptosis to allow efficient viral replication and promotion of viral gene expression (42). All of these processes are also necessary for survival of the virus and possibly viruses co-infected with HSV-1 and the interaction of US3 with the E1 and E7 proteins possibly enhance these activities. The HSV-1 US1 protein (also known as ICP22) is a transcriptional regulator of cellular and viral mRNAs. It facilitates the inhibition of host genome transcription, leading to cell cycle deregulation and loss of efficient antiviral response (195). Its interaction with the E1^E2C and the E7 proteins might also potentially play an important function in reducing the antiviral response and facilitating the survival of the viruses in the infected cells. HSV-1 UL25 plays a role in the encapsidation of viral genome and its packaging and also in the entry of viral genome into the nucleus. US5 (also called Glycoprotein J) is an anti-apoptotic protein, US9 is an envelope protein which plays a role in the spread of virus to the host nervous system whereas US10 is a capsid tegument protein (42). Their interactions with E1 and E2 respectively are also of potential interest.

UL48 or VP16 is a transcriptional activator which interacts with other viral and cellular transcription factors such as host cell factor 1 (HCF-1) to activate transcription of immediate early genes (196). It acts as a switch between lytic and latent stages of HSV-1 infection. When VP16 is activated, it promotes immediate early gene expression and causes lytic infection, when it is not activated, it causes in latent infection (197). Whether its interaction with the HPV proteins E6*^E4 and E1^E4* is involved in its transcriptional activity and whether VP16 plays a role in activation of HPV genes will be interesting to investigate.

RL1 (ICP 34.5) is a neuro-virulence factor of HSV-1. Upon viral infection, viral dsRNA is synthesized and through the activity of dsRNA induced interferon pathway, PKR is activated (198). PKR phosphorylates the translation initiation factor eIF-2A, thereby shutting off host protein synthesis and leading the cell to apoptosis. RL1 binds to PP1cα and recruits it to dephosphorylate translation initiation factor eIF-2A thereby maintaining protein synthesis (199). It also binds to proliferative cell nuclear antigen (PCNA) necessary for replication of host and viral DNA (200) and it is also involved in the evasion of MHC class II response (199). RS1 (ICP4) is a transcriptional regulator encoded by RS1 gene. It is necessary for transcriptional activation of both early and late gene expression and also causes repression of some genes (129). It interacts with general cellular transcription factors such as TBP and TFIIB (201) and with other viral transcription factors such as IPC27 for its transcriptional activity (202). Very interestingly, the HPV proteins E1^E4 and E1^E2C interact with RL1 and RS1 and HPV-18 E1 with RL1. These interactions are potentially relevant in the context of co-infections.

LUMIER assay was subsequently performed with ten of the seventeen interactions identified by the Y2H assay. The assay was unable to confirm any of the interactions positively which suggests that these might be false positives. Due to the scale of the study, where 2568 pair-wise interactions were tested at four different concentrations in a total of 108 96-well plates, the assay was not done in replicates. Additionally, most interactions could be significantly reduced or inhibited by use of high concentrations of inhibitor 3-AT of upto 5 mM. It is possible due to these reasons that the false positive rate in this assay is quite high. However,

LUMIER assay has its own limitations. Quite possibly, these interactions unconfirmed are false negatives of the LUMIER assay. Testing of these interactions with other protein-protein interaction techniques might be useful in this regard. Interestingly, among the seven interactions which were not tested by LUMIER assay due to unavailability of clones, were interactions of RL1 with HPV-18 E1, E1^E4 and E1^E2C and interactions of RS1a and RS1b both with E1^E4 and E1^E2C.

Future work will involve the validation of these interactions by other assays possibly, co-immunoprecipitation. Interactions of particular interest are those of ICP4 and ICP34.5 with HPV proteins. The study performed here provides a list of interactions between HPV and HSV-1 proteins. Since the HSV-1 and HSV-2 proteins are conserved, these interactions can possibly be extrapolated to HSV-2 and possible other herpesvirues such as CMV, EBV. Much future work is needed to elucidate the role of these viral protein interactions and the possible exploitation of this information in therapy against HPV-induced malignancies.

Chapter 5:

Virus-host interactions of HPV-16 proteins

5.1 Introduction

5.1.1 Virus-host protein interaction screens

Viruses need the host cell to survive and propagate. Once inside a cell, they use the host cell machinery for proliferation. Large viruses such as herpesviruses encode viral proteins necessary for functions such as replication and transcription but small DNA and RNA viruses such as papillomaviruses, poliomaviruses and retroviruses depend extensively on the host cell (42). Interactions of viruses with the host cell machinery are therefore critical for their survival and proliferation. High-throughput genome-wide assays such as yeast two-hybrid (Y2H), mass spectrometry, luminescence based mammalian interactome assay (LUMIER) provide a valuable tool to look at virus-host protein interactions (203). In the last ten years, Y2H has proved to be one of the most powerful tools to understand the interplay between viruses and their host, some of which are KSHV (141), HIV (204,205), vaccinia virus (206).

5.1.2 Interaction of HPV proteins with host proteins

As a small virus with only eight proteins, HPV depends extensively on the host machinery for many of its functions. To name a few important interactions, the E1 protein interacts with cellular factors such as replication protein A (RPA) and proliferative cell nuclear antigen (PCNA) for episomal replication (35), whilst E2 interacts with cellular transcription factors such as autocrine motility factor (AMF1) (50) for transcription of viral genes. However, the well characterised interactions of E6 with p53 and E7 with retinoblastoma protein (RB) play a central role in viral pathogenesis and transformation (9). The Y2H system has been used to generate interaction networks of individual HPV proteins such as E2 (208,209), E6 (210,211) and E7 (212,213).

Although it is important to perform large scale screens with individual viral proteins in order to increase the number of interactions, there is a bias towards the more extensively studied and significant proteins such as E2, E6 and E7 limiting the discovery of possibly important interactions of other lesser studied ones. Also, while most published studies

present a detailed analysis of one interaction, other identified but not analysed interactions remain unpublished which limits the available interactome. In this respect, systematic analysis of the whole viral genomes with host cellular libraries becomes important. The aim of the work presented in this Chapter was to perform a genome-wide interactome study of HPV-16 proteins against a human cDNA library to identify novel interaction partners. A further aim was to validate those interactions identified using biochemical assays, and to identify key interactions for further characterisation and elucidation.

5.2 Results

5.2.1 Y2H to identify novel cellular binding partners of HPV proteins

In order to identify novel interacting partners of HPV proteins, a Y2H screen was performed using HPV baits against a prey protein library derived from normalised cDNA from human testis epithelial cells with the help of Marcus Heinzelmann in Max von Pettenkofer Institute as described in Section 2.5.2.4. All HPV baits were transformed into the yeast strain AH109 and the prey library was obtained in the form of prey plasmids transformed into Y187 cells. In order to get high confidence interaction data, the use of an optimum concentration of inhibitor 3-AT is necessary. A very high 3-AT concentration will inhibit genuine interactions whilst a low 3-AT concentration will result in a high number of false positive interactions. To identify the optimal inhibitor concentration required for each bait, a pre-screen was performed using a range of inhibitor concentrations (0 mM, 0.1 mM, 0.5 mM, 1 mM, 2.5 mM, 5 mM and 10 mM). As the E2 bait was previously found to be auto-activating, it was not used in the screen (Section 3.2.1). For all the other HPV bait proteins a range of 3-AT concentration from 0.1 mM to 5 mM was identified and used for the screen (Appendix 3).

The screen was performed using the pre-determined 3-AT concentration by plating mated yeast in ten 96-well dishes per bait as described in Section 2.2.5.5. Individual colonies were picked, consolidated into multiple 96-well plates and grown on SD-LWH agar plates. Colonies were obtained for all the bait proteins except E4, E1^E4, E6 and E6*^E4 (Appendix

3). The prey gene in the colonies was identified by colony PCR amplification, sequencing and analysed by BLAST alignment against human genomic transcripts (NCBI BLAST software). This screen yielded 54 cellular interactions of HPV proteins which are listed in Appendix 5.

The identified HPV-host interactions were analyzed using the Ingenuity Pathway Analysis (IPA) software (Ingenuity® Systems, www.ingenuity.com). The IPA software uses the Ingenuity® Knowledge Base which is a repository of biological interactions and functional annotations created by manually reviewed publications. A data set containing all the host protein interactors of HPV identified in the study was uploaded into the application. The software then sorts the dataset of the proteins into well known pathways and develops networks of interactions and known functions of the proteins. To make the network more comprehensive, the HPV proteins were added by me manually into the network (Figure 5.1). The proteins in the dataset were broadly classified by IPA into four key functional interaction networks:

1) Infectious and dermatological diseases, and cellular development- CAMLG, CCDC136, PITRM1, SLC25A46, SLC30A1, TXNDC15, UBL3 and YIPF4 (Figure 5.2a).

2) Cancer, cell-to-cell signalling and renal and urological disorders- AIMP2, CCDC11, KIFC3, MRPL36, NUFIP1, PPIG, PSMD2, REEP6, RPS7, UCHL1, WDR48, ZNF451 (Figure 5.2b).

3) Inflammatory response and respiratory system development and function- ADORA3, DNAJB1, DNAJB6, EEF1A1, GLRX3, GRK5, HAX1, RNF141, SPZ1, TAF1A, XRCC6 (Figure 5.2c).

4) Cancer, haematological disease and cellular development- CLMN, CPT2, LDHC, MLL4, PRM2, RPL11, and ZBTB6 (Figure 5.2d).

These networks were subjected to functional analysis to identify the biological functions and/or diseases that were most significant to the proteins in the network. This was done by using Right-tailed Fisher's exact test and calculating a p-value determining the probability that each biological function and/or disease assigned to that network is due to chance alone. The functions identified by IPA are listed in Table 5.1.

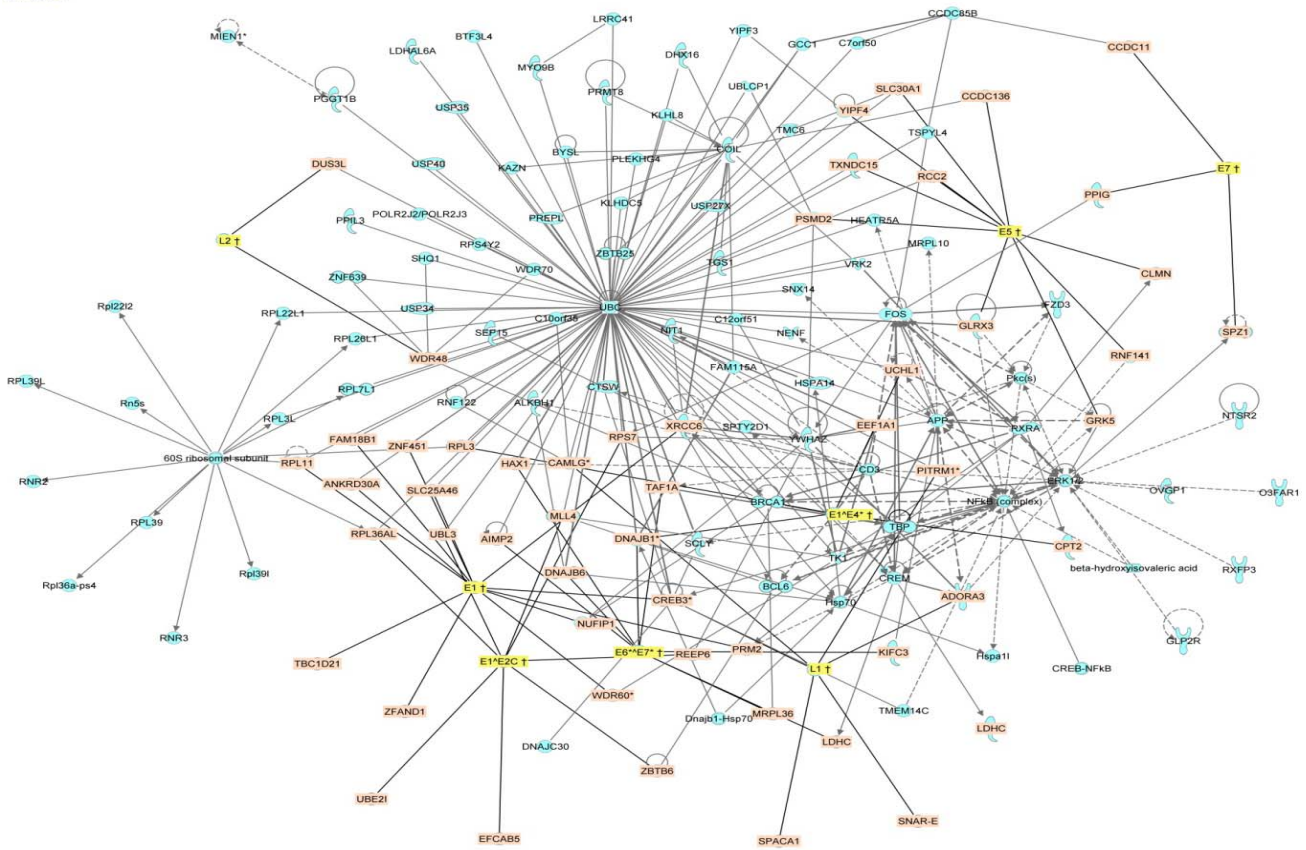

Figure 5.1: Virus-host interactome of HPV proteins. A network representing the interactome of HPV proteins with cellular interactions identified in the Y2H screen. The pathway map was created by Ingenuity Pathway Analysis software. Each node (cyan) represents a protein, with the shapes corresponding to the type of protein according to the software. HPV proteins are highlighted in yellow, and interacting partners identified in this screen are highlighted in orange. Each line represents an interaction, with solid (black) lines showing protein-protein interactions identified in this screen, solid (grey) lines are interactions identified by the software and dotted lines are interactions at transcriptional level.

a)

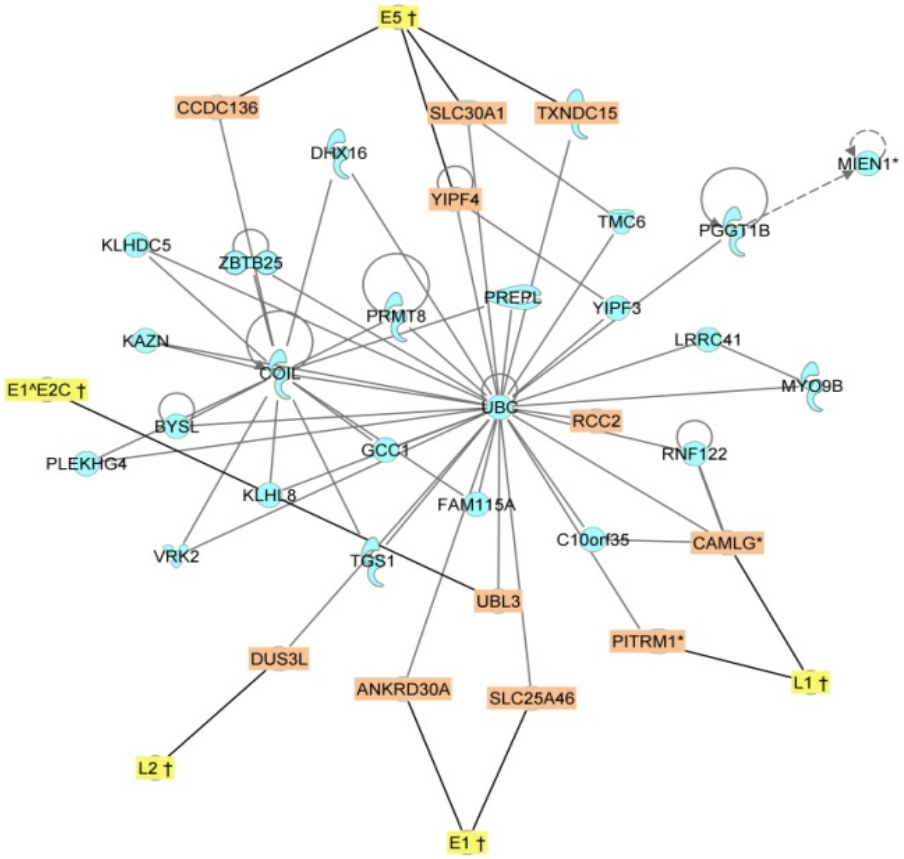
E5 †
CCDC136
SLC30A1
TXNDC15
DHX16
MIEN1*
YIPF4
TMC6
PGGT1B
KLHDC5
ZBTB25
PREPL
YIPF3
PRMT8
KAZN
LRRC41
COIL
MYO9B
E1^E2C †
UBC
BYSL
RCC2
GCC1
RNF122
PLEKHG4
KLHL8
FAM115A
C10orf35
CAMLG*
VRK2
TGS1
UBL3
PITRM1*
DUS3L
L1 †
ANKRD30A
SLC25A46
L2 †
E1 †

b)

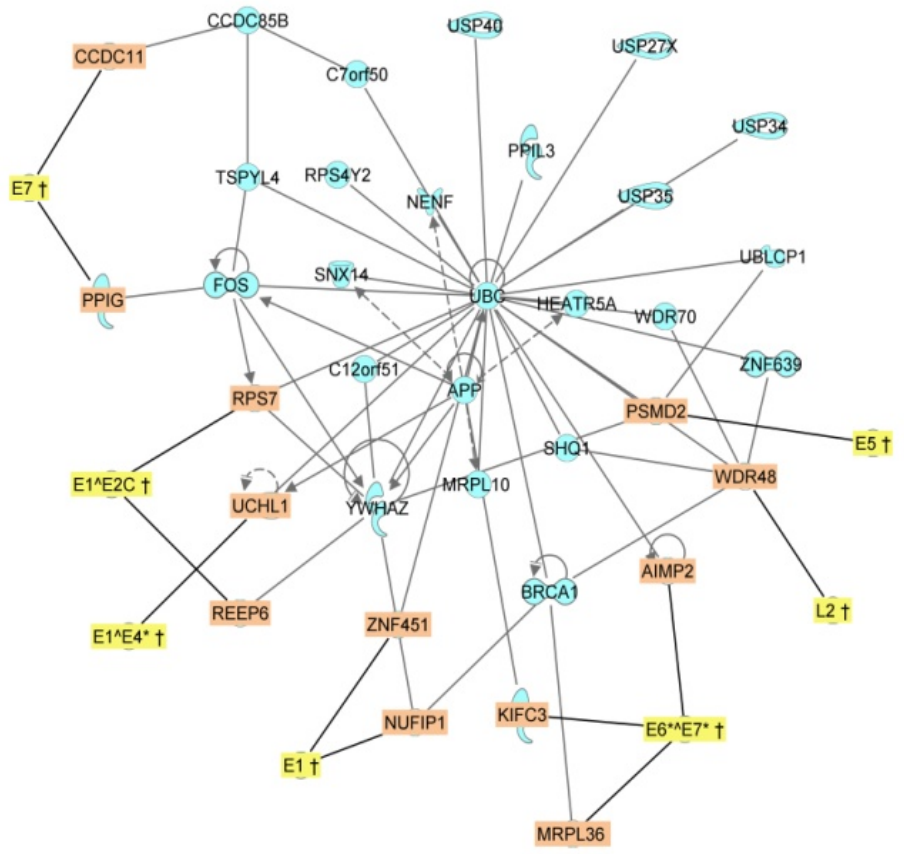
CCDC85B
USP40
USP27X
CCDC11
C7orf50
USP34
PPIL3
E7 †
TSPYL4
RPS4Y2
NENF
USP35
UBLCP1
SNX14
FOS
PPIG
UBC
HEATR5A
WDR70
ZNF639
C12orf51
APP
RPS7
PSMD2
E5 †
SHQ1
E1^E2C †
MRPL10
WDR48
UCHL1
YWHAZ
AIMP2
BRCA1
L2 †
REEP6
E1^E4* †
ZNF451
NUFIP1
KIFC3
E6*^E7* †
E1 †
MRPL36

c)

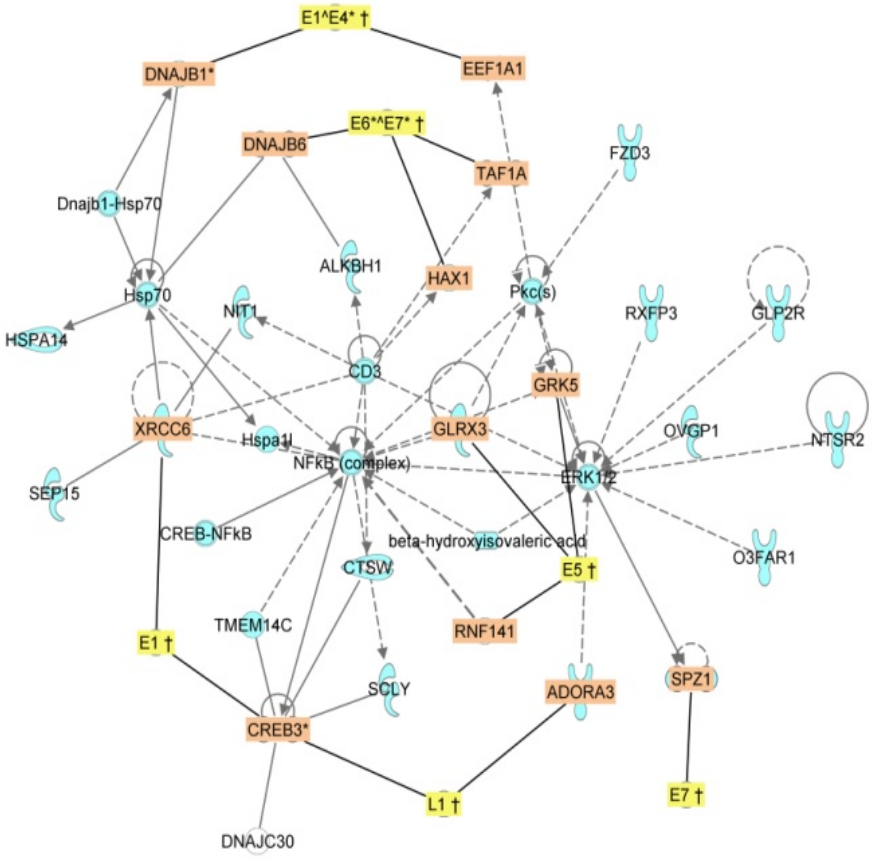
E1^E4* †
DNAJB1*
EEF1A1
E6*^E7* †
DNAJB6
TAF1A
FZD3
Dnajb1-Hsp70
ALKBH1
HAX1
Pkc(s)
Hsp70
NIT1
RXFP3
GLP2R
HSPA14
CD3
GRK5
XRCC6
Hspa1l
GLRX3
OVGP1
NTSR2
NFkB (complex)
ERK1/2
SEP15
CREB-NFkB
beta-hydroxyisovaleric acid
O3FAR1
CTSW
E5 †
TMEM14C
RNF141
E1 †
SCLY
ADORA3
SPZ1
CREB3*
L1 †
E7 †
DNAJC30

d)

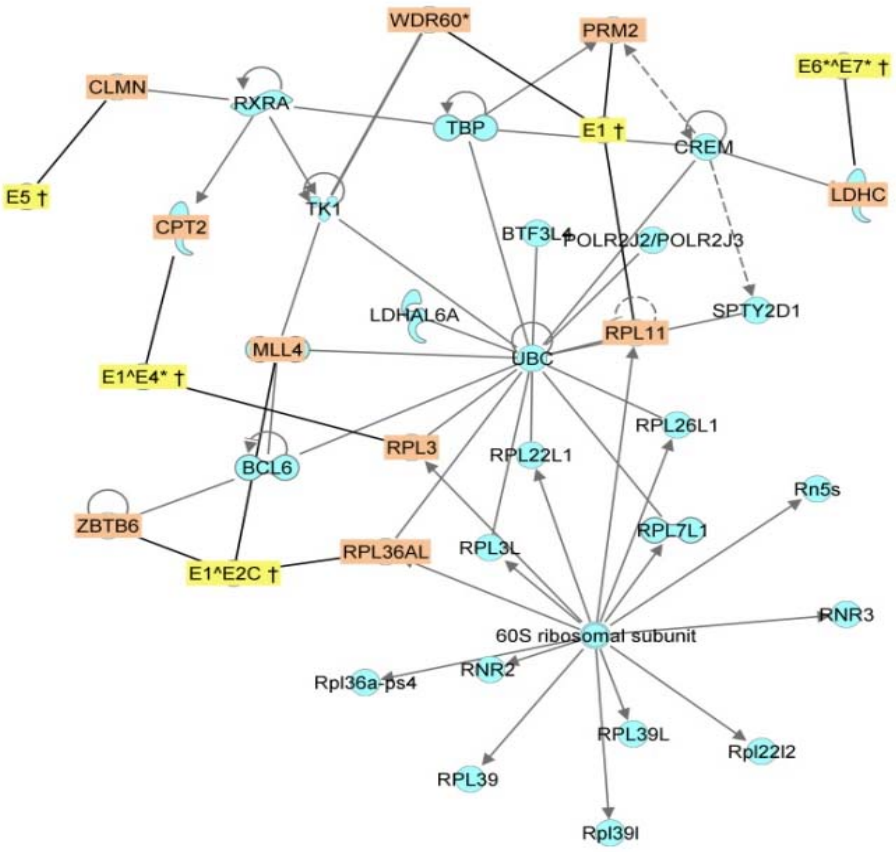
WDR60*
PRM2
E6*^E7* †
CLMN
RXRA
TBP
E1 †
CREM
E5 †
LDHC
TK1
CPT2
BTF3L4
POLR2J2/POLR2J3
LDHAL6A
SPTY2D1
RPL11
MLL4
UBC
E1^E4* †
RPL26L1
RPL3
RPL22L1
BCL6
Rn5s
ZBTB6
RPL7L1
RPL36AL
RPL3L
E1^E2C †
RNR3
60S ribosomal subunit
RNR2
Rpl36a-ps4
RPL39L
Rpl22l2
RPL39
Rpl39l

Figure 5.2: Interaction networks of HPV interacting proteins. Four functional networks representing the functional interactions of HPV binding proteins identified in the Y2H screen created by Ingenuity Pathway Analysis software. The maps correspond to proteins involved in a) infectious and dermatological diseases, and cellular development, b) Cancer, cell-to-cell signalling and renal and urological disorders, c) Inflammatory response and respiratory system development and function, d) Cancer, haematological disease and cellular development. Each node (cyan) represents a protein, with the shapes corresponding to the type of protein according to the software. HPV proteins are highlighted in yellow, and interacting partners identified in this screen are highlighted in orange. Each line represents an interaction, with solid (black) lines showing protein protein interactions identified in this screen, solid (grey) lines are interactions identified by the software and dotted lines are interactions at transcriptional level.

Diseases and Disorders

Name	p-value	Proteins
Neurological Disease	0.00016 - 0.0478	ADORA3, DNAJB1, DNAJB6, EEF1A1, GRK5, HAX1, RPL3, UCHL1, XRCC6
Skeletal and Muscular Disorders	0.00016 - 0.0176	ADORA3, DNAJB1, DNAJB6, EEF1A1, RPL3, UCHL1, XRCC6
Developmental Disorder	0.00026 - 0.0285	ADORA3, CPT2, HAX1, RPL11, RPS7, XRCC6
Haematological Disease	0.00026 - 0.0435	CPT2, HAX1, RPL3, RPL11, RPS7,
Hereditary Disorder	0.00026 - 0.0290	CPT2, DNAJB6, GRK5, HAX1, RPL11, RPS7, UCHL1, XRCC6

Molecular and Cellular functions

Name	p-value	Proteins
Post-Translational Modification	0.00213 -0.0 478	DNAJB1, GRK5, UCHL1,WDR48
Carbohydrate Metabolism	0.00222 -0.0456	ADORA3, EEF1A1, GRK5
Cell Morphology	0.00222 -0.0341	ADORA3, EEF1A1, XRCC6
Cellular Function and Maintenance	0.00222 – 0.0478	CAMLG, DNAJB6, EEF1A1, GRK5, KIFC3, PSMD2, SLC30A1, XRCC6, WDR48
DNA Replication, Recombination, and Repair	0.00222 – 0.0285	DNAJB1, PRM2, XRCC6

Physiological system development and function

Name	p-value	Proteins
Respiratory System Development and Function	0.000367 – 0.000367	ADORA3, GRK5
Hematological System Development and Function	0.00427 – 0.0475	ADORA3, CAMLG, HAX1, XRCC6
Humoral Immune Response	0.00427 – 0.0475	CAMLG, HAX1, XRCC6
Lymphoid Tissue Structure and Development	0.00427 – 0.00427	CAMLG, HAX1
Tissue Morphology	0.00427 – 0.0478	ADORA3, CAMLG, DNAJB6, HAX1, XRCC6

Table 5.1: Functional analysis of the HPV interactome. The functional analysis of the interactome dataset was performed to identify the biological functions and diseases that were most significant to the proteins in the dataset. Right-tailed Fisher's exact test was used to calculate a p-value determining the probability that each biological function and/or disease assigned to that network is due to chance alone. The proteins involved in each of the functions are listed.

5.2.2 Validation of interactions by LUMIER assay

In order to validate the interactions identified by Y2H, the LUMIER assay was performed for a subset of interactions. Out of the 54 interactions detected, cDNA clones expressing 37 of the proteins were obtained in pDONR223 vector. The genes were cloned into LUMIER vectors, pRenilla and pTREX-dest as described in Section 2.2.1.1. LUMIER assay for five interactions were performed at DKFZ, Heidelberg by Kerstin Mohr as described in Section 2.2.6.9.1 (Figure 5.3a). The remaining interactions were tested by me with a variation in analysis as described in Section 2.2.6.9.2 (Figure 5.3b). In DKFZ, the mean and standard deviations for the interactions were calculated from large datasets of protein pairs which were not expected to interact, i.e. from negative reference sets. Due to unavailability of a large dataset of non-interacting pairs, the mean and standard deviation was interactions performed by me were calculated from the entire dataset obtained from testing of protein pairs identified in the Y2H screen.

A known interaction between JUN and FOS in both cases was used as positive control and a z-score of >1 was considered a weak interaction and >1.5 as strong interaction. Nine of the interactions tested were validated LUMIER assay. These interactions are listed in Table 5.2. Among these, the highest z-score (=5) was found for an interaction between E7 and spermatogenic leucine zipper 1 (SPZ1). Being a proto-oncogene, SPZ1 was found to be a suitable candidate for further investigation (Chapter 6).

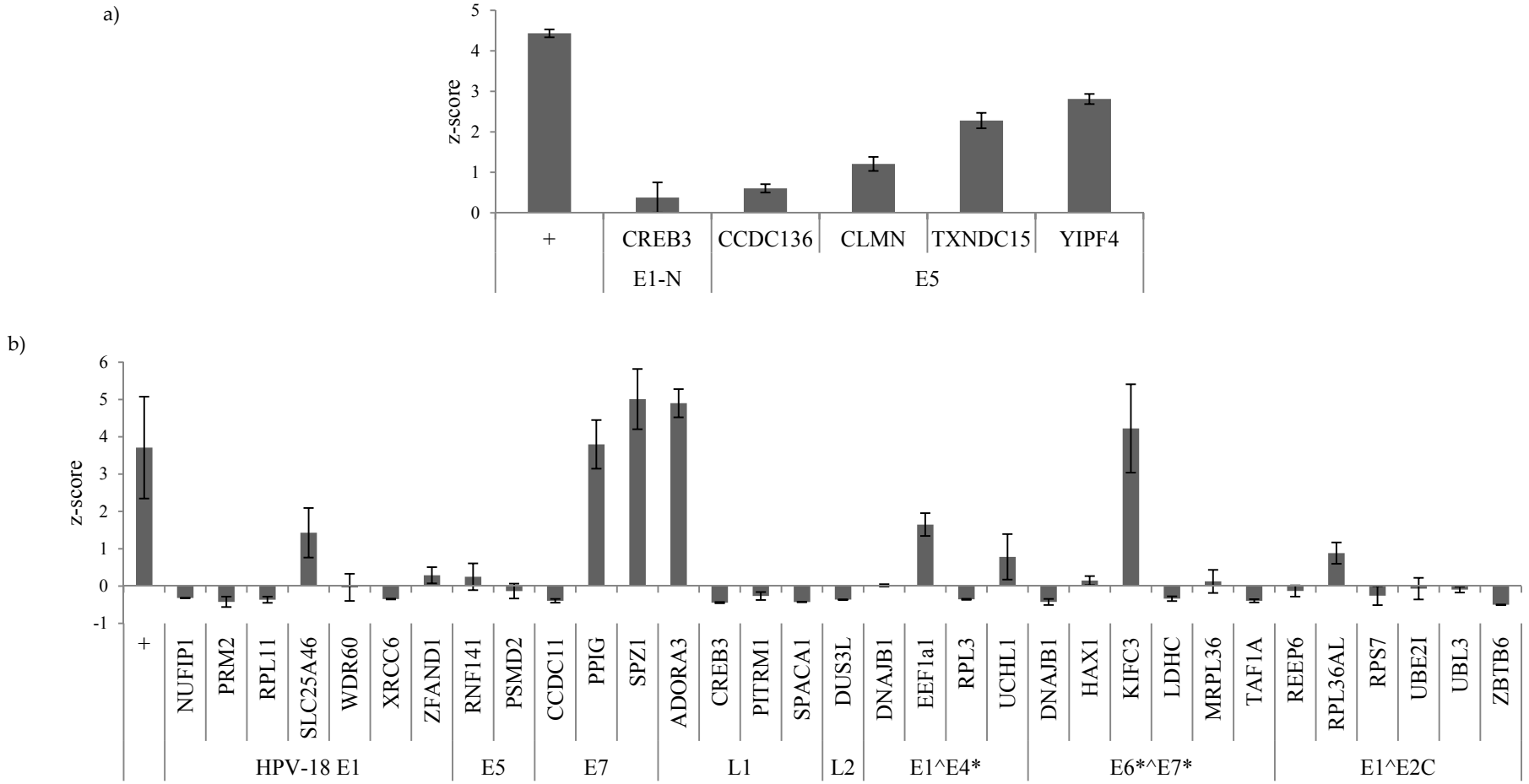

Figure 5.3: Confirmation of Y2H interactions using LUMIER assay. Virus-host interactions were tested by LUMIER assay in DKFZ (a) or in DPM (b) and observed luminescence is presented as z-score. A known interaction between JUN and FOS was used as positive control (+). Error bars represent standard deviation of triplicates in one representative experiment. z-score >1 represents positive interaction.

HPV proteins	Cellular proteins
HPV-18 E1	SLC25A46
HPV-16 E5	CLMN
HPV-16 E5	TXNDC15
HPV-16 E5	YIPF4
HPV-16 E7	PPIG
HPV-16 E7	SPZ1
HPV-16 L1	ADORA3
HPV-16 E1^E4*	EEF1A1
HPV-16 E6*^E7*	KIFC3

Table 5.2: List of validated HPV-host interactions. Validation of HPV-host interactions were performed by the LUMIER assay and the positive validated interactions are listed in the table.

5.3 Discussion

5.3.1 Virus-host interactome of HPV

Y2H is a very important tool in high-throughput studies due to its simplicity and cost-effectiveness. The Y2H screen performed in this study identified 54 interactions with nine of the thirteen HPV proteins tested. No interactions were identified with the HPV proteins E4, E1^E4, E6 and E6*^E4 despite sequence and restriction analysis verification of the bait clones. No interactions were seen with the E4, E6 and E6*^E4 proteins in the previous Y2H screens described in Chapter 3 and Chapter 4. There are several possible reasons for this: (i) it is possible that there was a spontaneous mutation in the GAL4 DNA-binding domain of the proteins which prevent binding of the fusion protein to the GAL4 promoter; (ii) the protein could be incorrectly folded or the fusion caused expression of unstable protein; (iii) there could be unforeseen technical issues while these screens were performed; (iv) the 3-AT concentration used for the screen could be too high which resulted in no interacting partners being detected. In order to test if this was due to a problem in expression of the bait proteins, western blot analysis or a more recent approach based on interaction with RanBPM (214) needs to be performed which could not be done within the time frame of this thesis.

Among the protein interactions observed in the screen, some have been previously identified, in particular, E1^E2C with Ubiquitin conjugating enzyme UBE2I (215), E1 and Zinc finger protein ZNF451 (215), and E5 and Zinc transporter ZnT1 (also known as SLC30A1)(216). The other 51 interactions identified were novel, out of which 38 were selected for validation by LUMIER assay in mammalian cell system. Some of these were tested in DKFZ while most were tested by me. Experiments carried out here were analysed using the complete dataset of the interactions tested in this study. As this dataset is biased towards previously identified interactions, the mean and the standard deviation is higher compared to a random dataset of non-interacting pairs (as used in DKFZ for calculation shown in data presented in Figure 3.3**,** Figure 4.4 and Figure 5.3a). This method of analysis therefore results in a relatively high cut-off and correspondingly low validation rate (29 %). Additionally a previously published interaction between E1^E2C and UBE2I was found negative in the LUMIER assay which can be attributed to false negatives in the system. Additional use of a range of different protein-protein interaction techniques such as co-immunoprecipitation, protein complementation assays (140) will enable further validation of the dataset and is something of interest for future studies.

5.3.2 Protein interactions of interest

While it is relatively easy to discover interactions using high-throughput assays, it is extremely time consuming and expensive to identify the functional relevance of these interactions. This study identified nine potentially relevant interactions (Table 5.2). The E1 protein interacted with a member of mitochondrial solute carrier family SLC25A46 (217). Member of the mitochondrial solute carrier family are localised in the mitochondria and transport molecules such as ATP/ADP, amino acids, malate, ornithine, and citruline (218). Although not much is known about the function of SLC25A46, other members of the SLC family are implicated in cell proliferation and cancers such as SLC25A43 (219)(220). Further investigation of this interaction might provide insights into the function of this member of the family and its role in HPV mediated cancers.

The E5 protein interacts with transmembrane proteins CLMN, TXNDC15 and YIPF4. Calmin (CLMN) contains a calponin homology (CH) domain at its N-terminal and a transmembrane domain at its C-terminus (221). The CH domain was first identified as a 100 aa actin binding region of calponin. This domain has since been identified in other signalling molecules and was proposed to be responsible for linking signal transduction molecules to the actin cytoskeleton (222). Although CLMN has homology to members of CH domain family, it is the only known member having a transmembrane region (221). The E5 protein is known to disrupt the actin cytoskeleton (223). CLMN might be an interesting interacting partner of E5 in this regard. Another interactor of E5, TXNDC15 is a thioredoxin domain containing protein involved in various redox reactions. A member of this family, TXNDC5, which is upregulated in cancers such as colorectal cancer (224) is shown to interact with HPV-16 E7, but the functional relevance of this interaction remains unknown (215). The interactions of E5 might provide evidence of an involvement of HPV in redox reactions.

Thirdly, YIPF4 is a member of the YIP domain containing proteins involved in transport of solutes across endoplasmic reticulum and golgi apparatus (225). The biological relevance of this interaction is currently being investigated in collaboration with Dr Andrew Macdonald at The University of Leeds.

The L1 protein interacts with an adenosine A3 receptor ADORA3, which belongs to a family of G protein coupled receptors involved in a variety of intracellular signaling pathways and physiological functions. ADORA3 mediates both cell proliferation and cell death (226) and is overexpressed in tumour cells and shown to be a possible target for therapeutics (227)(228). Its interaction with L1 might shed some light into this direction.

EEF1a1, eukayotic translation elongation factor 1 alpha 1(also known as, cervical cancer suppressor 32 or prostate tumour inducing protein) is responsible for the enzymatic delivery of aminoacyl tRNAs to the ribosome. It is a marker for cellular senescence (229). It is known to cause suppression of cell growth and induction of apoptosis when over expressed in cervical cancer cell lines (230). It is also involved in nuclear transport of machinery (231). HPV-38 E7 interacts with EEF1a1 for increasing cell proliferation (232). Its interaction with

E1^E4* therefore is a very relevant and investigation of this interaction will increase the understanding of its role.

KIFC3, Kinesin family member C3 belongs to a family of molecular motors involved in transport of cellular cargos across microtubules (233). KIFC3 plays a role in golgi positioning (234). Kinesins are implicated in several cancers and overexpression of KIFC3 in breast cancer cell line leads to resistance to docetaxel chemotherapy (235,236). Its interaction with E6*^E7* may implicate a role in tumour progression. It would also interesting to know if it interacts with E6 or E7 proteins as the splice variant contains both fragments.

The E7 protein interacts with cyclophilin G also known as peptidyl prolyl isomerase (PPIG). Cyclophilins are a class of proteins that were originally identified as intracellular receptors for immunosuppressive drug cyclosporin A (237). Since then they have been attributed to peptidyl prolyl isomerise activity and protein folding and have been shown to have a role in several cancers (238). It would be interesting to see how the interaction of E7 with PPIG is relevent to HPV induced cancers. Another interactor of E7 that has been further investigated in Chapter 6 is a proto-oncogene spermatogenic leucine zipper protein (SPZ1).

The Y2H screen presented in this Chapter provides a list of interesting interactions and opens up avenues for future work. It is necessary to perform additional validation of the interactions using other protein-protein interaction techniques such as co-immunoprecipitation, protein complementation assays (140). Also, the biological elucidation of the nine potentially interesting interactions will provide a better understanding of the biology of the virus and its effect on the host.

Chapter 6:

Elucidation of E7- SPZ1 interaction

6.1 Introduction

Spermatogenic leucine zipper protein (SPZ1) was first isolated in mouse testis (239). It is a basic helix-loop-helix leucine zipper transcription factor (bHLH-ZIP) that binds to E-box and G-box domains in the promoter regions of genes. The family of bHLH-ZIP proteins also contains other transcription factors such as MYC and MAX (240).

SPZ1 acts as a proto-oncogene via the MAPK pathway. It is phosphorylated by ERK1/2 and in turn binds to proliferative cell nuclear antigen (PCNA) promoter and induces cell proliferation. *SPZ1*-transfected cells can form foci on soft agar and develop tumours in nude mice (241). Furthermore, high levels of SPZ1 have been detected in murine tumour cell lines and in human brain tumour samples (242). Overexpression of SPZ1 in transgenic mice caused an increase in cell proliferation and reduction in spermatogenesis and fertility (241).

One of the direct protein interactions known for SPZ1 is with protein phosphatase 1 (PP1) (243). PP1 dephosphorylates a wide range of substrates with the help of catalytic subunits PP1c. There are four isoforms of PP1c in mammalian cells, α, β, $\gamma 1$ and $\gamma 2$, and these isoforms interact with several regulatory subunits which enhance its substrate specificity. It is believed that SPZ1 might be a novel regulatory subunit of PP1cγ2 (243) although its target specificity is unknown. All isoforms of PP1c are known to bind and dephosphorylate tumour suppressor retinoblastoma protein (RB) (244) thereby competing with CDKs to maintain control over cell cycle (244).

The virus host screen presented in Chapter 5 identified SPZ1 as a cellular target for HPV-16 E7 which was confirmed in mammalian LUMIER assay. Being a proto-oncogene, its interaction with E7 might play an important role in HPV pathogenesis. The aim of the work presented in this Chapter is to elucidate the biological mechanism and function of this interaction and to improve our limited understanding of the protein in order to explore diagnostic and therapeutic opportunities for cervical cancer.

6.2 Results

6.2.1 Comparison of SPZ1 interactions with E7 from different HPV types

In order to compare the relative affinities of interaction between SPZ1 and E7 from different HPV types, human and mouse SPZ1 were cloned into the Y2H prey vector as described in Section 2.2.1.1. These were then tested for interaction with E7 from high-risk HPV types -16, -18, -45 and low-risk type -11 (Figure 6.1). A strong interaction was seen for both human and mouse SPZ1 with E7 from the high-risk types. However, E7 from the low-risk HPV type -11 showed reduced interactions suggesting that the interaction affinity with SPZ1 was a characteristic of the high-risk HPV types.

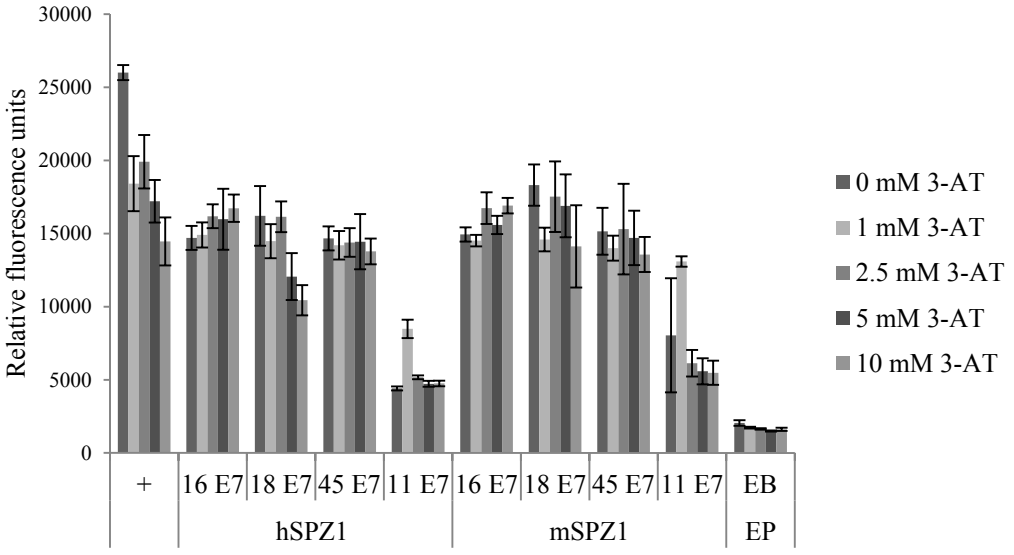

Figure 6.1: Interaction of SPZ1 with E7 from different HPV types. Interactions of human (hSPZ1) and mouse SPZ1 (mSPZ1) with E7 baits from HPV types -16, -18, -45 and -11 were tested. A known interaction between MYC and MAX proteins was used as positive control (+) and interaction between empty bait (EB) and prey (EP) protein was used as negative control. Relative fluorescence units were measured for five different inhibitor 3-AT concentrations (0 mM, 1 mM, 2.5 mM, 5 mM and 10 mM). Error bars represent standard deviation of quadruplicates in one representative experiment.

6.2.2 Mapping of the SPZ1 interaction domain on E7

In order to identify and map the interaction domains on E7 necessary for SPZ1 binding, mutants of HPV-16 E7 previously described in Section 3.2.4.1 were tested for interaction with SPZ1 by Y2H screen (Figure 6.2a). Mutants M2, M3, M4 retained over 80 % interaction affinities as compared to wild-type E7. The M4 mutant, comprising only of CRII domain and M2 and M3 which also retain the CRII domain are able to interact with SPZ1. The M5 mutant, which lacks the CRII domain has reduced interaction affinity (50 % at 10 mM concentration of inhibitor 3-AT). The M6 mutant, which lacks the CRII domain and amino acids 38-52 of CRIII showed significantly reduced interaction which is similar to interaction of SPZ1 to empty bait (Figure 6.2b). These data suggest that the CRII domain spanning amino acids 15-32 and possibly additional amino acids within 38-52 in CRIII play a role in SPZ1 interaction. The CRII domain of E7 contains an LxCxE domain necessary for binding RB (76) and therefore, it was hypothesized that this domain might also be involved in its interaction with SPZ1. E7 with mutant C24G within the LxCxE domain was cloned into pGBK-T7 plasmid as described in Section 2.2.1.1 and tested for interaction with SPZ1 by Y2H (Figure 6.2c) and co-immunoprecipitation (Figure 6.2d). E7 C24G retained its ability to interact with SPZ1 in indicating that the LxCxE domain is not involved in this interaction.

a)

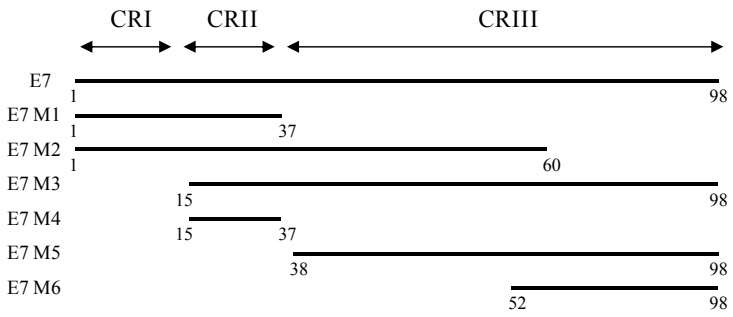
CRI
CRII
CRIII
E7
1
98
E7 M1
1
37
E7 M2
1
60
E7 M3
15
98
E7 M4
15
37
E7 M5
38
98
E7 M6
52
98

b)

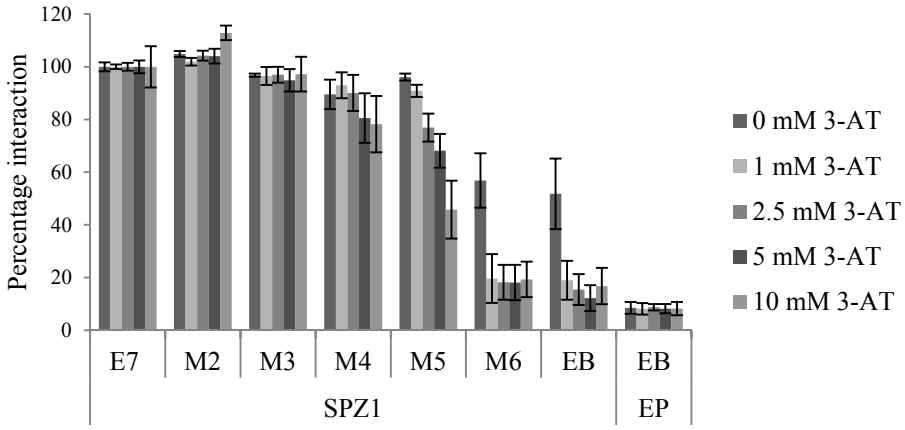
Percentage interaction
120
100
80
60
40
20
0
E7
M2
M3
M4
M5
M6
EB
EB
SPZ1
EP
0 mM 3-AT
1 mM 3-AT
2.5 mM 3-AT
5 mM 3-AT
10 mM 3-AT

c)

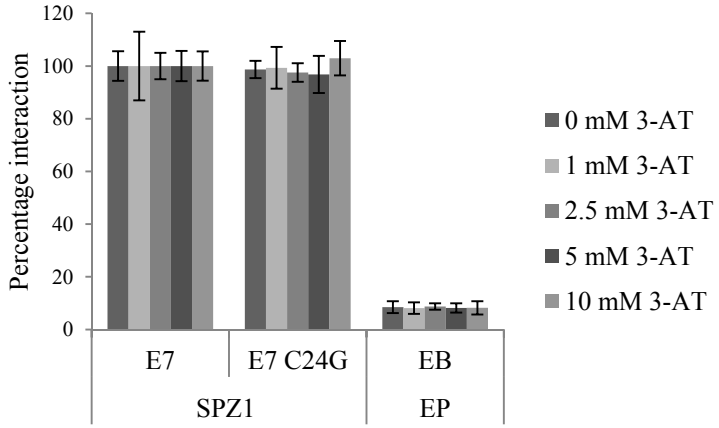
Percentage interaction
120
100
80
60
40
20
0
E7
E7 C24G
EB
SPZ1
EP
0 mM 3-AT
1 mM 3-AT
2.5 mM 3-AT
5 mM 3-AT
10 mM 3-AT

d)

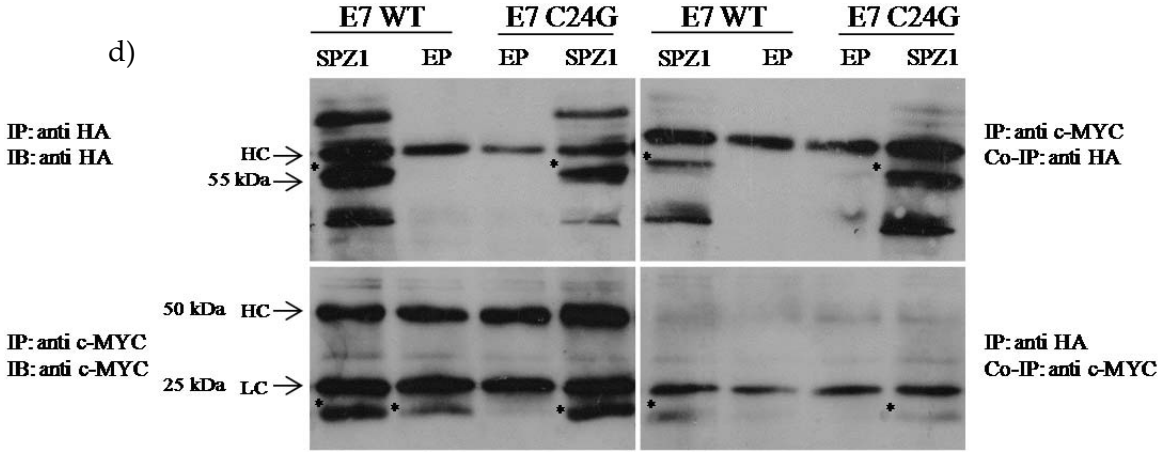
E7 WT
E7 C24G
E7 WT
E7 C24G
SPZ1
EP
EP
SPZ1
SPZ1
EP
EP
SPZ1
IP: anti HA
IB: anti HA
HC
55 kDa
IP: anti c-MYC
Co-IP: anti HA
50 kDa
HC
IP: anti c-MYC
IB: anti c-MYC
25 kDa
LC
IP: anti HA
Co-IP: anti c-MYC

Figure 6.2: Mapping of interaction domains of SPZ1 on E7. a) Schematic representation of the E7 deletion mutants. Interactions between b) E7 deletion mutants and SPZ1; and c) SPZ1 with E7 C24G was tested by Y2H assay. Relative fluorescence units were measured for five different 3-AT concentrations (0 mM, 1 mM, 2.5 mM, 5 mM, 10 mM). All interactions were normalised to positive control of wild-type E7 and SPZ1 (arbitrarily set to 100) for each 3-AT. Interaction between SPZ1 and empty bait (EB) and empty bait and empty prey (EP) were performed as negative controls. Error bars represent standard deviation of quadruplicates in one representative experiment. d) Co-immunoprecipitation of c-MYC tagged E7 and E7 C24G with HA tagged SPZ1 was performed and cell lysates **i**mmunoprecipitated (IP) with c-MYC and HA antibodies were lysed with 2 x laemelli buffer, separated on 15 % polyacrylamide gels and immunoblotted (IB) with either anti c-MYC or anti HA antibody as indicated. Both E7 and E7 C24G were tested for interaction with empty prey (EP) to rule out unspecific binding. The heavy (HC) and light chains (LC) of anti c-MYC and anti HA antibodies can be seen and are indicated by arrows. Specific bands corresponding to E7, E7 C24G and SPZ1 are indicated with *. The molecular weights are shown on the left.

6.2.3 Mapping the E7 interaction domain on SPZ1

In order to identify the E7 binding domain on SPZ1, three deletion mutants encompassing the bHLH domain and the leucine zipper domain were generated as described in Section 392.2.1.1 using sequence specific primers (Appendix 1) (Figure 6.3).

a)

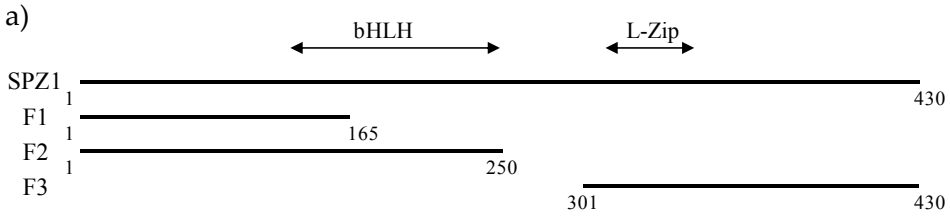

b)

Fragment	Amino acids	Domains
SPZ1	1-430	Full-length
SPZ1 F1	1-165	N-terminus
SPZ1 F2	1-250	bHLH domain
SPZ1 F3	301-430	Leucine zipper domain

Figure 6.3: Generation of SPZ1 deletion mutants. a) Schematic representation of the SPZ1 deletion mutants with the basic helix-loop-helix (bHLH) and the leucine zipper (L-Zip) domains shown above and the mutant fragments below. Number corresponding to the amino acids are shown b) The amino acids and domains spanned by each SPZ1 deletion mutant are listed.

The mutants were cloned into pGAD-T7 and tested for interaction with wild-type E7, E7 M4 (which was sufficient for interaction), and E7 M6 (which lacked the interaction with SPZ1) (Figure 6.4). SPZ1 mutants F1 and F2 showed a 50 % reduction in interaction affinity with all of the E7 fragments, however mutant F3 retained nearly 100 % interaction with E7 and M4 but not with M6 suggesting that the interaction domain of E7 is within the SPZ1 F3 fragment which comprises of the amino acids 301-430.

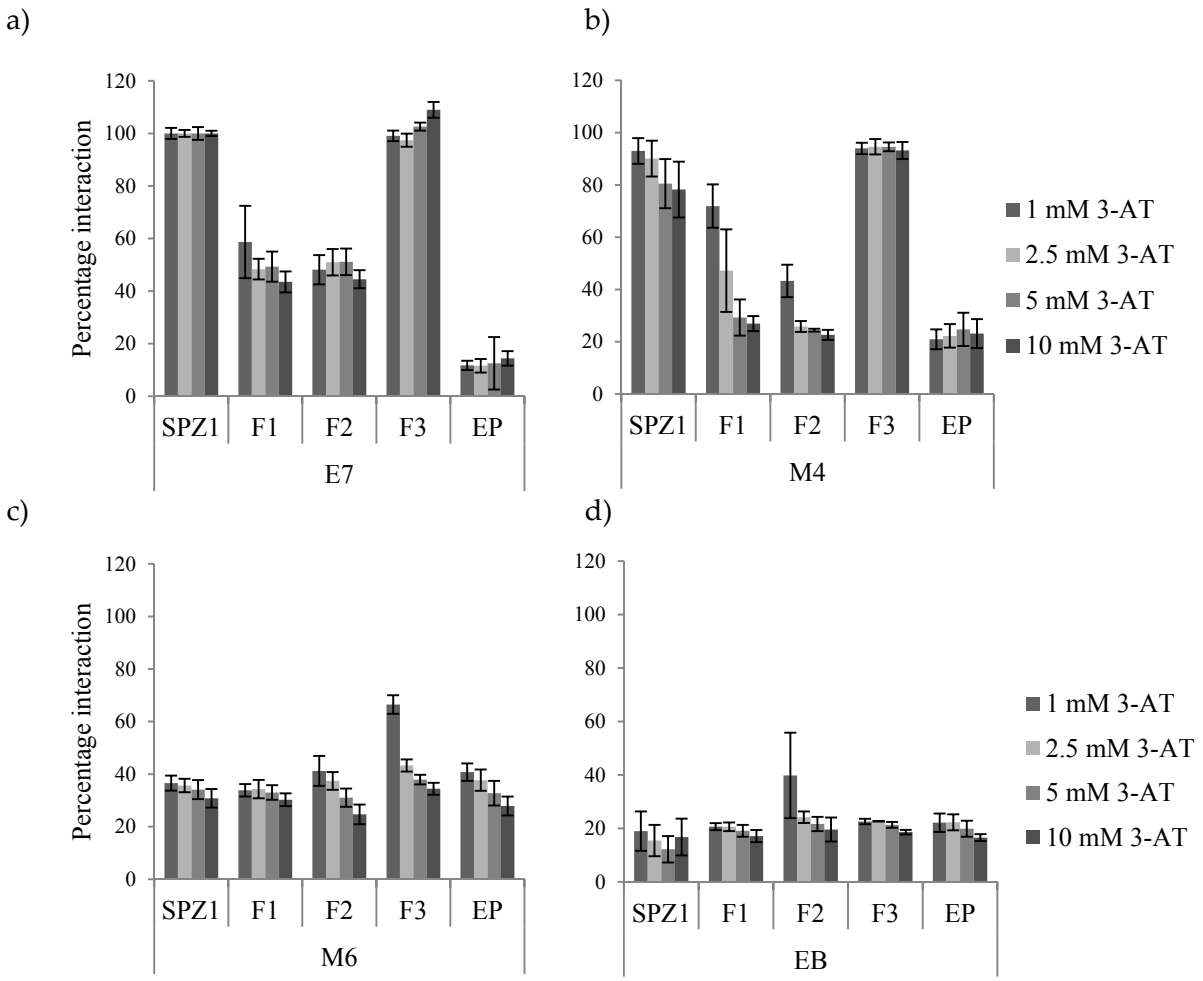

Figure 6.4: Mapping of the E7 interaction domain on SPZ1. The SPZ1 deletion mutants were tested for interaction with a) E7, b) M4, c) M6, d) empty bait (EB) using the Y2H assay. Relative fluorescence units were measured for four different 3-AT concentrations (1 mM, 2.5 mM, 5 mM, 10 mM). All interactions were normalised to positive control of wild-type E7 and SPZ1 interaction (arbitrarily set to 100) for each 3-AT. Each E7 bait was tested against empty prey (EP). Additionally, interaction between empty bait (EB) and empty prey (EP) was performed as negative control. Error bars represent standard deviation of quadruplicates in one representative experiment.

Since the fragment F3 contains a leucine zipper domain, it was hypothesized that mutations in the leucine residues could abrogate the interaction. In order to test this, four mutants were generated by site-directed point mutagenesis as described in Section 2.2.1.2 using pDONR223 SPZ1 as template and specific primers (Appendix 1). The mutants L1, L2 and L3 were generated using specific primers containing the desired mutation and sequence verified. L4 was generated by using the L1 mutant as template and the primer set for L2 (Figure 6.5). The mutants were then cloned into the Y2H prey vector and tested for interaction with E7 and EB using Y2H assay. Mutations of the leucine residues did not abrogate the interaction (Figure 6.5d) suggesting that the interaction domain might be on the

C-terminal region of the leucine zipper domain or mutations of all the leucine residues is needed to block this interaction.

a)

```
  1 MASSAKSAEM PTISKTVNPT PDPHQEYLDP RITIALFEIG SHSPSSWGSL PFLKNSSHQV
 61 TEQQTAQKFN NLLKEIKDIL KNMAGFEEKI TEAKELFEET NITEDVSAHK ENIRGLDKIN
121 EMLSTNLPVS LAPEKEDNEK KQEMILETNI TEDVSAHKEN IRGLDKINEM LSTNLPVSLA
181 PEKEDNEKKQ QMIMENQNSE NTAQVFARDL VNRLEEKKVL NETQQSQEKA KNRLNVQEET
241 MKIRNNMEQL LQEAEHWSKQ HTELSKLIKS YQKSQKDISE TLGNNGVGFQ TQPNNEVSAK
301 HELEEQVKKL SHDTYSLQLM AALLENECQI LQQRVEILKE LHHQKQGTLQ EKPIQINYKQ
361 DKKNQKPSEA KKVEMYKQNK QAMKGTFWKK DRSCRSLDVC LNKKACNTQF NIHVARKALR
421 GKMRSASSLR
```

b)

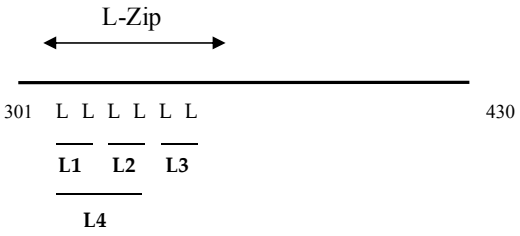

c)

Fragment	Mutation
SPZ1 L1	303, 310 L-A
SPZ1 L2	317, 324 L-A
SPZ1 L3	331, 338 L-A
SPZ1 L4	303, 310, 317, 324 L-A

d)

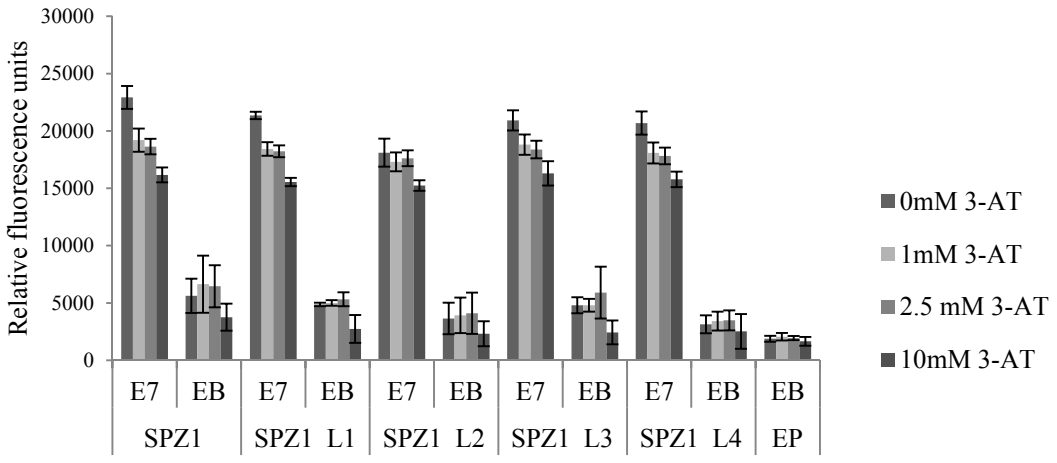

Figure 6.5: Interaction of SPZ1 leucine zipper mutants with E7. a) Sequence of SPZ1 with highlighted leucine residues that make up leucine zipper domain. b) Schematic representation of the leucine zipper domain (L-Zip) and the mutants generated. c) List of leucine residues mutated to alanine in each mutant. d) Interactions of SPZ1 leucine zipper mutants with E7 and empty bait (EB). Interaction between empty bait and prey protein was used as negative control. Relative fluorescence units were measured for four different inhibitor 3-AT concentrations (0 mM, 1 mM, 2.5 mM and 10 mM). Error bars represent standard deviation of quadruplicates in one representative experiment.

6.2.4 SPZ1 expression in HPV positive cell lines

SPZ1 was originally discovered in testis and its overexpression in several cancers has been reported (239). In order to check whether SPZ1 is expressed in cervical epithelial cells, western blot analysis was done using three cervical cancer cell lines - HeLa, CaSki and SiHa. HeLa cells contain 25-50 copies of integrated HPV-18 genome (245) whereas SiHa cells contain one to two copies and CaSki cell have about 600 copies of integrated HPV-16 genome per cell (246). Western blot analysis of equal protein amounts showed that HeLa cells express more SPZ1 compared to CaSki or SiHa cells (Figure 6.6a). Confocal microscopy of the three cell lines was performed as described in Section 2.2.6.7 which showed expression of SPZ1 in both nucleus and cytoplasm (Figure 6.6b) as previously described for other cell types (247).

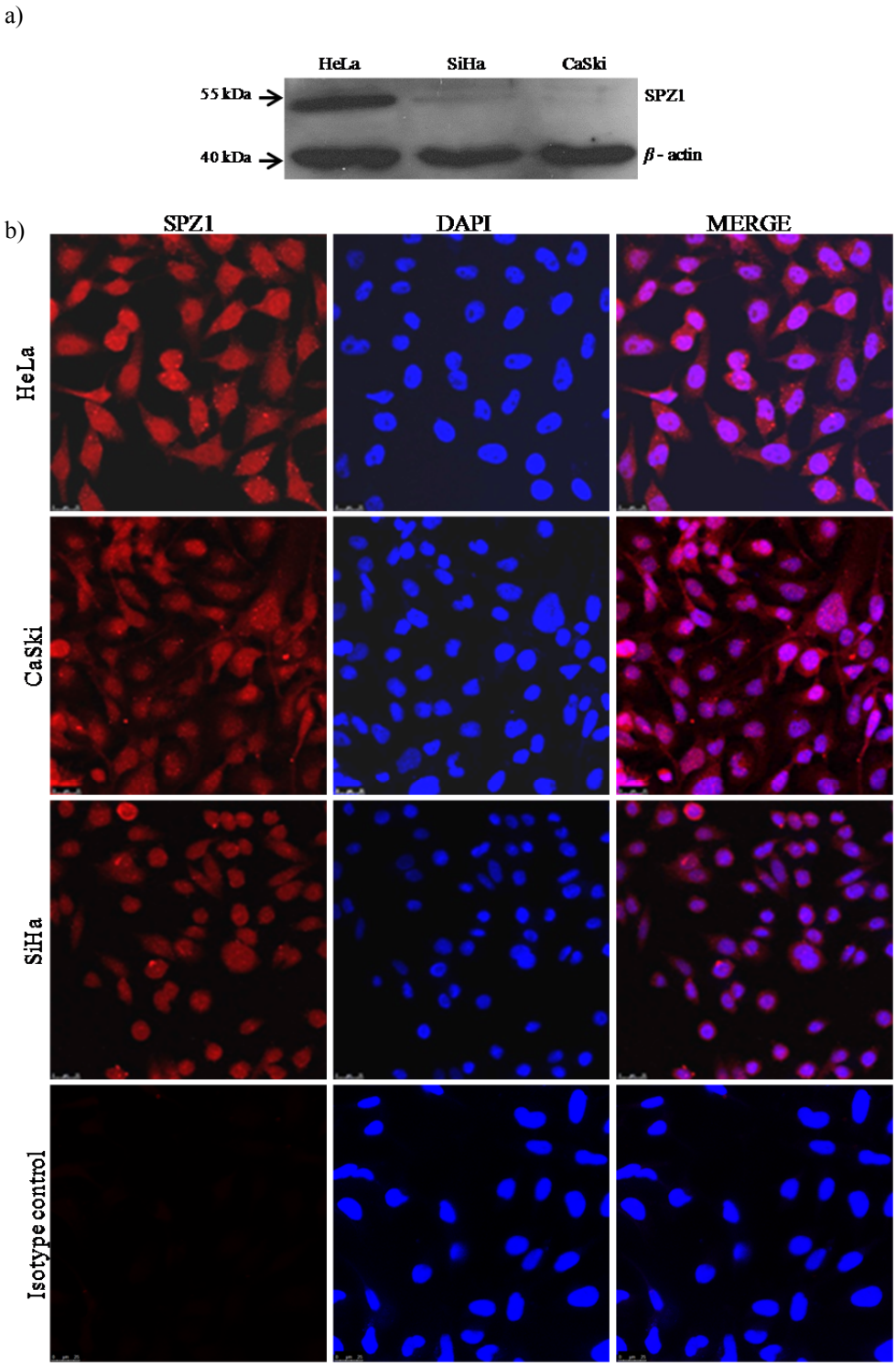

Figure 6.6: Expression of SPZ1 in cervical cancer cell lines. a) Western blot with human anti-SPZ1 was performed by isolating total cellular protein from cell lines HeLa, SiHa and CaSki. 50 µg of each protein extract was separated using SDS-PAGE followed by transfer onto nitro-cellulose membrane and immunoblotted with anti-SPZ1 antibody and anti-ACTIN antibody. b) Confocal microscopy was performed to visualise SPZ1 in HeLa, SiHa and CaSki cells. A rabbit isotype control was used in HeLa cells to check for unspecific binding of the antibody. The cells were fixed and stained with rabbit anti SPZ1 primary or rabbit isotype control (as indicated) and anti rabbit Alexa fluor 680 dye conjugated secondary antibody (red colour) for SPZ1 and DAPI staining to indicate nucleus. Images were taken using Leica SP5 confocal microscope using a 63.0X objective lens.

6.2.5 Colocalization of E7 and SPZ1

In order to check whether E7 and SPZ1 co-localize, confocal microscopy was performed as described in Section 2.2.6.7 .The cytoplasmic and nuclear localisation of SPZ1 previously described (248). The E7 protein is known to shuttle between nucleus and cytoplasm depending on cell confluence and cell cycle stage (249). HeLa cells were transfected with PCR3 plasmid expressing N-terminal HA tagged HPV-16 E7 and confocal microscopy was performed. Co-localization of E7 and SPZ1 can be seen both in the nucleus and cytoplasm (Figure 6.7b).

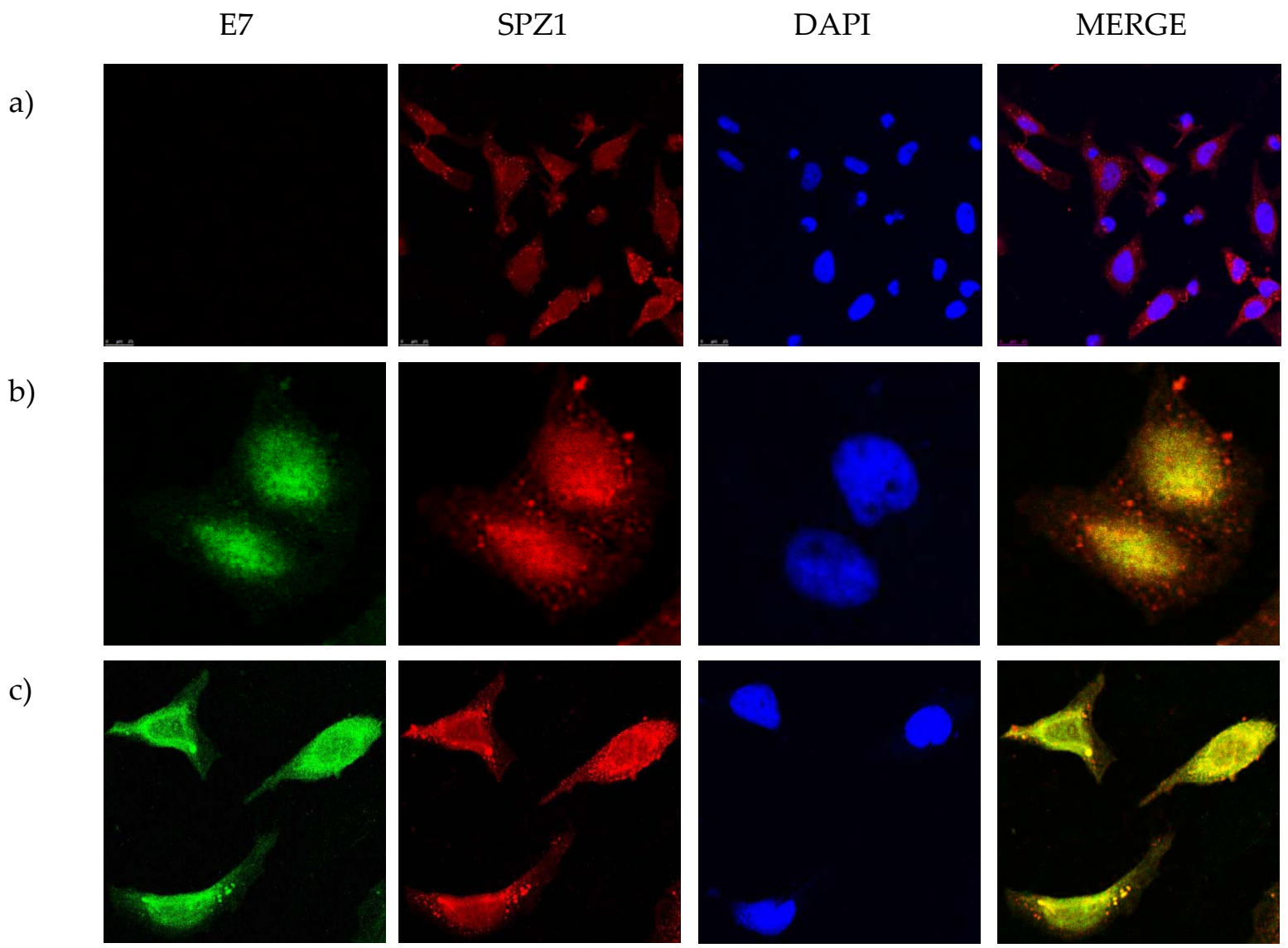
E7
SPZ1
DAPI
MERGE
a)
b)
c)

Figure 6.7: Co-localisation of E7 and SPZ1. HELA cells untransfected (a) or transfected with a plasmid expressing fusion protein of E7 with N-terminal HA tag (b and c) were fixed, 48 hours post transfection and stained with rabbit anti SPZ1 primary and anti rabbit Alexa fluor 680 dye conjugated secondary antibody (red colour) for SPZ1 and rat anti HA primary antibody and secondary antibody conjugated to Alexa Fluer 488 dye (green) for E7. DAPI staining was performed to indicate nucleus. Merge image on the right panel shows merge of red and green filters. Co-localisation of E7 with SPZ1 can be seen in the cell nucleus (b) and cytoplasm (c). Images were taken using Leica SP5 confocal microscope using a 63X objective lens.

6.2.6 E7 and SPZ1 upregulate PCNA promoter

It has previously been shown that mouse SPZ upregulates PCNA promoter (242). In order to investigate whether human SPZ1 similarly upregulates the PCNA promoter, a pGL3 plasmid containing the PCNA promoter was transfected into Cos7 cells along with expression plasmids for SPZ1 and E7 either alone or together and dual luciferase reporter assays were performed (Section 2.2.6.8) (Figure 6.8).Whilst E7 alone did activate the PCNA promoter, SPZ1 showed a moderate 1.5 fold activation. However, E7 and SPZ1 together show a significant three-fold increase in PCNA transcription.

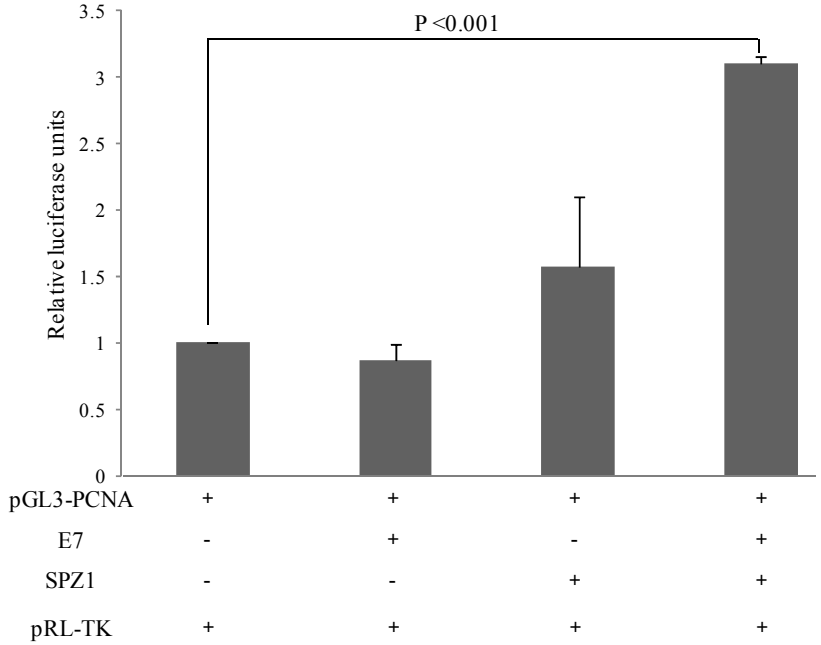

Figure 6.8: Upregulation of PCNA promoter transcription by E7 and SPZ1. Dual luciferase assay was performed by co-transfecting 50 ng pGL3-PCNA (firefly luciferase reporter) along with 150 ng of PCR3 plasmid expressing either SPZ1 or E7 as indicated genes. As a control 10 ng of pRL-TK (renilla luciferase) was also transfected for each sample total amount of tranfected DNA was made up to 360 ng with empty PCR3 plasmid where necessary. Cells were lysed 48 hours post transfection and luciferase activity was measured. Relative luciferase activity was calculated by normalising firefly luciferase activity by its respective renilla luciferase activity and normalising all samples to control sample with only reporter plasmid. Error bars indicate standard deviation in three independent experiments. Statistically significant activations are indicated with p-value.

6.2.7 Identification of novel cellular interactions of SPZ1

Being a recently identified protein, there remains much to discover about the functions and interactions of SPZ1 with other cellular proteins. In order to identify novel interaction partners, four Y2H screens were performed with SPZ1 bait and three human cellular prey libraries, a normalised library containing about 12,300 mainly full length human cDNAs from mammalian gene collection (MGC), a human epithelial testis and a human lymph library as described in Section 2.2.5.5. One of screens with the MGC library was performed under my supervision by Choi Sze Mak as part of Honours project. The Y2H screens identified 33 novel interacting partners: (i) 17 interactions with the MGC library; (ii) 17 with the human lymph library; and (iii) two with the human epithelial testis library. Of these, two interactions (KRT33B and MAGEA1) were identified in both the MGC and the lymph library and one interaction (RAD50) was identified both in the lymph and testis epithelial library. Multiple clones were identified for several interacting partners (13 clones for MAGEA1 and four clones each for RAD50 and KRT33) indicating them as high confidence interactions. The complete list of interactions is presented in Appendix 5.

The identified interaction partners were subjected to Ingenuity pathway analysis (Figure 6.9). Three clusters of functional protein networks were identified:

1) proteins involved in cell morphology, assembly and organization, and molecular transport-CCNI, CDK10, CENPM, CTSA, MAGEA1, METTL7B, MLLT6, MRPL51 NADKD1, PHF7, SERPINA6, TMCO1, VWA5A (Figure 6.10a)

2) proteins involved in cell to cell signalling and interaction and nervous system development and function- CRX, KCNN2, KRT33B, PTPRK, RAD50, SIKE1 and UBL3 (Figure 6.10b).

3) proteins involved in haematological, hereditary , immunological disorders and ribosomal proteins- CCL19, GRB2, HNRNPA2B1, IGF1R, IGLL5, MAX, NISCH, RPL4, RPL21 and RPL34 (Figure 6.10c)

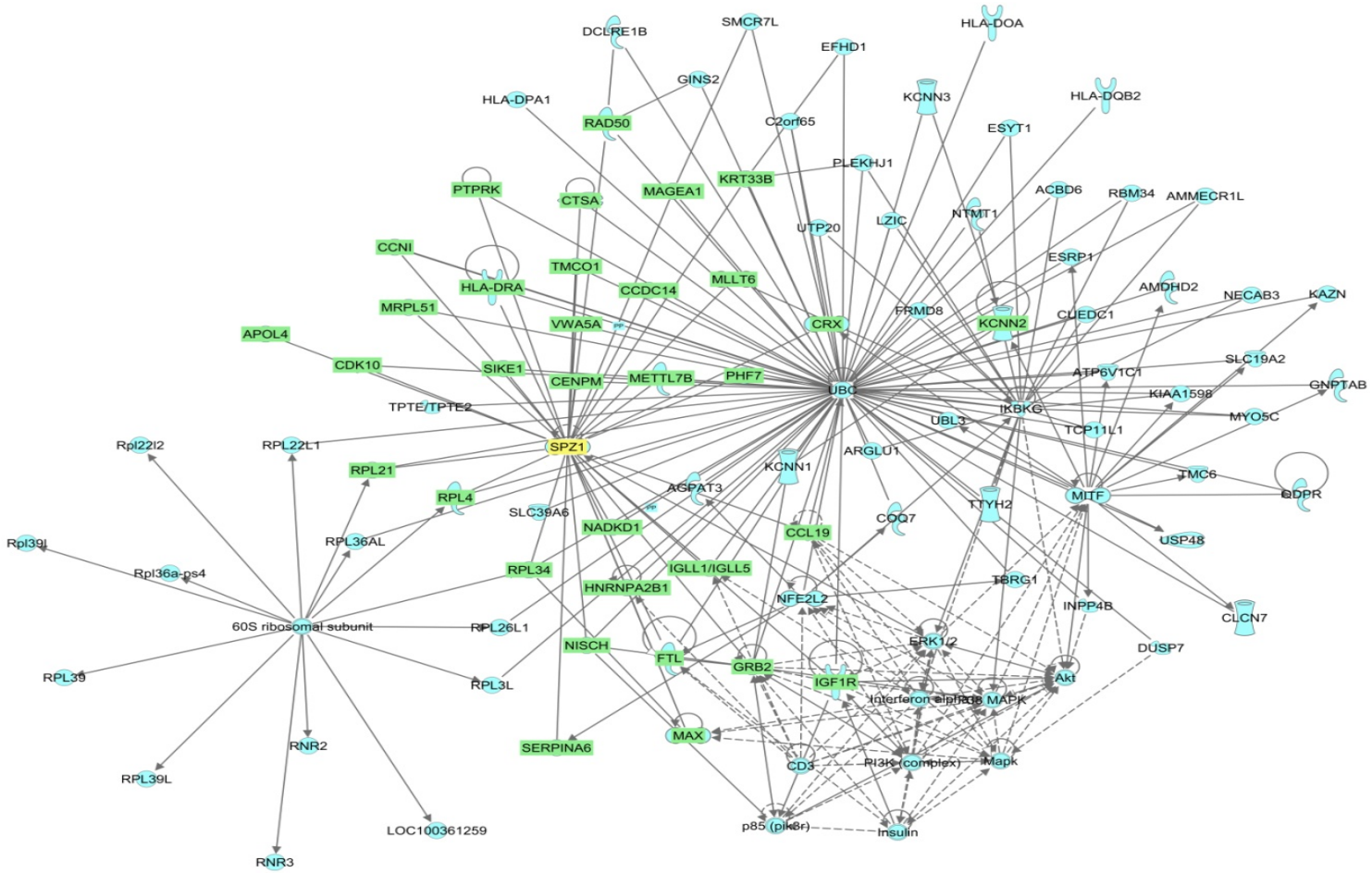

Figure 6.9: Pathway network analysis of SPZ1 interacting partners. Pathway network of interacting partners of SPZ1 (yellow) was done using Ingenuity pathway analysis. Each node (cyan) represents a protein, with the shapes corresponding to the type of protein according to the software. The interacting partners of SPZ1 identified in this screen are highlighted in green. Each line represents an interaction, with solid (black) lines showing protein protein interactions identified in this screen, solid (grey) lines are interactions identified by the software and dotted lines are interactions at transcriptional level.

a)

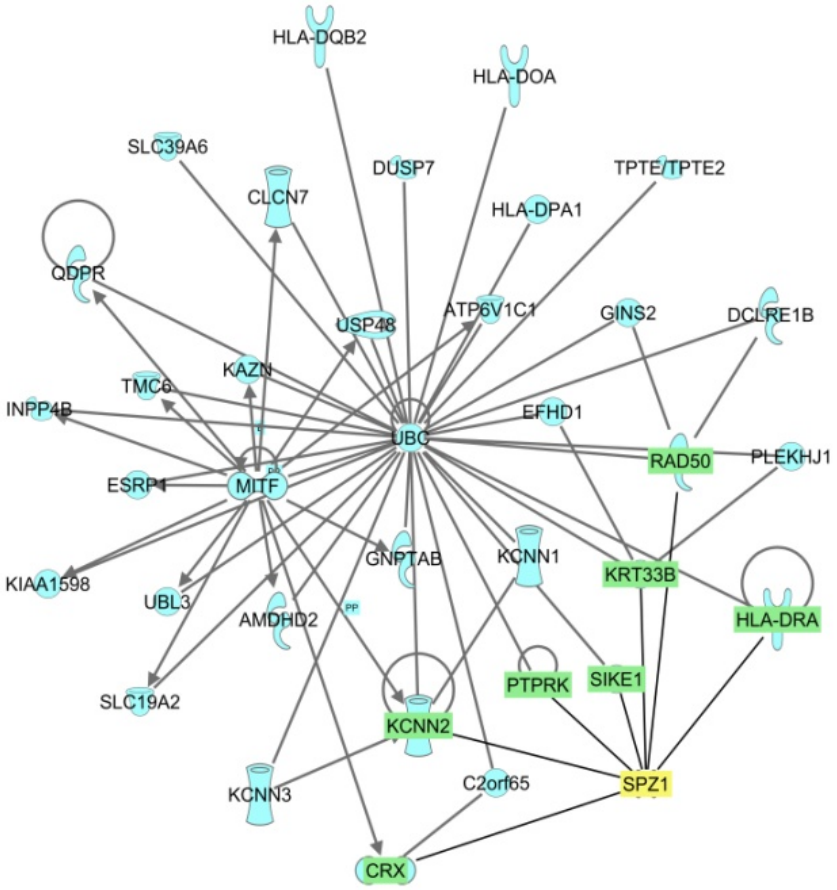
HLA-DQB2
HLA-DOA
SLC39A6
DUSP7
TPTE/TPTE2
CLCN7
HLA-DPA1
QDPR
ATP6V1C1
GINS2
DCLRE1B
USP48
KAZN
TMC6
INPP4B
EFHD1
UBC
RAD50
PLEKHJ1
ESRP1
MITF
GNPTAB
KCNN1
KRT33B
KIAA1598
UBL3
AMDHD2
HLA-DRA
PTPRK
SIKE1
SLC19A2
KCNN2
KCNN3
C2orf65
SPZ1
CRX

b)

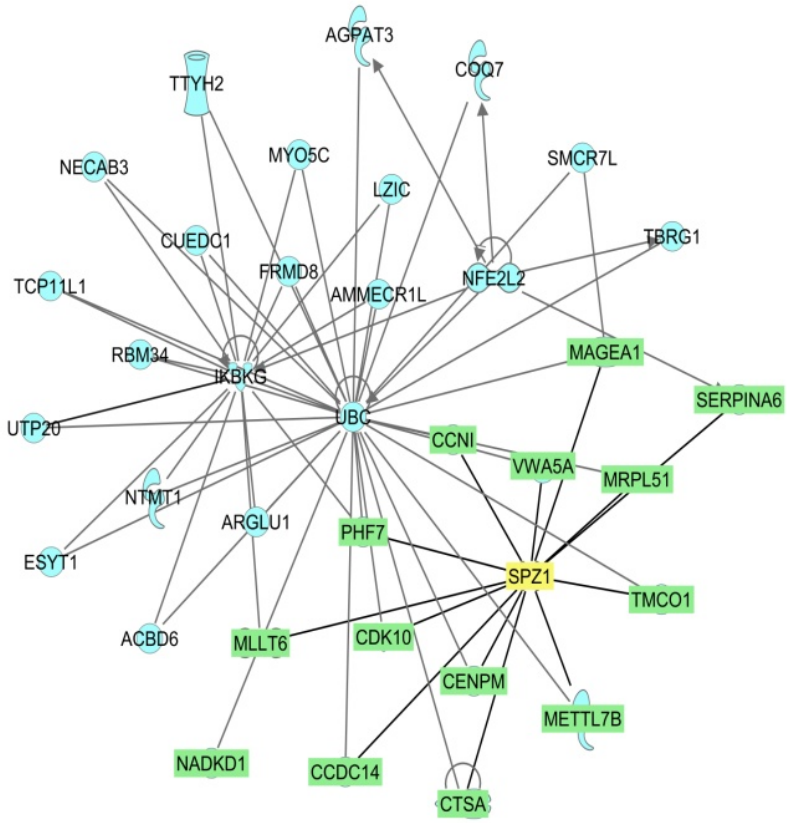
AGPAT3
TTYH2
COQ7
NECAB3
MYO5C
SMCR7L
LZIC
CUEDC1
TBRG1
FRMD8
NFE2L2
TCP11L1
AMMECR1L
RBM34
MAGEA1
IKBKG
SERPINA6
UTP20
UBC
CCNI
VWA5A
MRPL51
NTMT1
ARGLU1
PHF7
ESYT1
SPZ1
TMCO1
ACBD6
MLLT6
CDK10
CENPM
METTL7B
NADKD1
CCDC14
CTSA

c)

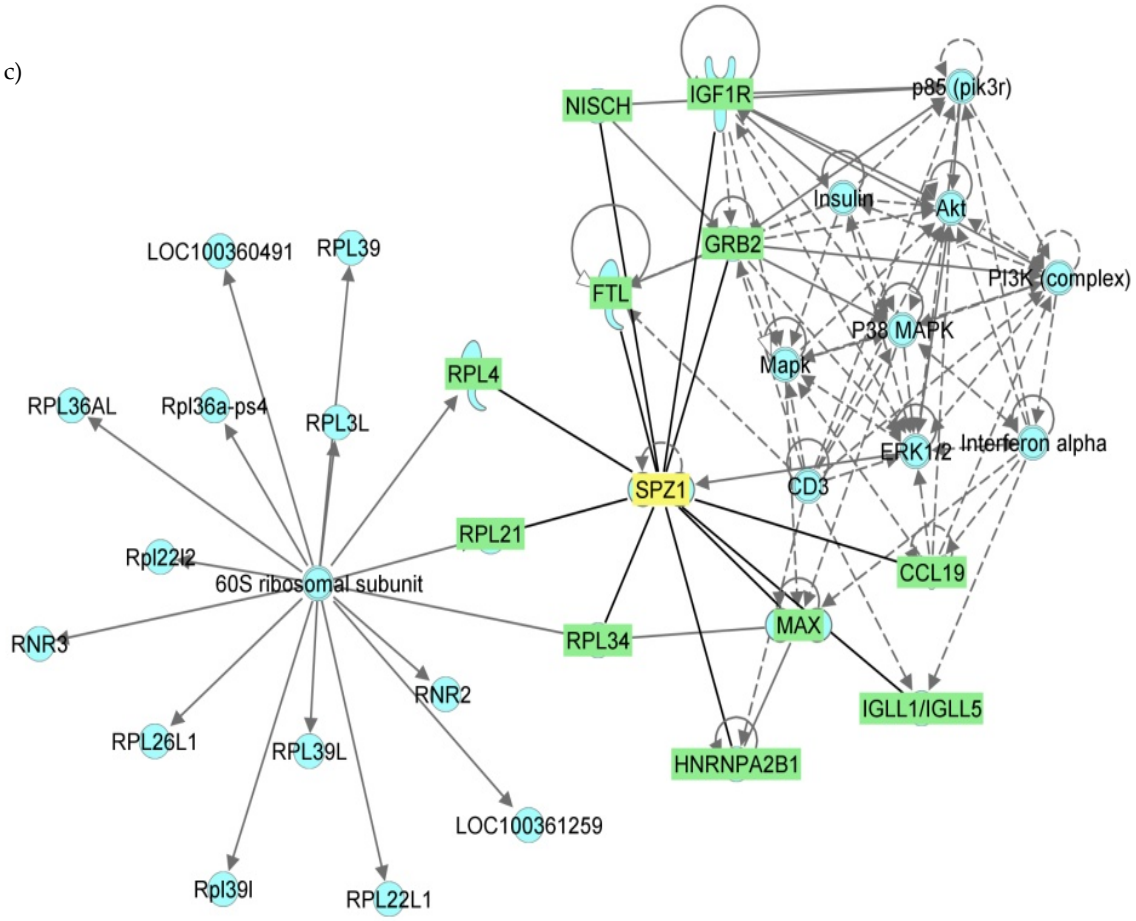

Figure 6.10: Interaction networks of SPZ1 interacting proteins. Three important networks representing the functional interactions of SPZ1 binding proteins identified in the Y2H screen were generated by Ingenuity Pathway Analysis software. The maps correspond to proteins involved in a) cell morphology, assembly and organization, and molecular transport b) cell to cell signaling and interaction and nervous system development and function and c) haematological, hereditary and immunological disorders. Each node (cyan) represents a protein, with the shapes corresponding to the type of protein according to the software. SPZ1 is highlighted in yellow, and interacting partners identified in this screen are highlighted in green. Each line represents an interaction, with solid (black) lines showing protein protein interactions identified in this screen, solid (grey) lines are interactions identified by the software and dotted lines are interactions at transcriptional level.

The network was also subjected to functional analysis to identify the biological functions and/or diseases that were most significant to the molecules in the network (Table 6.1). Right-tailed Fisher's exact test was used to calculate a p-value determining the probability that each biological function and/or disease assigned to that network is due to chance alone.

Diseases and Disorders

Name	p-Value	Proteins
Cancer	0.00135 – 0.0491	CCL19, FTL, GRB2, HLA-DRA, IGF1R, MAX, RAD50, RPL4, SERPINA6, TMCO1, VWA5A
Developmental Disorder	0.00188 – 0.0479	CTSA, IGF1R
Hematological Disease	0.00188 – 0.0476	IGLL1/IGLL5, MAX, RAD50
Hereditary Disorder	0.00188 – 0.0224	CRX, CTSA, IGF1R, IGLL1/IGLL5, FTL, SERPINA6,
Immunological Disease	0.00188 – 0.0476	CCL19, CTSA, HLA-DRA, IGF1R, IGLL1/IGLL5, MAX, RAD50

Molecular and Cellular Functions

Name	p-Value	Proteins
Cellular Growth and Proliferation	0.000414 – 0.0497	CCL19, CCNI, CDK10, FTL, GRB2, NRNPA2B1, KCNN2, IGF1R, IGLL1/IGLL5, MAX, MLLT6, PTPRK, RAD50, SPZ1
Protein Synthesis	0.0004 – 0.00043	GRB2, IGF1R, RAD50
Gene Expression	0.00125 – 0.00376	MAX, SPZ1
Cell-to-Cell Signaling and Interaction	0.00188 – 0.0497	CCL19, GRB2, IGF1R, KCNN2
Cellular Movement	0.00188 – 0.0495	CCL19, GRB2, HNRNPA2B1, IGF1R

Physiological system development and function

Name	p-Value	Proteins
Connective Tissue Development and Function	0.000414 – 0.0279	GRB2, IGF1R, MAX, MLLT6, SPZ1
Embryonic Development	0.00188 – 0.0479	CCL19, CRX, GRB2, IGF1R, MAX, RAD50
Hematological System Development and Function	0.00188 – 0.0497	CCL19, GRB2, HNRNPA2B1, IGLL1/IGLL5
Hematopoiesis	0.00188 – 0.0224	CCL19, IGLL1/IGLL5, GRB2
Immune Cell Trafficking	0.00188E – 0.00425	CCL19

Table 6.1: Functional analysis of SPZ1 interactions. The functional analysis of the interaction dataset was performed to identify the biological functions and diseases that were most significant to the proteins in the dataset. Right-tailed Fisher's exact test was used to calculate a p-value determining the probability that each biological function and/or disease assigned to that network is due to chance alone. The proteins involved in each of the functions are listed.

6.3 Discussion

6.3.1 Elucidation of E7-SPZ1 interaction

The interaction between E7 and proto-oncogene SPZ1 identified in the Y2H study was a very relevant interaction to study due to its upregulation in some cancers (242). Preliminary data suggests that the interaction between E7 and SPZ1 is a characteristic of the high-risk HPV types -16, -18 and -45 while the low-risk HPV-11 shows reduced interaction with SPZ1 (Figure 6.1). However, this needs to be further validated by Co-IP or other protein interaction studies and if true, may identify a mechanism of pathogenesis caused by the high-risk types.

The structural domains of this interaction with type-16 E7 were mapped to the CRII domain with possible additional low affinity sites between 38 and 52 amino acids (Figure 6.2). The CRII domain contains the LxCxE motif necessary for RB interaction (76) and other pocket proteins such as p107, p130, cyclin A and also the casein kinase CKII phosphorylation sites. A point mutant C24G unable to interact with RB still retained interaction with SPZ1 indicating that this residue is not necessary for the interaction (Figure 6.2). Further experiments to generate a short functional mutant of E7 that is unable to bind to SPZ1 will be useful to more specifically map this interaction. By deletion mutagenesis of SPZ1, it was found that the C–terminal domain containing the amino acids 301-430 was necessary and sufficient to maintain interaction with E7 (Figure 6.4). However, the substitution of the leucine zipper residues in the leucine zipper domain of SPZ1 did not abrogate the interaction (Figure 6.5) indicating that this domain may not necessary and the interaction domain was downstream of this region.

There is little data available about the expression of SPZ1 in epithelial cells and particularly cervical cancer cell lines. Therefore, in this study, western blot and confocal microscopy were performed to look at the expression of SPZ1 in HeLa, SiHa

and CaSki cell lines (Figure 6.6). HeLa cells seem to express more SPZ1 than SiHa and CaSki cell lines. This might be due to the fact that HeLa cells contain HPV-18 while the SiHa and CaSki cells contain HPV-16. A comparison of other cell lines infected with other types of HPV will be interesting to investigate. Further investigation into whether -16 E7 is causing downregulation or degradation of SPZ1 in these cell lines will also be important to investigate. The localisation of SPZ1 was found to be both cytoplasmic and nuclear in all three cell lines in line with previous literature (242,247). The endogenous SPZ1 in HeLa cells colocalised with E7 both in cytoplasm and nucleus and no change in localisation of SPZ1 was seen upon transcient overexpression of E7.

PCNA (also known as DNA processivity factor δ) is known for DNA synthesis and S-phase progression. It is upregulated in proliferative cells and it has been used as a marker in cancer cells including cervical cancer. In order to see if E7 and SPZ1 have a role in PCNA upregulation, the PCNA promoter region from nucleotides -560 to +60 containing the three SPZ1 binding sites was cloned and reporter assays performed. Whilst E7 and SPZ1 showed a significant upregulation of PCNA reporter, HPV-16 E7 alone did not cause any activation and SPZ1 alone showed a modest activation. While the upregulation of PCNA by E7 has been reported in raft culture experiments, E7 from HPV-18 in a similar study previously was shown to represses the PCNA promoter in the absence of E2F consensus binding sites (which are present in the first intron of PCNA) (251). Moreover, E7 is unable to cause activation or repression when these E2F binding sites are mutated (251). The promoter construct used in this study does not contain the E2F binding sites, which explains the absence of any response seen with E7 alone (Figure 6.11). SPZ1 alone shows a moderate 1.5 fold activation of the reporter as previously reported (250). These results suggest a novel mechanism of upregulation of PCNA by E7 independent of the E2F binding sites but via its interaction with SPZ1.

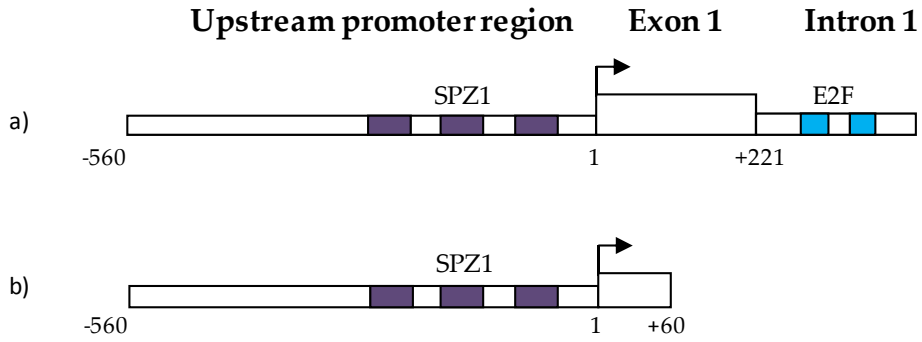

Figure 6.11: Promoter region of PCNA. a) The known sites in the PCNA promoter region along with the first exon and intron are shown. The SPZ1 binding site (250) and E2F sites (251) necessary for upregulation by E7 are highlighted. b) The promoter region used in this study which contains the SPZ1 binding site but not E2F binding sites.

Continued over-expression of SPZ1 may be a mechanism of upregulation of PCNA is necessary for DNA replication and maintenance of cell cycle. The role of E7 on SPZ1 in this context would be supportive, with E7 either stabilising the SPZ1 protein itself or facilitating increased DNA-binding of SPZ1. Additionally, it is quite possible that this effect is not mediated by a direct interaction but by the effects of E7 on other cellular factors such as cyclin-CDK2 complex or p21 or p53 which also regulate PCNA levels (252). The activation of PCNA promoter in this study was performed in Cos7 cells. Further investigation needs to be done to assess the activity in other cell lines and at different cell cycle stages which might indicate a regulated control of PCNA with SPZ1.

6.3.2 Protein interactions of SPZ1

SPZ1 interacts with PP1 and is hypothesized to be its regulatory substrate (247) . It is possible that SPZ1 might play a regulatory role in dephosphorylation of RB and/or E7 via its interactions with PP1 however, whether it has a tumour suppressor role or an oncogenic role remains to be studied. Future experiments will be directed to understand if SPZ1 helps/blocks the dephosphorylation of RB by PP1 using phosphatase assays and whether E7 plays a role in this activity of SPZ1. Alternatively,

whether SPZ1 directly plays a role in the dephosphorylation of E7 will also be interesting to investigate.

Apart from its known direct interaction with PP1cγ, SPZ1 is known to interact with homeobox protein HOXB9 (253), however the functional relevance of this interaction remains unknown. Being a proto-oncogene of the family of bHLH-Zip proteins, it is important to identify new protein interactors of SPZ1. An Y2H library screen performed led to the discovery of 33 novel interactors of the protein. The functional analysis of the interacting partners of SPZ1 done by IPA identified three clusters of functions: (i) cell morphology, assembly organization, and molecular transport; (ii) haematological, hereditary and immunological disorders and ribosomal proteins; (iii) cell to cell signalling, interaction and nervous system development. The list of significant biological and disease associations of SPZ1 is listed in Table 6.1.

One of the protein interactors, Melanoma antigen family A, 1 (MAGEA1) (also known as cancer testis antigen 1) was identified as interacting partner in thirteen clones. MAGEA1 was discovered as an antigen for melanoma cells detected by cytotoxic T lymphocytes (254). It is upregulated in a range of cancer including colorectal cancer (255), neuroblatoma tumours (256), hepatocellular carcinoma (257), prostate cancer (258), ovarian (259) and lung carcinomas (260). Its overexpression in cervical cancer cell line HeLa and in cancer patients has also been shown which suggests the use of it as a tumour marker and immunotherapy (261). Investigation of its interaction with SPZ1 in the context of cervical tumour samples will be interesting

Other interactors identified in four clones each are RAD50 and KRT33B. RAD50 is a member of MRN complex (which is made of MRE11, RAD50 and NBS1). This complex is involved in recognition of DNA double stranded breaks (DSB) and facilitation of DSB responses (262). It is of interest to see how SPZ1 might be involved in the MRN complex and whether it has any effects on DSB response. In the context of HPV

pathogenesis, DSB facilitates the integration of HPV genome into cellular DNA and this will be an interesting line of investigation.

Keratin 33B (KRT33B) belongs to the family of keratins which are filament forming proteins of epithelial cells. There are two types of keratins type I and type II that form heterodimers. KRT33B is a type-I hair keratin. Although keratins have been used extensively as cancer markers, there is also evidence of keratin in cancer cell invasion and metastasis (263). The role of KRT33B is not well studied however; its interaction with SPZ1 might provide important insights into its activity.

The Y2H screen also identified the MYC associated protein MAX as an interactor of SPZ1. MAX has a complex regulatory role in cells. MAX is a bHLH transcriptions factor that dimerises with itself and other bHLH transcription factors (264). Homodimers of MAX are weak and are transcriptionally inert but the MYC-MAX heterodimers transcriptionally activates a set of genes through its interaction with E-box domains (265). Alternatively MAX interacts with the MAD proteins (MAD1, MXI1, MAD3, MAD4) to transcriptional repress genes (266)(267)(256). Two more partners of MAX have been identified, MNT1 which causes repression of genes (258) and MGA which results in activation of genes through a T-box domain (258). The interaction identified between MAX and SPZ1 and the fact that SPZ1 is a bHLH transcription factor suggests that SPZ1 might be a new partner of MAX and whether it causes activation or repression of genes provides for an interesting line of investigation (Figure 6.12).

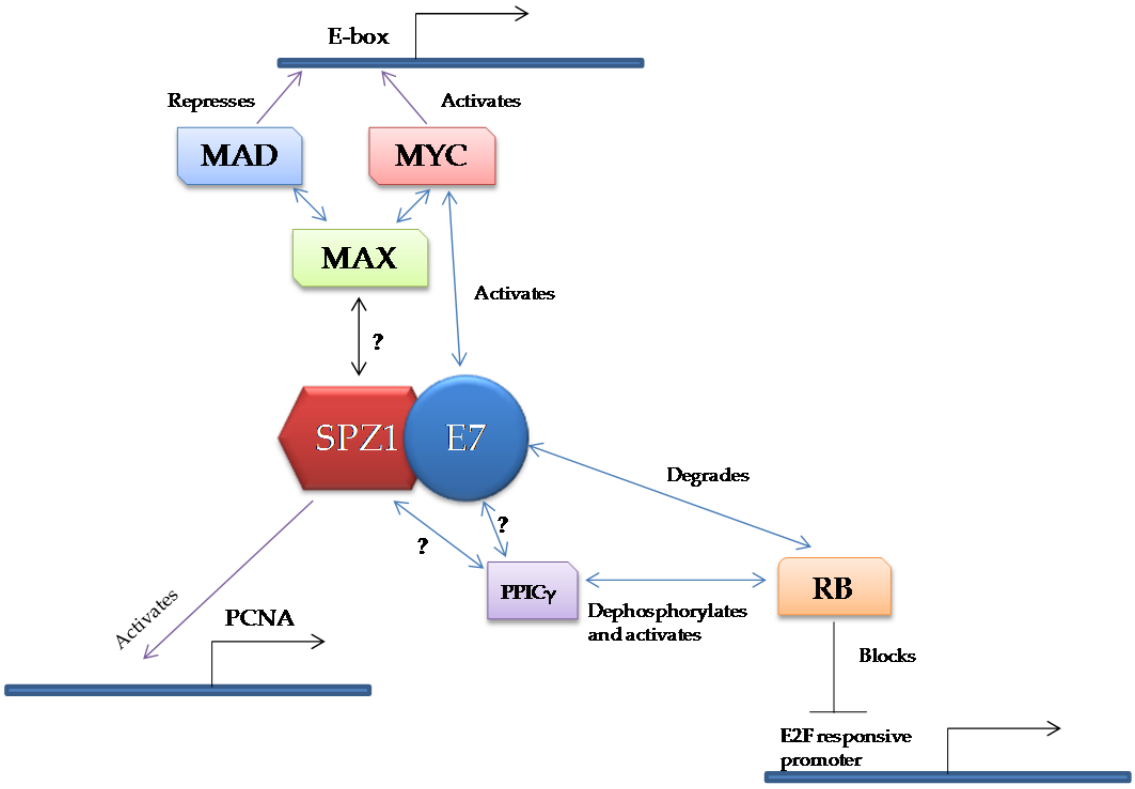

Figure 6.12: Hypothesis of transcriptional role of SPZ1-E7 interaction in gene regulation. Schematic representation of transcriptional activity of SPZ1. Protein-protein interactions are shown in blue double sided arrow, transcriptional control by purple single sided arrow, and the mechanism of action where known is mentioned. For roles to be investigated '?' is indicated.

Although much investigation is needed to understand the function of SPZ1, it proves to be an interesting transcription factor to study. Its transcriptional control of PCNA, E-box regulatory gene and E2F responsive promoters are directions of immediate future investigation which will provide an understanding of its mechanism of action (Figure 6.12). This study has shown evidence that E7 and SPZ1 co-operatively upregulate PCNA. The collective role of E7 and SPZ1 in the MYC/MAX transcriptional control can be studied using MYC/MAX responsive promoters. Additionally, the control of E2F responsive genes by E7 and SPZ1 can be investigated using E2F responsive promoter assays.

The work presented in this Chapter provides a novel E7 interacting protein, SPZ1 and a mechanism of upregulation of PCNA by E7. Additionally, a whole range of new

interacting partners were identified for SPZ1 which further enhance our understanding about this little characterised protein. Finally, this study opens up avenues to investigate the use of SPZ1 as a diagnostic marker for cancer progression and also possibly in reducing the burden of HPV related malignancies.

Chapter 7:

Conclusions and outlook

HPV is a medically important virus. Apart from causing cervical cancer, high-risk HPV types are also implicated in other genital and non-genital cancers including anal, penile, vaginal and vulval cancer. There is increasing evidence of the link between HPV and head and neck cancer. Also of relevance are the low-risk types that cause warts and benign lesions. While the implementation of HPV vaccination and screening programmes in many countries is leading to a reduction in the burden of cervical cancer, its effect on other malignancies is yet to be assessed. Additionally, there is increasing chances that while the incidence of high-risk types such as HPV-16 and -18 might be reducing, the incidence of the less prevalent and resistant strains might increase with the use of population-wide vaccination. Therefore, it is essential to identify newer and better diagnostics and therapeutics to combat this virus. In order to achieve this, it is important to obtain a better understanding of the life cycle of the virus and its effects on host. One of the ways of achieving this is by investigating its protein interactions.

The hypothesis of this study was to investigate the interactions of the viral proteins in three different contexts. Therefore, this thesis is divided into three separate sections which investigate each of these different types of interactions. The three individual screens are discussed in detail in Chapters 3, 4 and 5. The protein interactions among the viral proteins (Intra-viral interactions) are essential to mediate the basic functioning and life cycle of the virus such as replication and capsid formation. This study reports a novel interaction between the replication protein E1 and the transforming protein E7 (Chapter 3). The interaction domains of this interaction were mapped to the N-terminal 92 amino acids of E1 and the CxxC domain in the CRIII region of E7. Mutants of E7 which are unable to interact with E1 were generated (C58A, C59A, C61A). Transient replication assays indicate that E7, but not the mutants incapable of interacting with E1 cause a repression in HPV replication in vitro. Future work in this direction will be aimed at understanding the mechanism of the repression of replication by E7 including

looking at the replicative ability of viruses containing these mutations and investigating the use of mutant E7 as a therapeutic target towards HPV infection.

The interaction of HPV with co-infected viruses within the same cell at a protein level is an interesting line of investigation. There is no evidence of published studies looking into interactions between the proteins of two viruses. While a number of studies have suggested the role of HSV-1 and HSV-2 as co-factors in cervical carcinogenesis, this study presents evidence of direct protein interactions between the two viruses (Chapter 4). Future work will involve validation of these interactions. While it remains to be investigated, the interactions of E1, E1^E4 and E1^E2C with ICP4 and ICP34.5 may provide valuable insights into understanding the interplay between these two viruses.

Among all interactions of a virus, the most important ones are those with host proteins. These interactions, particularly for a small virus such as HPV are essential for its infection, survival and proliferation. This study has identified 53 interactions of HPV proteins, a majority of which are previously unknown (Chapter 5). The proteins identified as HPV interactors are involved in several cellular processes such as cell development, signalling, inflammation and also infectious diseases and cancer progression. Nine out of 37 interactions tested were positively validated in the LUMIER assay. Several avenues of future work have been opened by the data presented in this Chapter. Firstly, the validation of the remaining interactions needs to be performed. Secondly, nine of the interesting interactions have been discussed in the Chapter. Investigation of each of these individual interactions and the elucidation of their biological relevance will provide valuable insights into the virus.

Among the interactions identified in the screen, an interesting interaction between E7 and SPZ1 was investigated in some detail (Chapter 6). Since very little was known about this protein and its interactions, an Y2H screen was performed to identify new interactors of SPZ1 which identified 33 novel interactors. Among these interactors were

proteins involved in cell morphology, signalling and transport, and hereditary and immunological disorders. While it is known that SPZ1 is a bHLH transcription factor, this study identified its interaction with another bHLH transcription factor MAX. Apart from the role of SPZ1 in transcription of genes, a network of ribosomal proteins was identified as its interacting partners, which suggests its role in protein translation as well. An area of immediate interest with regards to this protein is the investigation of its role with MAX with the hypothesis that SPZ1 is a novel MAX dimerisation partner. Its role in immunological processes is also an interesting direction of research to pursue.

The investigation of the interaction between E7 and SPZ1 suggests that the CRII and additional domains in CRIII of E7 and the C-terminal region of SPZ1 might be necessary for this interaction. Transcient reporter assays suggest that E7 with the co-operation of SPZ1 upregulates PCNA, which presents a new mechanism of activation of PCNA by the virus. Whether E7 induces cell proliferation in co-operation with SPZ1 and activation of other genes having E-box promoters will be interesting to investigate. The proposed transcriptional control of SPZ1 and the role of E7 to be investigated are shown in Figure 6.13 which will be the basis of immediate future work. Also in the pipeline is the investigation of whether SPZ1 is unregulated in cervical cancer patients and its potential use as a biomarker. In long term, SPZ1 might prove to be an important oncogene implicated not only by E7 but other virus or non-virus mediated cancers.

This study aimed at providing a more detailed picture of interactions of HPV proteins among themselves, with HSV and with the host. Although it is near to impossible to identify all the interactions of the virus, this study provides the basis for several lines of future research and has added to the existing knowledge about the virus and the ultimate aim is to use some of the interactions identified in this screen and develop therapeutic strategies to decrease the burden of HPV.

APPENDICES

Appendix 1: Primers

Gateway® *att*B primers

Fwd	GGGGACAAGTTTGTACAAAAAAGCAGGCT
Rev	GGGGACCACTTTGTACAAGAAAGCTGGGT

Primers for HPV genes Gateway® recombinatorial cloning

GENE		**PRIMER**
HPV-16 E1-N	Fwd	AAAAAGCAGGCTCCGCCATGGCTGATCCTGCAGGTACC
	Rev	AGAAAGCTGGGTCTCATAATGTGTTAGTATTTTGTCC
HPV-16 E2	Fwd	AAA AAG CAG GCT CCG CCA TGG AGA CTC TTT GCC AAC G
	Rev	AGA AAG CTG GGT CTC ATA TAG ACA TAA ATC CAG TAG
HPV-16 E4	Fwd	AAA AAG CAG GCT CCG CCA TGT ATT ATG TCC TAC ATC TGT G
	Rev	AGA AAG CTG GGT CCT ATG GGT GTA GTG TTA CTA TTA C
HPV-16 E5	Fwd	AAA AAG CAG GCT CCG CCA TGA CAA ATC TTG ATA CTG C
	Rev	AGA AAG CTG GGT CTT ATG TAA TTA AAA AGC GTG C
HPV-16 E6	Fwd	AAA AAG CAG GCT CCG CCA TGC ACC AAA AGA GAA CTG C
	Rev	AGA AAG CTG GGT CTT ACA GCT GGG TTT CTC TAC
HPV-16 E7	Fwd	AAA AAG CAG GCT CCG CCA TGC ATG GAG ATA CAC CTA C
	Rev	AGA AAG CTG GGT CTT ATG GTT TCT GAG AAC AGA TG
HPV-16 L1	Fwd	AAA AAG CAG GCT CCG CCA TGC AGG TGA CTT TTA TTT AC
	Rev	AGA AAG CTG GGT CTTACA GCT TAC GTT TTT TGC G
HPV-16 L2	Fwd	AAA AAG CAG GCT CCG CCA TGC GAC ACA AAC GTT CTG C
	Rev	AGA AAG CTG GGT CCT AGG CAG CCA AAG AGA CAT C
HPV-16 E6*^E4	Fwd	AAAAAG CAG GCT CCG CCA TG TTT CAG GAC CCA CAG GAG C

	Rev	AGA AAG CTG GGT CTC AGG AGA GGA TAC TTC GTT GCT GCT CAC GTC GCA GTA ACT GTT GCT TGC
HPV-16 E1^E4*	Fwd	AAA AAG CAG GCT CCG CCA TGG CTG ATC CTG CAG GCA GCA CTT GGC CAA CCA CTCC GCC
	Rev	AGA AAG CTG GGT CCT ATG GGT GTA GTG TTA CTA TTA CAG TTA ATC CGT CC
HPV-16 E6*^E7	Fwd	AAA AAG CAG GCT CCG CCA TGT TTC AGG ACC CAC AGG AGC GAC
	Rev	AGAAAGCTGGGTCCTACGTGTGTGCTTTGTACGCACAACC GAAGCGTAGAGTCACCTCACGTCGCAGTAACTGTTGCTTG C
HPV-16 E1^E4	Fwd	AAA AAG CAG GCT CCG CCA TGG CTG ATC CTG CAG CAG CAA CGA AGT ATC CTC TCC
	Rev	AGA AAG CTG GGT CCT ATG GGT GTA GTG TTA CTA TTA CAG TTA ATC CGT CC
HPV-16 E1^E2C	Fwd	AAAAAGCAGGCTCCGCCATGGCAATACTGAAGTGGAAA CTCAGCAGATGTTACAGCAGCAACGAAGTATCCTCTCCTG
	Rev	AGA AAG CTG GGT CTC ATA TAG ACA TAA ATC CAG TAG AC
HPV-11 E7	Fwd	AAA AAG CAG GCT CCG CCA TG CATGGAA GACTTGTTAC CC
	Rev	AGA AAG CTG GGT CTT ATGGTTTTGGTGCGCAGATGGGACACAC
HPV-18 E7	Fwd	AAA AAG CAG GCT CCG CCA TGC ATG GAC CTA AGG CAA C
	Rev	AGA AAG CTG GGT CTT ACT GCT GGG ATG CAC ACC ACG G
HPV-45 E7	Fwd	AAA AAG CAG GCT CCG CCA TGC ATG GAC CCC GGG AAA CAC TGC
	Rev	AGA AAG CTG GGT CTT ATT GGT TAG TTG CAC ACC ACG GAC ACA C

Primers for E7 deletion mutants

GENE		PRIMER
E7 F2	Fwd	AAA AAG CAG GCT CCG CCA TGC ATG GAG ATA CAC CTA C
	Rev	AGA AAG CTG GGT CCA AAT CTA ACATATATTCATGC
E7 F3	Fwd	AAA AAG CAG GCT CCG CCA TGC ATG GAG ATA CAC CTA C
	Rev	AGA AAG CTG GGT CTTCATCCTCCTCCTCTGAGC
E7 F4	Fwd	AAA AAG CAG GCT CCG CCA TGC ATG GAG ATA CAC CTA C
	Rev	AGA AAG CTG GGT CCTTGCAACAAAAGGTTACAATATTG
E7 F5	Fwd	AAA AAG CAG GCT CCG CCA TGTTGCAACCAGAGACAACTGATCTC
	Rev	AGA AAG CTG GGT CTT ATG GTT TCT GAG AAC AGA TG
E7 F6	Fwd	AAA AAG CAG GCT CCG CCA TGTTGCAACCAGAGACAACTGATCTC
	Rev	AGA AAG CTG GGT CCA AAT CTA ACATATATTCATGC
E7 F7	Fwd	AAA AAG CAG GCT CCG CCA TGATAGATGGTCCAGCTGG
	Rev	AGA AAG CTG GGT CCA AAT CTA ACATATATTCATGC
E7 F8	Fwd	AAA AAG CAG GCT CCG CCA TGTACAATATTGTAACC
	Rev	AGA AAG CTG GGT CCA AAT CTA ACATATATTCATGC

Primers for SPZ1 deletion mutants

GENE		PRIMER
SPZ1-F1	Fwd	AAA AAG CAG GCT CCG CC ATGGCCAGCT CTGC
	Rev	AGA AAG CTG GGT C GTCAAGTCCTCTGATATTTTC
SPZ1-F2	Fwd	AAA AAG CAG GCT CCG CC ATGGCCAGCT CTGC
	Rev	AGA AAG CTG GGT C TAACTGCTCCATGTTG
SPZ1-F3	Fwd	AAA AAG CAG GCT CCG CC CAT GAG CTG GAG GAA C
	Rev	AGA AAG CTG GGT C TCTTAGGCTGCTAGC

Primers for overlap PCR

GENE		PRIMER
HPV-18 E1	Fwd-1	AAA AAG CAG GCT CCG CCA TGG CTG ATC CAG AAG GTA C
	Rev-1	CTAGTGGAATTCACAAATGATATTACTGC
	Fwd-2	TATCATTTGTGAATTCCACTAGTCATTTTTG
	Rev-2	AGA AAG CTG GGT CTC ATA GTG GTC TAT GAT TTT GTC C
HPV-16 L1	Fwd-1	AAA AAG CAG GCT CCG CCA TGC AGG TGA CTT TTA TTT AC
	Rev-1	GTACATGGGGATCCTTTGCCCCAGTGTTCCC
	Fwd-2	CTGGGGCAAAGGATCCCCATGTACCAATG
	Rev-2	AGA AAG CTG GGT CTTACA GCT TAC GTT TTT TGC G
HPV-16 E1-FL	Fwd-1	AAA AAG CAG GCT CCG CCA TGG CTG ATC CTG CAG GTA CC
	Rev-1	CACTAAGTGGACTTACCAAATACTTTCG
	Fwd-2	CGAAAGTATTTGGTAAGTCCACTTAGTG
	Rev-2	AGA AAG CTG GGT CTC ATA ATG TGT TAG TAT TTT GTC C

Primers for generation of E7 site-directed point mutants

GENE		PRIMER
H51A	Fwd	GAA CCG GAC AGA GCC GCT TAC AAT ATT GTA ACC
	Rev	GGTTACAATATTGTAAGCGGCTCTGTCCGGTTC
Y52A	Fwd	CCG GAC AGA GCC CAT GCC AAT ATT GTA ACC
	Rev	GGTTACAATATTGGCATGGGCTCTGTCCGG
N53A	Fwd	GAC AGA GCC CAT TAC GCT ATT GTA ACC TTT TG
	Rev	CAAAAGGTTACAATAGCGTAATGGGCTCTGTC
I54A	Fwd	AGA GCC CAT TAC AAT GCT GTA ACC TTT TGT TGC
	Rev	GCAACAAAAGGTTACAGCATTGTAATGGGCTCT
V55A	Fwd	GCC CAT TAC AAT ATT GCA ACC TTT TGT TGC AAG
	Rev	CTTGCAACAAAAGGTTGCAATATTGTAATGGGC
T56A	Fwd	GCC CAT TAC AAT ATT GTA GCC TTT TGT TGC AAG TGT GAC
	Rev	GTCACACTTGCAACAAAAGGCTACAATATTGTAATGGGC
F57A	Fwd	GCC CAT TAC AAT ATT GTA ACC GCT TGT TGC AAG TGT GAC
	Rev	GTCACACTTGCAACAAGCGGTTACAATATTGTAATGGGC
C58A	Fwd	C AAT ATT GTA ACC TTT GCT TGC AAG TGT GAC TCT ACG C
	Rev	GCGTAGAGTCACACTTGCAAGCAAAGGTTACAATATTG

C59A	Fwd	ATT GTA ACC TTT TGT GCC AAG TGT GAC TCT ACG
	Rev	CGTAGAGTCACACTTGGCACAAAAGGTTACAAT
K60A	Fwd	GTA ACC TTT TGT TGC GCG TGT GAC TCT ACG C
	Rev	GCGTAGAGTCACACGCGCAACAAAAGGTTAC
C61A	Fwd	ACC TTT TGT TGC AAG GCT GAC TCT ACG CTT CGG
	Rev	CCGAAGCGTAGAGTCAGCCTTGCAACAAAAGGT

Primers for generation of SPZ1 site-directed point mutants

GENE		**PRIMER**
SPZ1 L1	Fwd	TCGGCTAAGCATGAGGCGGAGGAACAGGTGAAGAAAGCGA GCCATGACACCTA
	Rev	TAGGTGTCATGGCTCGCTTTCTTCACCTGTTCCTCCGCCTCAT GCTTAGCCGA
SPZ1 L2	Fwd	CATGACACCTATTCAGCGCAGTTGATGGCAGCTTTGGCAGA GAATGAATGCCA
	Rev	TGGCATTCATTCTCTGCCAAAGCTGCCATCAACTGCGCTGAA TAGGTGTCATG
SPZ1 L3	Fwd	AATGAATGCCAAATCGCACAGCAGAGAGTAGAGATTGCCA AGGAACTCCATCA
	Rev	TGATGGAGTTCCTTGGCAATCTCTACTCTCTGCTGTGCGATTT GGCATTCATT

Appendix 2: HSV-1 genes used for Y2H inter-viral screen

Sl No.	Gene	Length	Full-length or domain (bp)	Protein description
1	UL1	672	Full-length	envelope glycoprotein L
2	UL1dSP	618	58-672	
3	UL2	1002	Full-length	uracil-DNA glycosylase
4	UL3	705	Full-length	nuclear protein
5	UL4	597	Full-length	nuclear protein
6	UL5	2646	Full-length	helicase-primase helicase subunit
7	UL6	2028	1-700, 1485-2028	capsid portal protein
8	UL7	888	Full-length	tegument protein
9	UL8	2250	1-530, 1760-2250	helicase-primase subunit
10	UL9a	1200	N-terminal 1200	DNA replication origin-binding helicase
11	UL9b	1353	C-terminal 1353	
12	UL10	1422	Full-length	envelope glycoprotein M
13	UL10C	390	1027-1422	
14	UL11	288	Full-length	myristylated tegument protein
15	UL12	1878	1-561, 1047-1878	deoxyribonuclease
16	UL13	1557	1-673, 977-1557	tegument serine/threonine protein kinase
17	UL14	657	Full-length	tegument protein
18	UL15	2208	1-650, 1652-2208	DNA packaging terminase subunit 1
19	UL16	1119	1-115, 606-1119	tegument protein
20	UL17	2109	1-739, 1258-2109	DNA packaging tegument protein
21	UL17N	1971	1-1971	
22	UL18	954	Full-length	capsid triplex subunit 2
23	UL19	4122	1-632, 3570-4122	major capsid protein
24	UL20	666	Full-length	envelope protein
25	UL20a	189	1-189	
26	UL21	1605	1-555, 1032-1605	tegument protein
27	UL22	2514	1-659, 1936-2514	envelope glycoprotein H
28	UL22NdSP	2358	55-2412	
29	UL23	1128	Full-length	thymidine kinase

30	UL24	807	Full-length	nuclear protein
31	UL25	1740	1-660, 1173-1740	DNA packaging tegument protein
32	UL26	1905	1-565, 1423-1-05	capsid maturation protease
33	UL26.5	987	1-454, 491-987	capsid scaffold protein
34	UL27NdSP	2151	91-2241	envelope glycoprotein B
35	UL27b	315	2397-2712	
36	UL28a	1029	N-terminal 1029	DNA packaging terminase subunit 2
37	UL29a	3348	N-terminal 3348	single-stranded DNA-binding protein
38	UL30	3708	1-639, 3149-3708	DNA polymerase catalytic subunit
39	UL31	921	Full-length	nuclear egress lamina protein
40	UL32	1791	1-276, 1237-1791	DNA packaging protein
41	UL33	393	Full-length	DNA packaging protein
42	UL34	825	Full-length	nuclear egress membrane protein
43	UL34a	741	1-741	
44	UL35	336	Full-length	small capsid protein
45	UL36a	3000	N-terminal 3000	large tegument protein
46	UL36b	3000	Central 3000	
47	UL37d11	3369	Full-length	tegument protein
48	UL37b	1869	C-terminal 1869	
49	UL38	1395	Full-length	capsid triplex subunit 1
50	UL39	3411	Full-length	ribonucleotide reductase subunit 1
51	UL40	1020	Full-length	ribonucleotide reductase subunit 2
52	UL40a	537	1-537	
53	UL40b	414	607-1020	
54	UL41	1467	Full-length	tegument host shutoff protein
55	UL42	1464	1-85, 760-1464	dsDNA-binding protein
56	UL43	1302	Full-length	envelope protein
57	UL43a	222	1-222	
58	UL43b	453	643-1095	
59	UL44	1533	1-74, 1017-1533	envelope glycoprotein C
60	UL44NdSP	1362	70-1431	

61	UL45	516	Full-length	membrane protein
62	UL45a	372	145-516	
63	UL46a	1008	N-terminal 1008	tegument protein VP11/12
64	UL46b	2514	C-terminal 2514	
65	UL47	2079	1-717, 1147-2079	tegument protein VP13/14
66	UL48	1470	Full-length	transactivating tegument protein VP16
67	UL49	903	Full-length	tegument protein VP22
68	UL49a	273	N-terminal 273	
69	UL50	1116	Full-length	deoxyuridine triphosphatase
70	UL51	732	Full-length	tegument protein UL51
71	UL52	3177	Full-length	helicase-primase primase subunit
72	UL53	1014	Full-length	envelope glycoprotein K
73	UL53a	270	97-366	
74	UL54	1539	Full-length	multifunctional expression regulator
75	UL55	558	Full-length	nuclear protein
76	UL56	702	Full-length	membrane protein
77	UL56N	630	1-630	
78	US1	1260	Full-length	regulatory protein ICP22
79	US2	873	Full-length	possibly envelope-associated
80	US3	1443	Full-length	serine/threonine protein kinase
81	US4	714	Full-length	envelope glycoprotein G
82	US4a	483	88-570	
83	US5	276	Full-length	envelope glycoprotein J
84	US5a	78	73-150	
85	US6	1182	Full-length	envelope glycoprotein D
86	US6a	1023	1-1023	
87	US6NdSP	948	76-1023	
88	US7	1170	Full-length	envelope glycoprotein I
89	US7a	819	1-819	
90	US7NdSP	759	61-819	
91	US7b	282	889-1170	
92	US8	1650	Full-length	envelope glycoprotein E
93	US8a	1263	1-1263	
94	US8NdSP	1200	63-1263	

95	US8b	318	1333-1650	
96	US9	270	Full-length	membrane protein
97	US9a	192	1-192	
98	US10	936	Full-length	virion protein
99	US11	483	Full-length	TAP transporter inhibitor ICP47
100	RL1	744	Full-length	Neurovirulence factor
101	RL2	666	Exon 2	
102	RS1a	897	265-1161	transcriptional regulator ICP4
103	RS1b	2157	1303-3459	

Appendix 3: Inhibitor 3-AT concentrations for Y2H assay

Bait	3-AT Conc.	Clones sequenced
HPV-16 E1-N	1 mM	1
HPV-16 E4	5 mM	0
HPV-16 E5	0.1 mM	11
HPV-16 E6	1 mM	0
HPV-16 E7	2.5 mM	16
HPV-16 L1	0.1 mM	28
HPV-16 L2	0.5 mM	7
HPV-16 E1^E4	1 mM	0
HPV-16 E1^E4*	0 mM	14
HPV-16 E1^E2C	0.1 mM	11
HPV-16 E6*^E4	0.5 mM	0
HPV-16 E6*^E7*	0.5 mM	26
HPV-18 E1	0.1 mM	38

Appendix 4: Virus-host Y2H assay and LUMIER validation

Sl no.	HPV Bait	Cellular interactor	NCBI accession number	No. of clones	LUMIER assay validation
1	E1-N	CREB3	NM_006368	1	Negative
2	E1	ZNF451	NM_015555	1	Not tested
3	E1	SLC25A46	NM_138773	1	Positive
4	E1	ZFAND1	NM_024699	1	Negative
5	E1	WDR60	NM_018051	3	Negative
6	E1	PRM2	NM_002762	1	Negative
7	E1	NUFIP1	NM_012345	1	Negative
8	E1	FAM18B1	NM_016078	1	Not tested
9	E1	ANKRD30A	NM_052997	1	Not tested
10	E1	XRCC6	NM_001469	1	Negative
11	E1	TBC1D21	NM_153356	1	Not tested
12	E1	RPL11	NM_000975	1	Not tested
13	E5	CCDC136	NM_022742	1	Negative
14	E5	SLC30A1	NM_021194	1	Not tested
15	E5	YIPF4	NM_032312	1	Positive
16	E5	CLMN	NM_024734	1	Positive
17	E5	TXNDC15	NM_024715	1	Positive
18	E5	RNF141	NM_016422	1	Negative
19	E5	GLRX3	NM_006541	1	Not tested
20	E5	RCC2	NM_018715	1	Not tested
21	E5	PSMD2	NM_002808	1	Negative
22	E5	GRK5	NM_005308.2	1	Not tested
23	E7	PPIG	NM_004792	1	Positive
24	E7	CCDC11	NM_145020	1	Negative
25	E7	SPZ1	NM_032567	1	Positive
26	L1	ADORA3	NM_001081976	1	Positive
27	L1	CAMLG	NM_001745	2	Not tested
28	L1	CREB3	NM_006368	7	Negative
29	L1	SPACA1	NM_030960	1	Negative
30	L1	SNAR-E	NR_024258	1	Not tested
31	L1	PITRM1	NM_014889	2	Negative
32	L2	DUS3L	NM_020175	1	Negative
33	L2	WDR48	NM_020839	1	Not tested
34	E1^ E4*	CPT2	NM_000098	1	Not tested
35	E1^ E4*	EEF1A1	NM_001402	1	Positive
36	E1^ E4*	DNAJB1	NM_006145	1	Negative
37	E1^ E4*	UCHL1	NM_004181	1	Negative
38	E1^ E4*	RPL3	NM_000967	1	Negative

39	E6*^E7*	MRPL36	NM_032479	1	Negative
40	E6*^E7*	AIMP2	NM_006303	1	Not tested
41	E6*^E7*	HAX1	NM_006118	1	Negative
42	E6*^E7*	DNAJB1	NM_006145	2	Negative
43	E6*^E7*	DNAJB6	NM_005494	1	Not tested
44	E6*^E7*	KIFC3	NM_001130100	1	Positive
45	E6*^E7*	LDHC	NM_017448	1	Negative
46	E6*^E7*	TAF1A	NM_005681	1	Negative
47	E1^ E2C	RPS7	NM_001011	1	Negative
48	E1^ E2C	MLL4	NM_014727	1	Not tested
49	E1^ E2C	ZBTB6	NM_006626	1	Not tested
50	E1^ E2C	UBE2I	NM_003345	2	Negative
51	E1^ E2C	UBL3	NM_007106	1	Negative
52	E1^ E2C	RPL36AL	NM_001001	1	Negative
53	E1^ E2C	EFCAB5	NR_026738	1	Not tested
54	E1^ E2C	REEP6	NM_138393	1	Negative

Appendix 5: Interactions identified in Y2H for SPZ1

Sl no.	SPZ1 Interactor	NCBI accession number	No. of Clones	Library
1	APOL4	NM_145660.1	1	MGC
2	BCSC-1	NM_001130142.1	1	MGC
3	CCDC14	NM_022757.4	1	Human lymph
4	CCL19	NM_006274.2	1	Human lymph
5	CCNI	NM_006835.2	1	MGC
6	CDK10	NR_027703	2	Human lymph
7	CENPM	NM_024053	1	Human lymph
8	CRX	NM_000554	1	MGC
9	CTSA	NM_000308	1	Human lymph
10	FTL	NM_000146	1	Human lymph
11	GRB2	NM_002086	1	Human lymph
12	HLA-DLR	NM_019111	1	MGC
13	HNRNPA2B1	NM_002137	1	Human lymph
14	IGF1R	NM_000875.3	1	MGC
15	IGLL5	NM_001178126.1	2	Human lymph
16	KCNN2	NM_170775	1	MGC
17	KRT33B	NM_002279	1	Human lymph
			2	MGC
18	MAGEA1	NM_004988	8	MGC
			5	Human lymph
19	MAX	NM_145112	1	MGC
20	METTL7B	NM_152637	1	MGC
21	MLLT6	NM_005937	1	MGC
22	MRPL51	NM_016497.3	1	MGC
23	NADKD1	NM_153013.3	1	MGC
24	NISCH	NM_007184	1	Human lymph
25	PHF7	NM_016483	1	Human Testis
26	PTPRK	NM_002844	1	MGC
27	RAD50	NM_005732	1	Human lymph
			3	Human Testis
28	RPL21	NM_000982	2	Human lymph
29	RPL34	NM_033625	1	Human lymph
30	RPL4	NM_000968	1	Human lymph
31	SERPINA6	NM_001756.3	1	MGC
32	SIKE1	NM_025073	1	MGC
33	TMCO1	NM_019026	1	Human lymph

Appendix 6: List of gene and protein names mentioned in the thesis

ADA3	Adenosine deaminase3
AMF-1	Transcription factor also known G-protein pathway suppressor 2 or GPS2
AP1	Activator protein 1
ATM	Ataxia telangiectasia mutated
ATR	Ataxia telangiectasia and Rad3 related
BAP31	B cell receptor associated protein 31
BRD4	Bromodomain containing protein 4
cAMP	Cyclic adenosine monophosphate
CREB3	cAMP response element protein 3
CBP	CREB binding protein
CDK2	Cyclin dependent kinase 2
ChIR1	Chitinase related protein 1
E4-DBP	E4 dead binding proteins
E6AP	E6 associated protein
E6BP	E6 binding protein
E6TP1	E6 targeted protein 1
EGFR	Epidermal growth factor receptor
ERK1/2	Extracellular signal regulated kinase
ET-1	Endothlin 1
ETA	Endothlin A receptor
EVER proteins	Epidermodysplasia verruciformis proteins
GPS2	G-protein pathway suppressor 2
HDAC	Histone deacetylase
hDIg	Human hopmologue of Drosphila disc large
hscrib	Human homologue of Drosphila scribble
HNAP1	Human nucleosome assembly protein 1
HSPGs	Heparin sulphate proteoglycans
hTERT	Human telomerase
INI1	Integrase interactor 1
MAPK	Mitogen activated protein kinase pathway
MAX	Myc binding protein
MCM7	Minichromosome maintenance 7
c-MYC	Cellular myelocytomatosis protein
MHC	Major histocompatibility complex
NCoR1	Nuclear receptor corepressor 1

NFX1	Nuclear factor, X box binding
NFX123	Nuclear factor, X box binding 123
PCNA	Proliferative cell nuclear antigen
PDZ	A domain, an acronym combining the first letters of three proteins— post synaptic density protein (PSD95), Drosophila disc large tumor suppressor (Dlg1), and zonula occludens-1 protein (zo-1)
PDGF	Platelet derived growth factor
RB	Retinoblastoma gene
RPA	Replication protein A
SET domain	Zeste domain
SETB1	SET domain, bifurcated 1
SP1	Specifity protein 1
SWI/SNF complex	SWItch/Sucrose Non-Fermentable
TBP	TATA binding protein
TBLR1	Transducin (beta)-like 1 X-linked receptor 1
TopBP1	Topoisomerase 2- binding protein 1
TRIM28	Tripartite motif-containing 28
UBC9	Ubiquitin conjugating enzyme
ZNT1	Zinc transporter 1

REFERENCES

1. Shope RE, Hurst EW. Infectious papillomatosis of rabbits. J Exp Med. 1933 Oct 31;58(5):607–24.

2. Parsons RJ, Kidd JG. Oral papillomatosis of rabbits: a virus disease. J Exp Med. 1943 Mar 1;77(3):233–50.

3. Lowy DR. History of Papillomavirus Research. In: Garcea RL, DiMaio D, editors. The Papillomaviruses. Springer US; 2007. page 13–28.

4. Bernard H-U, Burk RD, Chen Z, Van Doorslaer K, Hausen H zur, De Villiers E-M. Classification of papillomaviruses (PVs) based on 189 PV types and proposal of taxonomic amendments. Virology. 2010 May 25;401(1):70–9.

5. Chen EY, Howley PM, Levinson AD, Seeburg PH. The primary structure and genetic organization of the bovine papillomavirus type 1 genome. Nature. 1982;299:529–34.

6. Regenmortel MHV van, Fauquet CM, Bishop DHL, Carsten EB, Estes MK, Lemon SM, et al., editors. Virus Taxonomy: Seventh Report of the International Committee on Taxonomy of Viruses. 1st ed. Academic Press; 2000.

7. De Villiers E-M, Fauquet C, Broker TR, Bernard H-U, Zur Hausen H. Classification of papillomaviruses. Virology. 2004 Jun 20;324(1):17–27.

8. Muñoz N, Bosch FX, De Sanjosé S, Herrero R, Castellsagué X, Shah KV, et al. Epidemiologic Classification of Human Papillomavirus Types Associated with Cervical Cancer. New England Journal of Medicine. 2003;348(6):518–27.

9. Moody CA, Laimins LA. Human papillomavirus oncoproteins: pathways to transformation. Nat. Rev. Cancer. 2010 Aug;10(8):550–60.

10. Ho GYF, Bierman R, Beardsley L, Chang CJ, Burk RD. Natural History of Cervicovaginal Papillomavirus Infection in Young Women. New England Journal of Medicine. 1998;338(7):423–8.

11. Wentzensen N, Vinokurova S, Von Knebel Doeberitz M. Systematic review of genomic integration sites of human papillomavirus genomes in epithelial dysplasia and invasive cancer of the female lower genital tract. Cancer Res. 2004 Jun 1;64(11):3878–84.

12. Longworth MS, Laimins LA. Pathogenesis of Human Papillomaviruses in Differentiating Epithelia. Microbiol. Mol. Biol. Rev. 2004 Jun 1;68(2):362–72.

13. Woodman CBJ, Collins SI, Young LS. The natural history of cervical HPV infection: unresolved issues. Nature Reviews Cancer. 2007 Jan 1;7(1):11–22.

14. Zheng Z-M, Baker CC. Papillomavirus Genome Structure, Expression, And Post-Transcriptional Regulation. Front Biosci. 2006 Sep 1;11:2286–302.

15. Conway MJ, Meyers C. Replication and Assembly of Human Papillomaviruses. J Dent Res. 2009 Apr 1;88(4):307–17.

16. McLaughlin-Drubin ME, Meyers C. Propagation of infectious, high-risk HPV in organotypic "raft" culture. Methods Mol. Med. 2005;119:171–86.

17. Dollard SC, Wilson JL, Demeter LM, Bonnez W, Reichman RC, Broker TR, et al. Production of human papillomavirus and modulation of the infectious program in epithelial raft cultures. Genes Dev. 1992 Jul 1;6(7):1131–42.

18. Finnen RL, Erickson KD, Chen XS, Garcea RL. Interactions between Papillomavirus L1 and L2 Capsid Proteins. J. Virol. 2003 Apr 15;77(8):4818–26.

19. Lowe J, Panda D, Rose S, Jensen T, Hughes WA, Tso FY, et al. Evolutionary and structural analyses of alpha-papillomavirus capsid proteins yields novel insights into L2 structure and interaction with L1. Virology Journal. 2008 Dec 17;5(1):150.

20. Trus BL, Roden RB, Greenstone HL, Vrhel M, Schiller JT, Booy FP. Novel structural features of bovine papillomavirus capsid revealed by a three-dimensional reconstruction to 9 A resolution. Nat. Struct. Biol. 1997 May;4(5):413–20.

21. Giroglou T, Florin L, Schäfer F, Streeck RE, Sapp M. Human Papillomavirus Infection Requires Cell Surface Heparan Sulfate. J Virol. 2001 Feb;75(3):1565–70.

22. Shafti-Keramat S, Handisurya A, Kriehuber E, Meneguzzi G, Slupetzky K, Kirnbauer R. Different heparan sulfate proteoglycans serve as cellular receptors for human papillomaviruses. J. Virol. 2003 Dec;77(24):13125–35.

23. Horvath C, Boulet G, Renoux V, Delvenne P, Bogers J-P. Mechanisms of cell entry by human papillomaviruses: an overview. Virology Journal. 2010 Jan 20;7(1):11.

24. Sapp M, Day PM. Structure, attachment and entry of polyoma- and papillomaviruses. Virology. 2009 Feb 20;384(2):400–9.

25. Bousarghin L, Touzé A, Sizaret P-Y, Coursaget P. Human papillomavirus types 16, 31, and 58 use different endocytosis pathways to enter cells. J. Virol. 2003 Mar;77(6):3846–50.

26. Spoden G, Freitag K, Husmann M, Boller K, Sapp M, Lambert C, et al. Clathrin- and caveolin-independent entry of human papillomavirus type 16--involvement of tetraspanin-enriched microdomains (TEMs). PLoS ONE. 2008;3(10):e3313.

27. Sapp M, Bienkowska-Haba M. Viral entry mechanisms: human papillomavirus and a long journey from extracellular matrix to the nucleus. FEBS J. 2009 Dec;276(24):7206–16.

28. Florin L, Becker KA, Lambert C, Nowak T, Sapp C, Strand D, et al. Identification of a Dynein Interacting Domain in the Papillomavirus Minor Capsid Protein L2. J Virol. 2006 Jul;80(13):6691–6.

29. Schneider MA, Spoden GA, Florin L, Lambert C. Identification of the dynein light chains required for human papillomavirus infection. Cell. Microbiol. 2011 Jan;13(1):32–46.

30. Ustav M, Ustav E, Szymanski P, Stenlund A. Identification of the origin of replication of bovine papillomavirus and characterization of the viral origin recognition factor E1. EMBO Journal. 1991;10(13):4321–9.

31. Chiang CM, Ustav M, Stenlund A, Ho TF, Broker TR, Chow LT. Viral E1 and E2 proteins support replication of homologous and heterologous papillomaviral origins. Proc Natl Acad Sci U S A. 1992 Jul 1;89(13):5799–803.

32. Kadaja M, Silla T, Ustav E, Ustav M. Papillomavirus DNA replication — From initiation to genomic instability. Virology. 2009 Feb 20;384(2):360–8.

33. Clertant P, Seif I. A common function for polyoma virus large-T and papillomavirus E1 proteins? Nature. 1984 Sep 20;311(5983):276–9.

34. F J Hughes MAR. E1 protein of human papillomavirus is a DNA helicase/ATPase. Nucleic acids research. 1994;21(25):5817–23.

35. Melendy T, Sedman J, Stenlund A. Cellular factors required for papillomavirus DNA replication. J. Virol. 1995 Dec;69(12):7857–67.

36. Wilson VG, West M, Woytek K, Rangasamy D. Papillomavirus E1 Proteins: Form, Function, and Features. Virus Genes. 2002;24(3):275–90.

37. Le Moal MA, Yaniv M, Thierry F. The bovine papillomavirus type 1 (BPV1) replication protein E1 modulates transcriptional activation by interacting with BPV1 E2. J. Virol. 1994 Feb;68(2):1085–93.

38. Chiang CM, Broker TR, Chow LT. An E1M--E2C fusion protein encoded by human papillomavirus type 11 is asequence-specific transcription repressor. J Virol. 1991 Jun;65(6):3317–29.

39. Swindle CS, Engler JA. Association of the human papillomavirus type 11 E1 protein with histone H1. J. Virol. 1998 Mar;72(3):1994–2001.

40. Belyavskyi M, Westerman M, DiMichele L, Wilson VG. Perturbation of the host cell cycle and DNA replication by the bovine papillomavirus replication protein E1. Virology. 1996 May 1;219(1):206–19.

41. Romanczuk H, Howley PM. Disruption of either the E1 or the E2 regulatory gene of human papillomavirus type 16 increases viral immortalization capacity. Proc Natl Acad Sci U S A. 1992 Apr 1;89(7):3159–63.

42. Fields BN, Knipe DM, Howley PM. Fields virology. Philadelphia: Wolters Kluwer Health/Lippincott Williams & Wilkins; 2007.

43. Milligan SG, Veerapraditsin T, Ahamet B, Mole S, Graham SV. Analysis of novel human papillomavirus type 16 late mRNAs in differentiated W12 cervical epithelial cells. Virology. 2007 Mar 30;360(1-5):172–81.

44. Rosenstierne MW, Vinther J, Hansen CN, Prydsoe M, Norrild B. Identification and characterization of a cluster of transcription start sites located in the E6 ORF of human papillomavirus type 16. J. Gen. Virol. 2003 Nov;84(Pt 11):2909–20.

45. Doorbar J, Parton A, Hartley K, Banks L, Crook T, Stanley M, et al. Detection of novel splicing patterns in a HPV16-containing keratinocyte cell line. Virology. 1990 Sep;178(1):254–62.

46. Stubenrauch F, Hummel M, Iftner T, Laimins LA. The E8^E2C Protein, a Negative Regulator of Viral Transcription and Replication, Is Required for Extrachromosomal Maintenance of Human Papillomavirus Type 31 in Keratinocytes. J. Virol. 2000 Feb 1;74(3):1178–86.

47. Hegde RS. The Papillomavirus E2 Proteins: Structure, Function, and Biology. Annual Review of Biophysics and Biomolecular Structure. 2002;31(1):343–60.

48. Ammermann I, Bruckner M, Matthes F, Iftner T, Stubenrauch F. Inhibition of transcription and DNA replication by the papillomavirus E8-E2C protein is mediated by interaction with corepressor molecules. J. Virol. 2008 Jun;82(11):5127–36.

49. Powell MLC, Smith JA, Sowa ME, Harper JW, Iftner T, Stubenrauch F, et al. NCoR1 mediates papillomavirus E8;E2C transcriptional repression. J. Virol. 2010 May;84(9):4451–60.

50. Breiding DE, Sverdrup F, Grossel MJ, Moscufo N, Boonchai W, Androphy EJ. Functional interaction of a novel cellular protein with the papillomavirus E2 transactivation domain. Mol. Cell. Biol. 1997 Dec;17(12):7208–19.

51. Rehtanz M, Schmidt H-M, Warthorst U, Steger G. Direct interaction between nucleosome assembly protein 1 and the papillomavirus E2 proteins involved in activation of transcription. Mol. Cell. Biol. 2004 Mar;24(5):2153–68.

52. Dong G, Broker TR, Chow LT. Human papillomavirus type 11 E2 proteins repress the homologous E6 promoter by interfering with the binding of host transcription factors to adjacent elements. J. Virol. 1994 Feb;68(2):1115–27.

53. Johansson C, Somberg M, Li X, Backström Winquist E, Fay J, Ryan F, et al. HPV-16 E2 contributes to induction of HPV-16 late gene expression by inhibiting early polyadenylation. EMBO J. 2012 Jul 18;31(14):3212–27.

54. McBride AA, McPhillips MG, Oliveira JG. Brd4: tethering, segregation and beyond. Trends Microbiol. 2004 Dec;12(12):527–9.

55. Parish JL, Bean AM, Park RB, Androphy EJ. ChlR1 is required for loading papillomavirus E2 onto mitotic chromosomes and viral genome maintenance. Mol. Cell. 2006 Dec 28;24(6):867–76.

56. Boner W, Taylor ER, Tsirimonaki E, Yamane K, Campo MS, Morgan IM. A Functional interaction between the human papillomavirus 16 transcription/replication factor E2 and the DNA damage response protein TopBP1. J. Biol. Chem. 2002 Jun 21;277(25):22297–303.

57. Donaldson MM, Boner W, Morgan IM. TopBP1 regulates human papillomavirus type 16 E2 interaction with chromatin. J. Virol. 2007 Apr;81(8):4338–42.

58. Brown C, Kowalczyk AM, Taylor ER, Morgan IM, Gaston K. P53 represses human papillomavirus type 16 DNA replication via the viral E2 protein. Virol. J. 2008;5:5.

59. Thierry F, Demeret C. Direct activation of caspase 8 by the proapoptotic E2 protein of HPV18 independent of adaptor proteins. Cell Death Differ. 2008 Sep;15(9):1356–63.

60. Doorbar J, Coneron I, Gallimore PH. Sequence divergence yet conserved physical characteristics among the E4 proteins of cutaneous human papillomaviruses. Virology. 1989 Sep;172(1):51–62.

61. Tan CL, Gunaratne J, Lai D, Carthagena L, Wang Q, Xue YZ, et al. HPV-18 E2^E4 chimera: 2 new spliced transcripts and proteins induced by keratinocyte differentiation. Virology. 2012 Jul 20;429(1):47–56.

62. Raj K, Berguerand S, Southern S, Doorbar J, Beard P. E1 empty set E4 protein of human papillomavirus type 16 associates with mitochondria. J. Virol. 2004 Jul;78(13):7199–207.

63. Ashmole I, Gallimore PH, Roberts S. Identification of conserved hydrophobic C-terminal residues of the human papillomavirus type 1 E1E4 protein necessary for E4 oligomerisation in vivo. Virology. 1998 Jan 20;240(2):221–31.

64. Doorbar J, Ely S, Sterling J, McLean C, Crawford L. Specific interaction between HPV-16 E1–E4 and cytokeratins results in collapse of the epithelial cell intermediate filament network. Nature. 1991 Aug 29;352(6338):824–7.

65. Roberts S, Ashmole I, Gibson LJ, Rookes SM, Barton GJ, Gallimore PH. Mutational analysis of human papillomavirus E4 proteins: identification of structural features important in the formation of cytoplasmic E4/cytokeratin networks in epithelial cells. J. Virol. 1994 Oct;68(10):6432–45.

66. Wang Q, Griffin H, Southern S, Jackson D, Martin A, McIntosh P, et al. Functional analysis of the human papillomavirus type 16 E1=E4 protein provides a mechanism for in vivo and in vitro keratin filament reorganization. J. Virol. 2004 Jan;78(2):821–33.

67. Khan J, Davy CE, McIntosh PB, Jackson DJ, Hinz S, Wang Q, et al. Role of calpain in the formation of human papillomavirus type 16 E1^E4 amyloid fibers and reorganization of the keratin network. J. Virol. 2011 Oct;85(19):9984–97.

68. Davy CE, Jackson DJ, Wang Q, Raj K, Masterson PJ, Fenner NF, et al. Identification of a G(2) arrest domain in the E1 wedge E4 protein of human papillomavirus type 16. J. Virol. 2002 Oct;76(19):9806–18.

69. Knight GL, Turnell AS, Roberts S. Role for Wee1 in inhibition of G2-to-M transition through the cooperation of distinct human papillomavirus type 1 E4 proteins. J. Virol. 2006 Aug;80(15):7416–26.

70. Phelps WC, Yee CL, Münger K, Howley PM. The human papillomavirus type 16 E7 gene encodes transactivation and transformation functions similar to those of adenovirus E1A. Cell. 1988 May 20;53(4):539–47.

71. Klingelhutz AJ, Roman A. Cellular transformation by human papillomaviruses: Lessons learned by comparing high- and low-risk viruses. Virology. 2012 Mar 15;424(2):77–98.

72. Giacinti C, Giordano A. RB and cell cycle progression. Oncogene. 2006 Aug 28;25(38):5220–7.

73. Nevins JR. The Rb/E2F pathway and cancer. Hum. Mol. Genet. 2001 Apr 1;10(7):699–703.

74. Vietri M, Bianchi M, Ludlow JW, Mittnacht S, Villa-Moruzzi E. Direct interaction between the catalytic subunit of Protein Phosphatase 1 and pRb. Cancer Cell Int. 2006 Feb 8;6:3.

75. Edmonds C, Vousden KH. A point mutational analysis of human papillomavirus type 16 E7 protein. J. Virol. 1989 Jun;63(6):2650–6.

76. Lee JO, Russo AA, Pavletich NP. Structure of the retinoblastoma tumour-suppressor pocket domain bound to a peptide from HPV E7. Nature. 1998 Feb 26;391(6670):859–65.

77. Todorovic B, Massimi P, Hung K, Shaw GS, Banks L, Mymryk JS. Systematic analysis of the amino acid residues of human papillomavirus type 16 E7 conserved region 3 involved in dimerization and transformation. J. Virol. 2011 Oct;85(19):10048–57.

78. Hwang SG, Lee D, Kim J, Seo T, Choe J. Human papillomavirus type 16 E7 binds to E2F1 and activates E2F1-driven transcription in a retinoblastoma protein-independent manner. J. Biol. Chem. 2002 Jan 25;277(4):2923–30.

79. Funk JO, Waga S, Harry JB, Espling E, Stillman B, Galloway DA. Inhibition of CDK activity and PCNA-dependent DNA replication by p21 is blocked by interaction with the HPV-16 E7 oncoprotein. Genes Dev. 1997 Aug 15;11(16):2090–100.

80. Münger K, Baldwin A, Edwards KM, Hayakawa H, Nguyen CL, Owens M, et al. Mechanisms of Human Papillomavirus-Induced Oncogenesis. J Virol. 2004 Nov;78(21):11451–60.

81. Werness BA, Levine AJ, Howley PM. Association of human papillomavirus types 16 and 18 E6 proteins with p53. Science. 1990 Apr 6;248(4951):76–9.

82. Vousden KH, Lu X. Live or let die: the cell's response to p53. Nature Reviews Cancer. 2002 Aug 1;2(8):594–604.

83. Huibregtse JM, Scheffner M, Howley PM. Cloning and expression of the cDNA for E6-AP, a protein that mediates the interaction of the human papillomavirus E6 oncoprotein with p53. Mol Cell Biol. 1993 Feb;13(2):775–84.

84. Kao WH, Beaudenon SL, Talis AL, Huibregtse JM, Howley PM. Human Papillomavirus Type 16 E6 Induces Self-Ubiquitination of the E6AP Ubiquitin-Protein Ligase. J Virol. 2000 Jul;74(14):6408–17.

85. Lechner MS, Laimins LA. Inhibition of p53 DNA binding by human papillomavirus E6 proteins. J. Virol. 1994 Jul;68(7):4262–73.

86. Kranjec C, Banks L. A Systematic Analysis of Human Papillomavirus (HPV) E6 PDZ Substrates Identifies MAGI-1 as a Major Target of HPV Type 16 (HPV-16) and HPV-18 Whose Loss Accompanies Disruption of Tight Junctions. J Virol. 2011 Feb;85(4):1757–64.

87. Thomas M, Laura R, Hepner K, Guccione E, Sawyers C, Lasky L, et al. Oncogenic human papillomavirus E6 proteins target the MAGI-2 and MAGI-3 proteins for degradation. Oncogene. 2002 Aug 1;21(33):5088–96.

88. Klingelhutz AJ, Foster SA, McDougall JK. Telomerase activation by the E6 gene product of human papillomavirus type 16. Nature. 1996 Mar 7;380(6569):79–82.

89. Howie HL, Katzenellenbogen RA, Galloway DA. Papillomavirus E6 proteins. Virology. 2009 Feb 20;384(2):324–34.

90. Conrad M, Bubb VJ, Schlegel R. The human papillomavirus type 6 and 16 E5 proteins are membrane-associated proteins which associate with the 16-kilodalton pore-forming protein. J. Virol. 1993 Oct;67(10):6170–8.

91. Leechanachai P, Banks L, Moreau F, Matlashewski G. The E5 gene from human papillomavirus type 16 is an oncogene which enhances growth factor-mediated signal transduction to the nucleus. Oncogene. 1992 Jan;7(1):19–25.

92. Crusius K, Rodriguez I, Alonso A. The human papillomavirus type 16 E5 protein modulates ERK1/2 and p38 MAP kinase activation by an EGFR-independent process in stressed human keratinocytes. Virus Genes. 2000;20(1):65–9.

93. Venuti A, Salani D, Poggiali F, Manni V, Bagnato A. The E5 oncoprotein of human papillomavirus type 16 enhances endothelin-1-induced keratinocyte growth. Virology. 1998 Aug 15;248(1):1–5.

94. Tsao YP, Li LY, Tsai TC, Chen SL. Human papillomavirus type 11 and 16 E5 represses p21(WafI/SdiI/CipI) gene expression in fibroblasts and keratinocytes. J. Virol. 1996 Nov;70(11):7535–9.

95. Chen SL, Lin YK, Li LY, Tsao YP, Lo HY, Wang WB, et al. E5 proteins of human papillomavirus types 11 and 16 transactivate the c-fos promoter through the NF1 binding element. J. Virol. 1996 Dec;70(12):8558–63.

96. Zhang B, Li P, Wang E, Brahmi Z, Dunn KW, Blum JS, et al. The E5 protein of human papillomavirus type 16 perturbs MHC class II antigen maturation in human foreskin keratinocytes treated with interferon-gamma. Virology. 2003 May 25;310(1):100–8.

97. Ashrafi GH, Brown DR, Fife KH, Campo MS. Down-regulation of MHC class I is a property common to papillomavirus E5 proteins. Virus Res. 2006 Sep;120(1-2):208–11.

98. Regan JA, Laimins LA. Bap31 is a novel target of the human papillomavirus E5 protein. J. Virol. 2008 Oct;82(20):10042–51.

99. Lazarczyk M, Pons C, Mendoza J-A, Cassonnet P, Jacob Y, Favre M. Regulation of cellular zinc balance as a potential mechanism of EVER-mediated protection against pathogenesis by cutaneous oncogenic human papillomaviruses. J. Exp. Med. 2008 Jan 21;205(1):35–42.

100. Stanley M. Immune responses to human papillomavirus. Vaccine. 2006 Mar 30;24, Supplement 1(0):S16–S22.

101. Stanley MA. Epithelial Cell Responses to Infection with Human Papillomavirus. Clin. Microbiol. Rev. 2012 Apr 1;25(2):215–22.

102. Karim R, Meyers C, Backendorf C, Ludigs K, Offringa R, Van Ommen G-JB, et al. Human Papillomavirus Deregulates the Response of a Cellular Network Comprising of Chemotactic and Proinflammatory Genes. PLoS ONE. 2011 Mar 14;6(3):e17848.

103. Leong CM, Doorbar J, Nindl I, Yoon H-S, Hibma MH. Loss of Epidermal Langerhans Cells Occurs in Human Papillomavirus α, γ, and μ but Not β Genus Infections. J Invest Dermatol. 2009 Sep 17;130(2):472–80.

104. Caberg J-H, Hubert P, Herman L, Herfs M, Roncarati P, Boniver J, et al. Increased migration of Langerhans cells in response to HPV16 E6 and E7 oncogene silencing: role of CCL20. Cancer Immunol. Immunother. 2009 Jan;58(1):39–47.

105. Sperling T, Ołdak M, Walch-Rückheim B, Wickenhauser C, Doorbar J, Pfister H, et al. Human papillomavirus type 8 interferes with a novel C/EBPβ-mediated mechanism of keratinocyte CCL20 chemokine expression and Langerhans cell migration. PLoS Pathog. 2012;8(7):e1002833.

106. Nees M, Geoghegan JM, Hyman T, Frank S, Miller L, Woodworth CD. Papillomavirus type 16 oncogenes downregulate expression of interferon-responsive genes and upregulate proliferation-associated and NF-kappaB-responsive genes in cervical keratinocytes. J. Virol. 2001 May;75(9):4283–96.

107. Ronco LV, Karpova AY, Vidal M, Howley PM. Human papillomavirus 16 E6 oncoprotein binds to interferon regulatory factor-3 and inhibits its transcriptional activity. Genes Dev. 1998 Jul 1;12(13):2061–72.

108. Barnard P, McMillan NA. The human papillomavirus E7 oncoprotein abrogates signaling mediated by interferon-alpha. Virology. 1999 Jul 5;259(2):305–13.

109. Stanley M. HPV - immune response to infection and vaccination. Infect Agent Cancer. 2010 Oct 20;5:19.

110. Moscicki A-B, Schiffman M, Kjaer S, Villa LL. Chapter 5: Updating the natural history of HPV and anogenital cancer. Vaccine. 2006 Aug 31;24 Suppl 3:S3/42–51.

111. Rogers HD, MacGregor JL, Nord KM, Tyring S, Rady P, Engler DE, et al. Acquired epidermodysplasia verruciformis. Journal of the American Academy of Dermatology. 2009 Feb;60(2):315–20.

112. Walboomers JMM, Jacobs MV, Manos MM, Bosch FX, Kummer JA, Shah KV, et al. Human papillomavirus is a necessary cause of invasive cervical cancer worldwide. The Journal of Pathology. 1999;189(1):12–9.

113. Pfister H. Chapter 8: Human papillomavirus and skin cancer. J. Natl. Cancer Inst. Monographs. 2003;(31):52–6.

114. Harwood CA, McGregor JM, Proby CM, Breuer J. Human papillomavirus and the development of non-melanoma skin cancer. J. Clin. Pathol. 1999 Apr;52(4):249–53.

115. Crum CP, McLachlin CM, Tate JE, Mutter GL. Pathobiology of vulvar squamous neoplasia. Curr. Opin. Obstet. Gynecol. 1997 Feb;9(1):63–9.

116. Uronis HE, Bendell JC. Anal Cancer: An Overview. The Oncologist. 2007 May 1;12(5):524–34.

117. Marur S, D'Souza G, Westra WH, Forastiere AA. HPV-associated head and neck cancer: a virus-related cancer epidemic. Lancet Oncol. 2010 Aug;11(8):781–9.

118. Bosch FX, Lorincz A, Muñoz N, Meijer CJLM, Shah KV. The causal relation between human papillomavirus and cervical cancer. J. Clin. Pathol. 2002 Apr;55(4):244–65.

119. Kraft S, Faquin WC, Krane JF. HPV-associated neuroendocrine carcinoma of the oropharynx: a rare new entity with potentially aggressive clinical behavior. Am. J. Surg. Pathol. 2012 Mar;36(3):321–30.

120. Wheeler CM. Advances in primary and secondary interventions for cervical cancer: human papillomavirus prophylactic vaccines and testing. Nature Clinical Practice Oncology. 2007 Apr;4(4):224–35.

121. Burchell AN, Winer RL, De Sanjosé S, Franco EL. Chapter 6: Epidemiology and transmission dynamics of genital HPV infection. Vaccine. 2006 Aug 31;24 Suppl 3:S3/52–61.

122. Matsumoto K, Oki A, Furuta R, Maeda H, Yasugi T, Takatsuka N, et al. Tobacco smoking and regression of low-grade cervical abnormalities. Cancer Sci. 2010 Sep;101(9):2065–73.

123. Smith JS, Green J, Berrington de Gonzalez A, Appleby P, Peto J, Plummer M, et al. Cervical cancer and use of hormonal contraceptives: a systematic review. Lancet. 2003 Apr 5;361(9364):1159–67.

124. Simonetti AC, Melo JH de L, De Souza PRE, Bruneska D, De Lima Filho JL. Immunological's host profile for HPV and Chlamydia trachomatis, a cervical cancer cofactor. Microbes Infect. 2009 Apr;11(4):435–42.

125. Szostek S, Zawilinska B, Kopec J, Kosz-Vnenchak M. Herpesviruses as possible cofactors in HPV-16-related oncogenesis. Acta Biochim. Pol. 2009;56(2):337–42.

126. Simon JW. The association of Herpes simplex virus and cervical cancer: A review. Gynecologic Oncology. 1976 Mar;4(1):108–16.

127. Rawls WE, Tompkins W a. F, Figueroa ME, Melnick JL. Herpesvirus Type 2: Association with Carcinoma of the Cervix. Science. 1968 Sep 20;161(3847):1255–6.

128. Weir JP. Regulation of herpes simplex virus gene expression. Gene. 2001 Jun 27;271(2):117–30.

129. Yamakawa Y, Forslund O, Chua KL, Dillner L, Boon ME, Hansson BG. Detection of the BC 24 transforming fragment of the herpes simplex virus type 2 (HSV-2) DNA in cervical carcinoma tissue by polymerase chain reaction (PCR). APMIS. 1994 Jun;102(6):401–6.

130. DiPaolo JA, Woodworth CD, Coutlée F, Zimonic DB, Bryant J, Kessous A. Relationship of stable integration of herpes simplex virus-2 BglII N subfragmentXho2 to malignant transformation of human papillomavirus-immortalized cervical keratinocytes. International Journal of Cancer. 1998;76(6):865–71.

131. Smith JS, Herrero R, Bosetti C, Muñoz N, Bosch FX, Eluf-Neto J, et al. Herpes simplex virus-2 as a human papillomavirus cofactor in the etiology of invasive cervical cancer. J. Natl. Cancer Inst. 2002 Nov 6;94(21):1604–13.

132. Zur Hausen H. Human genital cancer: synergism between two virus infections or synergism between a virus infection and initiating events? Lancet. 1982 Dec 18;2(8312):1370–2.

133. Muñoz N, Bosch FX, Castellsagué X, Díaz M, De Sanjose S, Hammouda D, et al. Against which human papillomavirus types shall we vaccinate and screen? The international perspective. Int. J. Cancer. 2004 Aug 20;111(2):278–85.

134. Lin K, Doolan K, Hung C-F, Wu TC. Perspectives for Preventive and Therapeutic HPV Vaccines. Journal of the Formosan Medical Association. 2010 Jan;109(1):4–24.

135. Fields S, Song O. A novel genetic system to detect protein–protein interactions. , Published online: 20 July 1989; | doi:10.1038/340245a0. 1989 Jul 20;340(6230):245–6.

136. Clemens KE, Brent R, Gyuris J, Munger K. Dimerization of the Human Papillomavirus E7 Oncoproteinin Vivo. Virology. 1995 Dec 1;214(1):289–93.

137. Brückner A, Polge C, Lentze N, Auerbach D, Schlattner U. Yeast two-hybrid, a powerful tool for systems biology. Int J Mol Sci. 2009 Jun;10(6):2763–88.

138. Van Criekinge W, Beyaert R. Yeast Two-Hybrid: State of the Art. Biol Proced Online. 1999 Oct 4;2:1–38.

139. Barrios-Rodiles M, Brown KR, Ozdamar B, Bose R, Liu Z, Donovan RS, et al. High-throughput mapping of a dynamic signaling network in mammalian cells. Science. 2005 Mar 11;307(5715):1621–5.

140. Braun P, Tasan M, Dreze M, Barrios-Rodiles M, Lemmens I, Yu H, et al. An experimentally derived confidence score for binary protein-protein interactions. Nature Methods. 2009;6(1):91–7.

141. Fossum E, Friedel CC, Rajagopala SV, Titz B, Baiker A, Schmidt T, et al. Evolutionarily Conserved Herpesviral Protein Interaction Networks. PLoS Pathog. 2009;5(9):e1000570.

142. Bernard P, Couturier M. Cell killing by the F plasmid CcdB protein involves poisoning of DNA-topoisomerase II complexes. Journal of Molecular Biology. 1992 Aug 5;226(3):735–45.

143. Seedorf K, Krämmer G, Dürst M, Suhai S, Röwekamp WG. Human papillomavirus type 16 DNA sequence. Virology. 1985 Aug;145(1):181–5.

144. Parrish JR, Yu J, Liu G, Hines JA, Chan JE, Mangiola BA, et al. A proteome-wide protein interaction map for Campylobacter jejuni. Genome Biol. 2007;8(7):R130.

145. Uetz P, Giot L, Cagney G, Mansfield TA, Judson RS, Knight JR, et al. A comprehensive analysis of protein-protein interactions in Saccharomyces cerevisiae. Nature. 2000 Feb 10;403(6770):623–7.

146. Li S, Armstrong CM, Bertin N, Ge H, Milstein S, Boxem M, et al. A map of the interactome network of the metazoan C. elegans. Science. 2004 Jan 23;303(5657):540–3.

147. Giot L, Bader JS, Brouwer C, Chaudhuri A, Kuang B, Li Y, et al. A Protein Interaction Map of Drosophila melanogaster. Science. 2003 Dec 5;302(5651):1727–36.

148. LaCount DJ, Vignali M, Chettier R, Phansalkar A, Bell R, Hesselberth JR, et al. A protein interaction network of the malaria parasite Plasmodium falciparum. Nature. 2005 Nov 3;438(7064):103–7.

149. Uhrig JF. Protein interaction networks in plants. Planta. 2006 Sep;224(4):771–81.

150. Stelzl U, Worm U, Lalowski M, Haenig C, Brembeck FH, Goehler H, et al. A Human Protein-Protein Interaction Network: A Resource for Annotating the Proteome. Cell. 2005 Sep 23;122(6):957–68.

151. Von Brunn A, Teepe C, Simpson JC, Pepperkok R, Friedel CC, Zimmer R, et al. Analysis of intraviral protein-protein interactions of the SARS coronavirus ORFeome. PLoS ONE. 2007;2(5):e459.

152. Bartel PL, Roecklein JA, SenGupta D, Fields S. A protein linkage map of Escherichia coli bacteriophage T7. Nature Genetics. 1996 Jan 1;12(1):72–7.

153. McCraith S, Holtzman T, Moss B, Fields S. Genome-wide analysis of vaccinia virus protein-protein interactions. Proc. Natl. Acad. Sci. U.S.A. 2000 Apr 25;97(9):4879–84.

154. Flajolet M, Rotondo G, Daviet L, Bergametti F, Inchauspé G, Tiollais P, et al. A genomic approach of the hepatitis C virus generates a protein interaction map. Gene. 2000 Jan 25;242(1-2):369–79.

155. Rozen R, Sathish N, Li Y, Yuan Y. Virion-Wide Protein Interactions of Kaposi's Sarcoma-Associated Herpesvirus. J. Virol. 2008 May 15;82(10):4742–50.

156. Calderwood MA, Venkatesan K, Xing L, Chase MR, Vazquez A, Holthaus AM, et al. Epstein–Barr virus and virus human protein interaction maps. PNAS. 2007 May 1;104(18):7606–11.

157. Lee JH, Vittone V, Diefenbach E, Cunningham AL, Diefenbach RJ. Identification of structural protein–protein interactions of herpes simplex virus type 1. Virology. 2008 Sep 1;378(2):347–54.

158. Yasugi T, Benson JD, Sakai H, Vidal M, Howley PM. Mapping and characterization of the interaction domains of human papillomavirus type 16 E1 and E2 proteins. J. Virol. 1997 Feb 1;71(2):891–9.

159. Bryan JT, Fife KH, Brown DR. The intracellular expression pattern of the human papillomavirus type 11 E1--E4 protein correlates with its ability to self associate. Virology. 1998 Feb 1;241(1):49–60.

160. Gammoh N, Grm HS, Massimi P, Banks L. Regulation of Human Papillomavirus Type 16 E7 Activity through Direct Protein Interaction with the E2 Transcriptional Activator. J Virol. 2006 Feb;80(4):1787–97.

161. Davy C, McIntosh P, Jackson DJ, Sorathia R, Miell M, Wang Q, et al. A novel interaction between the human papillomavirus type 16 E2 and E1--E4 proteins leads to stabilization of E2. Virology. 2009 Nov 25;394(2):266–75.

162. Okoye A, Cordano P, Taylor ER, Morgan IM, Everett R, Campo MS. Human papillomavirus 16 L2 inhibits the transcriptional activation function, but not the DNA replication function, of HPV-16 E2. Virus Research. 2005 Mar;108(1–2):1–14.

163. Zheng X, Yang M, Tan J, Pan Q, Long Z, Dai H, et al. Screening of LRRK2 interactants by yeast 2-hybrid analysis. Zhong Nan Da Xue Xue Bao Yi Xue Ban. 2008 Oct;33(10):883–91.

164. Jones RE, Wegrzyn RJ, Patrick DR, Balishin NL, Vuocolo GA, Riemen MW, et al. Identification of HPV-16 E7 peptides that are potent antagonists of E7 binding to the retinoblastoma suppressor protein. J. Biol. Chem. 1990 Aug 5;265(22):12782–5.

165. Patrick DR, Oliff A, Heimbrook DC. Identification of a novel retinoblastoma gene product binding site on human papillomavirus type 16 E7 protein. J. Biol. Chem. 1994 Mar 4;269(9):6842–50.

166. Swindle CS, Engler JA. Association of the Human Papillomavirus Type 11 E1 Protein with Histone H1. J. Virol. 1998 Mar 1;72(3):1994–2001.

167. Wang W-S, Lee M-S, Tseng C-E, Liao I-H, Huang S-P, Lin R-I, et al. Interaction between human papillomavirus type 5 E2 and polo-like kinase 1. J. Med. Virol. 2009 Mar;81(3):536–44.

168. Wilson VG, West M, Woytek K, Rangasamy D. Papillomavirus E1 proteins: form, function, and features. Virus Genes. 2002 Jun;24(3):275–90.

169. Huang H, Jedynak BM, Bader JS. Where have all the interactions gone? Estimating the coverage of two-hybrid protein interaction maps. PLoS Comput. Biol. 2007 Nov;3(11):e214.

170. Van Criekinge W, Beyaert R. Yeast Two-Hybrid: State of the Art. Biol Proced Online. 1999 Oct 4;2:1–38.

171. Lina Villa L, Schlegel R. Differences in transformation activity between HPV-18 and HPV-16 map to the viral LCR-E6-E7 region. Virology. 1991 Mar;181(1):374–7.

172. Liu J-S, Kuo S-R, Broker TR, Chow LT. The Functions of Human Papillomavirus Type 11 E1, E2, and E2C Proteins in Cell-free DNA Replication. J. Biol. Chem. 1995 Nov 10;270(45):27283–91.

173. Munger K, Halpern AL. HPV16 E7 : Primary Structure and Biological Properties. Pathology. 1995;17–36.

174. Phelps WC, Münger K, Yee CL, Barnes JA, Howley PM. Structure-function analysis of the human papillomavirus type 16 E7 oncoprotein. J. Virol. 1992 Apr;66(4):2418–27.

175. Storey A, Almond N, Osborn K, Crawford L. Mutations of the human papillomavirus type 16 E7 gene that affect transformation, transactivation and phosphorylation by the E7 protein. J. Gen. Virol. 1990 Apr;71 (Pt 4):965–70.

176. S Watanabe TK. Mutational analysis of human papillomavirus type 16 E7 functions. Journal of virology. 1990;64(1):207–14.

177. Park P, Copeland W, Yang L, Wang T, Botchan MR, Mohr IJ. The cellular DNA polymerase alpha-primase is required for papillomavirus DNA replication and associates with the viral E1 helicase. Proc. Natl. Acad. Sci. U.S.A. 1994 Aug 30;91(18):8700–4.

178. Clower RV, Fisk JC, Melendy T. Papillomavirus E1 Protein Binds to and Stimulates Human Topoisomerase I. J. Virol. 2006 Feb 1;80(3):1584–7.

179. Flores ER, Allen-Hoffmann BL, Lee D, Lambert PF. The Human Papillomavirus Type 16 E7 Oncogene Is Required for the Productive Stage of the Viral Life Cycle. J. Virol. 2000 Jul 15;74(14):6622–31.

180. Antinore MJ, Birrer MJ, Patel D, Nader L, McCance DJ. The human papillomavirus type 16 E7 gene product interacts with and trans-activates the AP1 family of transcription factors. EMBO J. 1996 Apr 15;15(8):1950–60.

181. Massimi P, Pim D, Banks L. Human papillomavirus type 16 E7 binds to the conserved carboxy-terminal region of the TATA box binding protein and this contributes to E7 transforming activity. J. Gen. Virol. 1997 Oct;78 (Pt 10):2607–13.

182. Massimi P, Banks L. Transformation assays for HPV oncoproteins. Methods Mol. Med. 2005;119:381–95.

183. Gupta R, Warren T, Wald A. Genital herpes. The Lancet. 2007 Dec 22;370(9605):2127–37.

184. Huang W, Hu K, Luo S, Zhang M, Li C, Jin W, et al. Herpes Simplex Virus Type 2 Infection of Human Epithelial Cells Induces CXCL9 Expression and CD4+ T Cell Migration via Activation of p38-CCAAT/Enhancer-Binding Protein-β Pathway. J Immunol. 2012 Jun 15;188(12):6247–57.

185. MacDonald EM, Savoy A, Gillgrass A, Fernandez S, Smieja M, Rosenthal KL, et al. Susceptibility of Human Female Primary Genital Epithelial Cells to Herpes Simplex Virus, Type-2 and the Effect of TLR3 Ligand and Sex Hormones on Infection. Biol Reprod. 2007 Dec 1;77(6):1049–59.

186. Horbul JE, Schmechel SC, Miller BRL, Rice SA, Southern PJ. Herpes Simplex Virus-Induced Epithelial Damage and Susceptibility to Human Immunodeficiency Virus Type 1 Infection in Human Cervical Organ Culture. PLoS One [Internet].

2011 Jul 27 [cited 2013 Jun 24];6(7). Available from: http://www.ncbi.nlm.nih.gov/pmc/articles/PMC3144918/

187. Karlen S, Offord EA, Beard P. Herpes simplex virions interfere with the expression of human papillomavirus type 18 genes. J. Gen. Virol. 1993 Jun;74 (Pt 6):965–73.

188. Kari I, Syrjänen S, Johansson B, Peri P, He B, Roizman B, et al. Antisense RNA directed to the human papillomavirus type 16 E7 mRNA from herpes simplex virus type 1 derived vectors is expressed in CaSki cells and downregulates E7 mRNA. Virol. J. 2007;4:47.

189. Fang L, Ward MG, Welsh PA, Budgeon LR, Neely EB, Howett MK. Suppression of human papillomavirus gene expression in vitro and in vivo by herpes simplex virus type 2 infection. Virology. 2003 Sep 15;314(1):147–60.

190. Lou E, Kellman RM, Shillitoe EJ. Effect of herpes simplex virus type-1 on growth of oral cancer in an immunocompetent, orthotopic mouse model. Oral Oncol. 2002 Jun;38(4):349–56.

191. Nguyen ML, Kraft RM, Blaho JA. Susceptibility of cancer cells to herpes simplex virus-dependent apoptosis. J. Gen. Virol. 2007 Jul;88(Pt 7):1866–75.

192. Griffith C, Noonan S, Lou E, Shillitoe EJ. An oncolytic mutant of herpes simplex virus type-1 in which replication is governed by a promoter/enhancer of human papillomavirus type-16. Cancer Gene Ther. 2007 Dec;14(12):985–93.

193. Green KL, Southgate TD, Mulryan K, Fairbairn LJ, Stern PL, Gaston K. Diffusible VP22-E2 protein kills bystander cells and offers a route for cervical cancer gene therapy. Hum. Gene Ther. 2006 Feb;17(2):147–57.

194. Zhao Y, Cao X, Tang J, Zhou L, Gao Y, Wang J, et al. A novel multiplex real-time PCR assay for the detection and quantification of HPV16/18 and HSV1/2 in cervical cancer screening. Mol. Cell. Probes. 2012 Apr;26(2):66–72.

195. Orlando JS, Astor TL, Rundle SA, Schaffer PA. The products of the herpes simplex virus type 1 immediate-early US1/US1.5 genes downregulate levels of S-phase-specific cyclins and facilitate virus replication in S-phase Vero cells. J. Virol. 2006 Apr;80(8):4005–16.

196. Narayanan A, Nogueira ML, Ruyechan WT, Kristie TM. Combinatorial transcription of herpes simplex virus and varicella zoster virus immediate early genes is strictly determined by the cellular coactivator HCF-1. J. Biol. Chem. 2005 Jan 14;280(2):1369–75.

197. Thompson RL, Preston CM, Sawtell NM. De Novo Synthesis of VP16 Coordinates the Exit from HSV Latency In Vivo. PLoS Pathog. 2009 Mar 27;5(3):e1000352.

198. Williams BR. PKR; a sentinel kinase for cellular stress. Oncogene. 1999 Nov 1;18(45):6112–20.

199. He B, Gross M, Roizman B. The gamma(1)34.5 protein of herpes simplex virus 1 complexes with protein phosphatase 1alpha to dephosphorylate the alpha subunit of the eukaryotic translation initiation factor 2 and preclude the shutoff of protein synthesis by double-stranded RNA-activated protein kinase. Proc. Natl. Acad. Sci. U.S.A. 1997 Feb 4;94(3):843–8.

200. Brown SM, MacLean AR, McKie EA, Harland J. The herpes simplex virus virulence factor ICP34.5 and the cellular protein MyD116 complex with proliferating cell nuclear antigen through the 63-amino-acid domain conserved in ICP34.5, MyD116, and GADD34. J. Virol. 1997 Dec;71(12):9442–9.

201. Carrozza MJ, DeLuca NA. Interaction of the viral activator protein ICP4 with TFIID through TAF250. Mol Cell Biol. 1996 Jun;16(6):3085–93.

202. Panagiotidis CA, Lium EK, Silverstein SJ. Physical and functional interactions between herpes simplex virus immediate-early proteins ICP4 and ICP27. J. Virol. 1997 Feb;71(2):1547–57.

203. Bailer SM, Haas J. Connecting viral with cellular interactomes. Curr. Opin. Microbiol. 2009 Aug;12(4):453–9.

204. Das S, Kalpana GV. Reverse two-hybrid screening to analyze protein-protein interaction of HIV-1 viral and cellular proteins. Methods Mol. Biol. 2009;485:271–93.

205. Rain J-C, Cribier A, Gérard A, Emiliani S, Benarous R. Yeast two-hybrid detection of integrase-host factor interactions. Methods. 2009 Apr;47(4):291–7.

206. Zhang L, Villa NY, Rahman MM, Smallwood S, Shattuck D, Neff C, et al. Analysis of vaccinia virus-host protein-protein interactions: validations of yeast two-hybrid screenings. J. Proteome Res. 2009 Sep;8(9):4311–8.

207. Bellanger S, Tan CL, Xue YZ, Teissier S, Thierry F. Tumor suppressor or oncogene? A critical role of the human papillomavirus (HPV) E2 protein in cervical cancer progression. Am J Cancer Res. 2011 Jan 24;1(3):373–89.

208. Muller M, Jacob Y, Jones L, Weiss A, Brino L, Chantier T, et al. Large Scale Genotype Comparison of Human Papillomavirus E2-Host Interaction Networks Provides New Insights for E2 Molecular Functions. PLoS Pathog. 2012 Jun 28;8(6):e1002761.

209. Olejnik-Schmidt AK, Schmidt MT, Kedzia W, Goździcka-Józefiak A. Search for cellular partners of human papillomavirus type 16 E2 protein. Arch. Virol. 2008;153(5):983–90.

210. Li S, Liu P, Xi L, Jiang X, Zhou J, Wang S, et al. Screening for novel binding proteins interacting with human papillomavirus type 18 E6 oncogene in the Hela cDNA library by yeast two-hybrid system. J. Huazhong Univ. Sci. Technol. Med. Sci. 2008 Feb;28(1):93–6.

211. White EA, Kramer RE, Tan MJA, Hayes SD, Harper JW, Howley PM. Comprehensive Analysis of Host Cellular Interactions with Human Papillomavirus E6 Proteins Identifies New E6 Binding Partners and Reflects Viral Diversity. J. Virol. 2012 Dec 15;86(24):13174–86.

212. Neveu G, Cassonnet P, Vidalain P-O, Rolloy C, Mendoza J, Jones L, et al. Comparative analysis of virus–host interactomes with a mammalian high-throughput protein complementation assay based on Gaussia princeps luciferase. Methods. 2012 Dec;58(4):349–59.

213. White EA, Sowa ME, Tan MJA, Jeudy S, Hayes SD, Santha S, et al. Systematic identification of interactions between host cell proteins and E7 oncoproteins from diverse human papillomaviruses. PNAS. 2012 Jan 31;109(5):E260–E267.

214. Tucker CL, Peteya LA, Pittman AMC, Zhong J. A Genetic Test for Yeast Two-Hybrid Bait Competency Using RanBPM. Genetics. 2009 Aug 1;182(4):1377–9.

215. Gulbahce N, Yan H, Dricot A, Padi M, Byrdsong D, Franchi R, et al. Viral Perturbations of Host Networks Reflect Disease Etiology. PLoS Comput Biol. 2012 Jun 28;8(6):e1002531.

216. Lazarczyk M, Pons C, Mendoza J-A, Cassonnet P, Jacob Y, Favre M. Regulation of cellular zinc balance as a potential mechanism of EVER-mediated protection against pathogenesis by cutaneous oncogenic human papillomaviruses. J Exp Med. 2008 Jan 21;205(1):35–42.

217. Haitina T, Lindblom J, Renström T, Fredriksson R. Fourteen novel human members of mitochondrial solute carrier family 25 (SLC25) widely expressed in the central nervous system. Genomics. 2006 Dec;88(6):779–90.

218. Palmieri F. The mitochondrial transporter family (SLC25): physiological and pathological implications. Pflugers Arch. 2004 Feb;447(5):689–709.

219. Tina E, Lindqvist B, Gabrielson M, Lubovac Z, Wegman P, Wingren S. The mitochondrial transporter SLC25A43 is frequently deleted and may influence cell proliferation in HER2-positive breast tumors. BMC Cancer. 2012 Aug 10;12(1):350.

220. Palmieri F. Diseases caused by defects of mitochondrial carriers: A review. Biochimica et Biophysica Acta (BBA) - Bioenergetics. 2008 Jul;1777(7–8):564–78.

221. Ishisaki Z, Takaishi M, Furuta I, Huh N. Calmin, a protein with calponin homology and transmembrane domains expressed in maturing spermatogenic cells. Genomics. 2001 Jun 1;74(2):172–9.

222. Stradal T, Kranewitter W, Winder SJ, Gimona M. CH domains revisited. FEBS Letters. 1998 Jul 17;431(2):134–7.

223. Thomsen P, Van Deurs B, Norrild B, Kayser L. The HPV16 E5 oncogene inhibits endocytic trafficking. Oncogene. 2000 Dec 7;19(52):6023–32.

224. Wang Y, Ma Y, Lü B, Xu E, Huang Q, Lai M. Differential expression of mimecan and thioredoxin domain-containing protein 5 in colorectal adenoma and cancer: a proteomic study. Exp. Biol. Med. (Maywood). 2007 Oct;232(9):1152–9.

225. Tanimoto K, Suzuki K, Jokitalo E, Sakai N, Sakaguchi T, Tamura D, et al. Characterization of YIPF3 and YIPF4, cis-Golgi Localizing Yip domain family proteins. Cell Struct. Funct. 2011;36(2):171–85.

226. Fishman P, Bar-Yehuda S, Synowitz M, Powell JD, Klotz KN, Gessi S, et al. Adenosine receptors and cancer. Handb Exp Pharmacol. 2009;(193):399–441.

227. Madi L, Ochaion A, Rath-Wolfson L, Bar-Yehuda S, Erlanger A, Ohana G, et al. The A3 adenosine receptor is highly expressed in tumor versus normal cells: potential target for tumor growth inhibition. Clin. Cancer Res. 2004 Jul 1;10(13):4472–9.

228. Panjehpour M, Karami-Tehrani F. Adenosine modulates cell growth in the human breast cancer cells via adenosine receptors. Oncol. Res. 2007;16(12):575–85.

229. Byun H-O, Han N-K, Lee H-J, Kim K-B, Ko Y-G, Yoon G, et al. Cathepsin D and Eukaryotic Translation Elongation Factor 1 as Promising Markers of Cellular Senescence. Cancer Res. 2009 Jun 1;69(11):4638–47.

230. Rho SB, Park YG, Park K, Lee S-H, Lee J-H. A novel cervical cancer suppressor 3 (CCS-3) interacts with the BTB domain of PLZF and inhibits the cell growth by inducing apoptosis. FEBS Letters. 2006 Jul 24;580(17):4073–80.

231. Khacho M, Mekhail K, Pilon-Larose K, Pause A, Côté J, Lee S. eEF1A Is a Novel Component of the Mammalian Nuclear Protein Export Machinery. Mol Biol Cell. 2008 Dec;19(12):5296–308.

232. Yue J, Shukla R, Accardi R, Zanella-Cleon I, Siouda M, Cros M-P, et al. Cutaneous Human Papillomavirus Type 38 E7 Regulates Actin Cytoskeleton

Structure for Increasing Cell Proliferation through CK2 and the Eukaryotic Elongation Factor 1A▽. J Virol. 2011 Sep;85(17):8477–94.

233. Noda Y, Okada Y, Saito N, Setou M, Xu Y, Zhang Z, et al. KIFC3, a microtubule minus end-directed motor for the apical transport of annexin XIIIb-associated Triton-insoluble membranes. J. Cell Biol. 2001 Oct 1;155(1):77–88.

234. Xu Y, Takeda S, Nakata T, Noda Y, Tanaka Y, Hirokawa N. Role of KIFC3 motor protein in Golgi positioning and integration. J. Cell Biol. 2002 Jul 22;158(2):293–303.

235. De S, Cipriano R, Jackson MW, Stark GR. Overexpression of kinesins mediates docetaxel resistance in breast cancer cells. Cancer Res. 2009 Oct 15;69(20):8035–42.

236. Rath O, Kozielski F. Kinesins and cancer. Nature Reviews Cancer. 2012 Jul 24;12(8):527–39.

237. Handschumacher RE, Harding MW, Rice J, Drugge RJ, Speicher DW. Cyclophilin: a specific cytosolic binding protein for cyclosporin A. Science. 1984 Nov 2;226(4674):544–7.

238. Yao Q, Li M, Yang H, Chai H, Fisher W, Chen C. Roles of cyclophilins in cancers and other organ systems. World J Surg. 2005 Mar;29(3):276–80.

239. Hsu SH, Shyu HW, Hsieh-Li HM, Li H. Spz1, a novel bHLH-Zip protein, is specifically expressed in testis. Mech. Dev. 2001 Feb;100(2):177–87.

240. Jones S. An overview of the basic helix-loop-helix proteins. Genome Biology. 2004 May 28;5(6):226.

241. Hsu S-H, Hsieh-Li H-M, Li H. Dysfunctional spermatogenesis in transgenic mice overexpressing bHLH-Zip transcription factor, Spz1. Experimental cell research. 2004 Mar 10;294(1):185–98.

242. Hsu S-H, Hsieh-Li H-M, Huang H-Y, Huang P-H, Li H. bHLH-zip transcription factor Spz1 mediates mitogen-activated protein kinase cell proliferation, transformation, and tumorigenesis. Cancer research. 2005 May;65(10):4041–50.

243. Hrabchak C, Varmuza S. Identification of the spermatogenic zip protein Spz1 as a putative protein phosphatase-1 (PP1) regulatory protein that specifically binds the PP1cgamma2 splice variant in mouse testis. The Journal of biological chemistry. 2004 Aug 27;279(35):37079–86.

244. Ludlow JW, Glendening CL, Livingston DM, DeCarprio J a. Specific enzymatic dephosphorylation of the retinoblastoma protein. Molecular and cellular biology. 1993 Jan;13(1):367–72.

245. Schwarz E, Freese UK, Gissmann L, Mayer W, Roggenbuck B, Stremlau A, et al. Structure and transcription of human papillomavirus sequences in cervical carcinoma cells. Nature. 1985 Mar 7;314(6006):111–4.

246. Baker CC, Phelps WC, Lindgren V, Braun MJ, Gonda MA, Howley PM. Structural and transcriptional analysis of human papillomavirus type 16 sequences in cervical carcinoma cell lines. J. Virol. 1987 Apr 1;61(4):962–71.

247. Hrabchak C, Varmuza S. Identification of the Spermatogenic Zip Protein Spz1 as a Putative Protein Phosphatase-1 (PP1) Regulatory Protein That Specifically Binds the PP1c{gamma}2 Splice Variant in Mouse Testis. Journal of Biological Chemistry. 2004 Aug 27;279(35):37079.

248. Hrabchak C, Varmuza S. Identification of the Spermatogenic Zip Protein Spz1 as a Putative Protein Phosphatase-1 (PP1) Regulatory Protein That Specifically Binds the PP1c{gamma}2 Splice Variant in Mouse Testis. Journal of Biological Chemistry. 2004 Aug 27;279(35):37079.

249. Laurson J, Raj K. Localisation of Human Papillomavirus 16 E7 Oncoprotein Changes with Cell Confluence. PLoS ONE. 2011 Jun 29;6(6):e21501.

250. Hsu S-H, Hsieh-Li H-M, Huang H-Y, Huang P-H, Li H. bHLH-zip Transcription Factor Spz1 Mediates Mitogen-Activated Protein Kinase Cell Proliferation, Transformation, and Tumorigenesis. Cancer Res. 2005 May 15;65(10):4041–50.

251. Noya F, Chien W-M, Wu X, Banerjee NS, Kappes JC, Broker TR, et al. The Promoter of the Human Proliferating Cell Nuclear Antigen Gene Is Not Sufficient for Cell Cycle-dependent Regulation in Organotypic Cultures of Keratinocytes. J. Biol. Chem. 2002 May 10;277(19):17271–80.

252. Morris GF, Bischoff JR, Mathews MB. Transcriptional activation of the human proliferating-cell nuclear antigen promoter by p53. Proc. Natl. Acad. Sci. U.S.A. 1996 Jan 23;93(2):895–9.

253. Ravasi T, Suzuki H, Cannistraci CV, Katayama S, Bajic VB, Tan K, et al. An Atlas of Combinatorial Transcriptional Regulation in Mouse and Man. Cell. 2010 Mar 5;140(5):744–52.

254. Van der Bruggen P, Traversari C, Chomez P, Lurquin C, De Plaen E, Van den Eynde B, et al. A gene encoding an antigen recognized by cytolytic T lymphocytes on a human melanoma. Science. 1991 Dec 13;254(5038):1643–7.

255. Kim K-H, Choi J-S, Kim I-J, Ku J-L, Park J-G. Promoter hypomethylation and reactivation of MAGE-A1 and MAGE-A3 genes in colorectal cancer cell lines and cancer tissues. World J. Gastroenterol. 2006 Sep 21;12(35):5651–7.

256. Grau E, Oltra S, Martínez F, Orellana C, Cañete A, Fernández JM, et al. MAGE-A1 expression is associated with good prognosis in neuroblastoma tumors. J. Cancer Res. Clin. Oncol. 2009 Apr;135(4):523–31.

257. Chen H, Cai S, Wang Y, Zhao H, Peng J, Pang X, et al. Expression of the MAGE-1 gene in human hepatocellular carcinomas. Chin. Med. J. 2000 Dec;113(12):1112–8.

258. Hudolin T, Juretic A, Spagnoli GC, Pasini J, Bandic D, Heberer M, et al. Immunohistochemical expression of tumor antigens MAGE-A1, MAGE-A3/4, and NY-ESO-1 in cancerous and benign prostatic tissue. Prostate. 2006 Jan 1;66(1):13–8.

259. Zhang S, Zhou X, Yu H, Yu Y. Expression of tumor-specific antigen MAGE, GAGE and BAGE in ovarian cancer tissues and cell lines. BMC Cancer. 2010;10:163.

260. Jang SJ, Soria JC, Wang L, Hassan KA, Morice RC, Walsh GL, et al. Activation of melanoma antigen tumor antigens occurs early in lung carcinogenesis. Cancer Res. 2001 Nov 1;61(21):7959–63.

261. Sarcevic B, Spagnoli GC, Terracciano L, Schultz-Thater E, Heberer M, Gamulin M, et al. Expression of Cancer/Testis Tumor Associated Antigens in Cervical Squamous Cell Carcinoma. Oncology. 2003;64(4):443–9.

262. Bosch M van den, Bree RT, Lowndes NF. The MRN complex: coordinating and mediating the response to broken chromosomes. EMBO reports. 2003 Sep 1;4(9):844–9.

263. Karantza V. Keratins in health and cancer: more than mere epithelial cell markers. Oncogene. 2011 Jan 13;30(2):127–38.

264. Grandori C, Cowley SM, James LP, Eisenman RN. The Myc/Max/Mad Network and the Transcriptional Control of Cell Behavior. Annual Review of Cell and Developmental Biology. 2000;16(1):653–99.

265. Amati B, Dalton S, Brooks MW, Littlewood TD, Evan GI, Land H. Transcriptional activation by the human c-Myc oncoprotein in yeast requires interaction with Max. Nature. 1992 Oct 1;359(6394):423–6.

266. Ayer DE, Kretzner L, Eisenman RN. Mad: A heterodimeric partner for Max that antagonizes Myc transcriptional activity. Cell. 1993 Jan 29;72(2):211–22.

267. Zervos AS, Gyuris J, Brent R. Mxi1, a protein that specifically interacts with Max to bind Myc-Max recognition sites. Cell. 1993 Jan 29;72(2):223–32.

268. Hurlin PJ, Quéva C, Koskinen PJ, Steingrímsson E, Ayer DE, Copeland NG, et al. Mad3 and Mad4: novel Max-interacting transcriptional repressors that suppress c-myc dependent transformation and are expressed during neural and epidermal differentiation. EMBO J. 1995 Nov 15;14(22):5646–59.

269. Hurlin PJ, Quéva C, Eisenman RN. Mnt, a novel Max-interacting protein is coexpressed with Myc in proliferating cells and mediates repression at Myc binding sites. Genes Dev. 1997 Jan 1;11(1):44–58.

270. Hurlin PJ, Steingrìmsson E, Copeland NG, Jenkins NA, Eisenman RN. Mga, a dual-specificity transcription factor that interacts with Max and contains a T-domain DNA-binding motif. EMBO J. 1999 Dec 15;18(24):7019–28.